



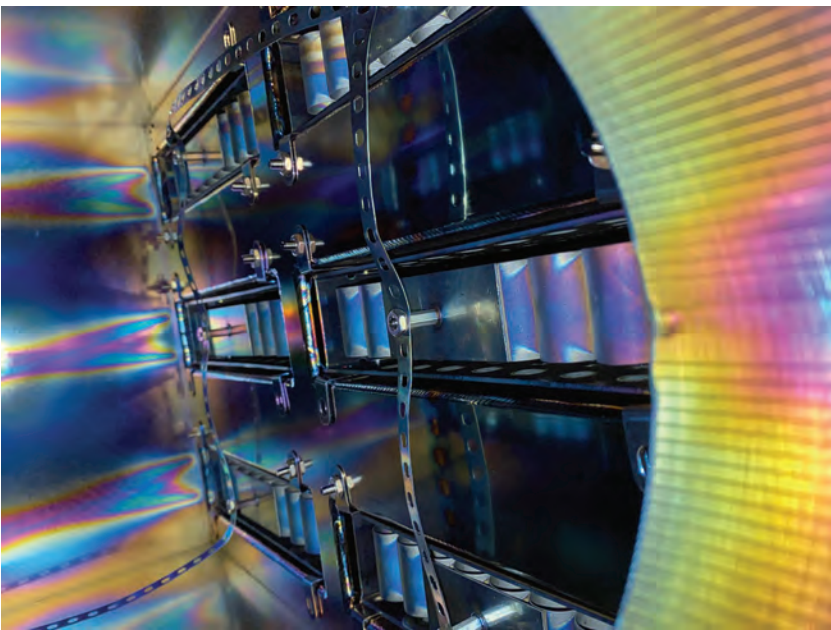
J-PARC

ANNUAL

REPORT

2 0 2 2

Vol.1: Highlight



Editorial Board (April 2023 – March 2024)



Yong LIU (*Accelerator Division*)



Kaoru SAKASAI (*Materials and Life Science Division*)



Toshiyuki TAKAHASHI (*Particle and Nuclear Physics Division*)



Masami IIO (*Cryogenics Section*)



Shigeru SAITO (*Transmutation Division*)



Fumihiro MASUKAWA (*Safety Division*)



Masatoshi TSUKADA (*Users Office Team*)



Narumi SUGIYAMA (*Public Relations Section*)

Cover photographs



Photograph ① : Do specular reflection images in quadrupole magnet ducts dream of ray tracing?
Image credit: Masahiko UOTA



Photograph ② : The art inside the ion pump
Image credit: Masahiko UOTA



Photograph ③ : Large aerogel Cherenkov detector under construction
Image credit: Takeshi YAMAMOTO

J-PARC Annual Report 2022

Contents

Preface	1
Accelerators	3
Overview of the Accelerator.....	3
Linac	5
RCS	8
MR	11
Materials and Life Science Experimental Facility	15
Overview	15
Neutron Source Section	16
Neutron Science Section	17
Neutron Instrumentation Section	18
Muon Section	19
Technology Development Section	21
Particle and Nuclear Physics	23
Neutrino Experimental Facility	23
Hadron Experimental Facility (HEF)	24
Particle and Nuclear Physics Experiments at MLF	25
Theory group	26
Technical Support Group (Esys-Tokai)	26
— Research Highlight —	
Mass and Width of the $\Lambda(1405)$ Hyperon Resonance.....	27
Cryogenics Section	29
Overview	29
Cryogen Supply and Technical Support	30
Superconducting Magnet System for T2K	30
Superconducting Magnet Systems at the MLF	31
Superconducting Magnet Systems at the HEF	31
R&D for the Future Projects at J-PARC	32
Information System	35
Overview	35
Status of Networking	35
Internet Connection Services for Visitors and Public Users of J-PARC	38
Status of Computing	38

Transmutation Studies	41
Overview	41
Research and development	42
International and Domestic Cooperation	45
Safety	47
Safety	48
User Service	51
Users Office (UO)	52
User Statistics	54
MLF Proposals Summary - FY2022	55
J-PARC PAC Approval Summary for the 2022 Rounds	57
Organization and Committees	61
Organization Structure	62
Members of the Committees Organized for J-PARC	63
Main Parameters	69
Events	71
Events	71
Publications	79
Publications in Periodical Journals	80
Conference Reports and Books	90
KEK Reports	95
JAEA Reports	96
Others	97



Preface

In Japanese fiscal year (JFY) 2022, from April 2022 through March 2023, we made great progress at J-PARC on many fronts and a few of our achievements are covered below.

We succeeded in delivering 830kW stable beam to the MLF at a very high availability of about 96%. A major challenge in JFY2022 was the soaring electricity prices, which initially hindered to plan 7.2 cycle operation for the MLF within the allocated budget. However, the allocation of a supplementary budget to offset the

increased electricity costs, enabled us to restore the operation back to 6.6 cycles, 92% of 7.2 cycles, which allowed the execution of 418 general user experiments.

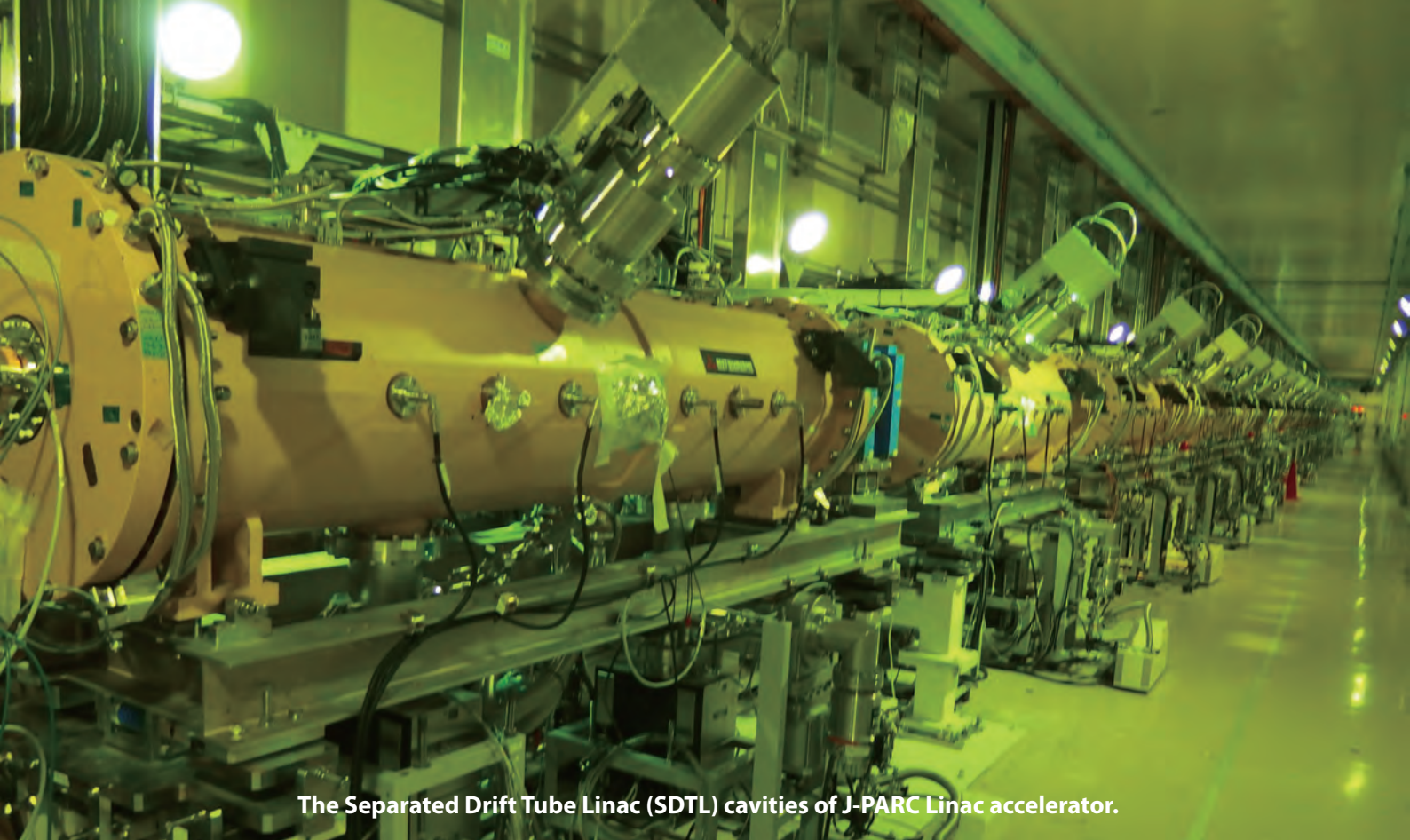
The major upgrade of the MR for higher beam power was completed in JFY2021, with its commissioning scheduled for JFY2022. However, initial failures in the upgraded components significantly reduced the beam time for the beam commissioning.

A major milestone achieved in the HD experimental facility was the completion of the C-line for the COMET experiment after long preparation. By the end of JFY2022, we successfully commissioned the slow extraction beam and bunched slow extraction at 8GeV in the C-line. At the same time, the upgrade of the neutrino beam facility to achieve a higher beam power upto 1.3MW for the HyperKamiokande project is ongoing. One of the most important scientific achievements from the particle and nuclear physics experiments was the results from E40 experiment on hyperon - proton scattering, which reveal insights into the nature of the strong force acting between nucleons at short distances.

In this volume, we report the progress made at J-PARC in JFY2022.

On behalf of the J-PARC staff members,
Director of J-PARC Center

Takashi Kobayashi



The Separated Drift Tube Linac (SDTL) cavities of J-PARC Linac accelerator.

Accelerators

Overview of the Accelerator

The J-PARC accelerator complex consists of a 400 MeV linac, a 3 GeV Rapid Cycling Synchrotron (RCS) and a Main Ring Synchrotron (MR, 30 GeV). The proton beam from the RCS is delivered to the Materials and Life Science Experimental Facility (MLF) for neutron and muon experiments as well as injected to the MR. The MR has two beam extraction modes: fast extraction (FX) mode for the Neutrino experimental facility (NU) and slow extraction (SX) mode for the Hadron experimental facility (HD).

The operation in Japanese fiscal year (JFY) 2022 is illustrated in Fig. 1. The topics related to the beam operation are as follows:

(1) Operation for the MLF

The beam operation as an operation run of Run#89, which started in the middle of January 2022 continued until the end of April on schedule. The beam power for the Materials and Life Science experimental facility (MLF) user program increased from 720 kW to 830 kW.



Fig. 1. Accelerator operation in JFY2022.

After almost a ten-day shutdown at the beginning of May, the user program resumed for the MLF at 830 kW beam power on May 11. However, the beam power for the MLF user program had to be reduced from 830 kW to 770 kW from June 7 due to insufficient cooling capacity of the cooling water system of the RCS in summer. The MLF user program has been performed on schedule until June 24, before the summer shutdown.

The user program for the MLF resumed on schedule at 800kW beam power, which was almost the same value as the power before the summer shutdown, as an operation run of Run#90 on November 21. This program has been performed on schedule until March 15, 2023, with a New Year's break of about two weeks in the middle.

The MLF operation statistics for JFY2022 (from April 2022 to March 2023) are shown in Table 1. The net user operation hours and the beam availability rate for the MLF facility were as follows: 3,440 hours (96.0%). These statistics show that the linac, and the RCS operated with high availabilities.

Figure 3 shows the number of stop events and stop time by components in JFY2022. The stop time includes not only the stop events during scheduled operation but also during beam studies and tuning. There were several causes of the stop.

For the linac, HVDC were still dominant. The RCS outage was mainly due to RF. The RF outage was not due to the cavity, but to the failure of the capacitor, the life of the vacuum tube in the amplifier and transformer

rectifier. There were three main causes of the MR downtime events, which were the trouble of the power supply of the BM and the QM and beam fast extraction magnets.

(2) The MR upgrade work and beam operation

The MR upgrade work had been performed since July 2021. Manufacture of new power supplies for the main magnets (BM and QM), new 2nd harmonic RF system, and new injection and extraction magnets and so on were scheduled during this upgrade work. This work should have been completed by the end of May 2022, but it was not completed as scheduled, specifically, the tuning of the new power supplies for the main magnets was delayed due to failures that occurred twice, in May and June. Beam commissioning, scheduled from June 1 before the summer shutdown, was delayed by about a month, reducing its duration from a month to almost a week due to these power supply failures.

Beam commissioning, scheduled from the middle of November after the summer shutdown, was also delayed by two months due to failure of the new power supply for the main magnet, and coil failure of the septum magnet for the fast beam extraction magnet. As response emergency measures for this magnet failure, the coil joints of the same type of electromagnet were reinforced and partially repaired electromagnets were reinstalled. The MR beam operations in February and March were a combination of slow beam extraction adjustment and COMET operation 8GeV pattern.

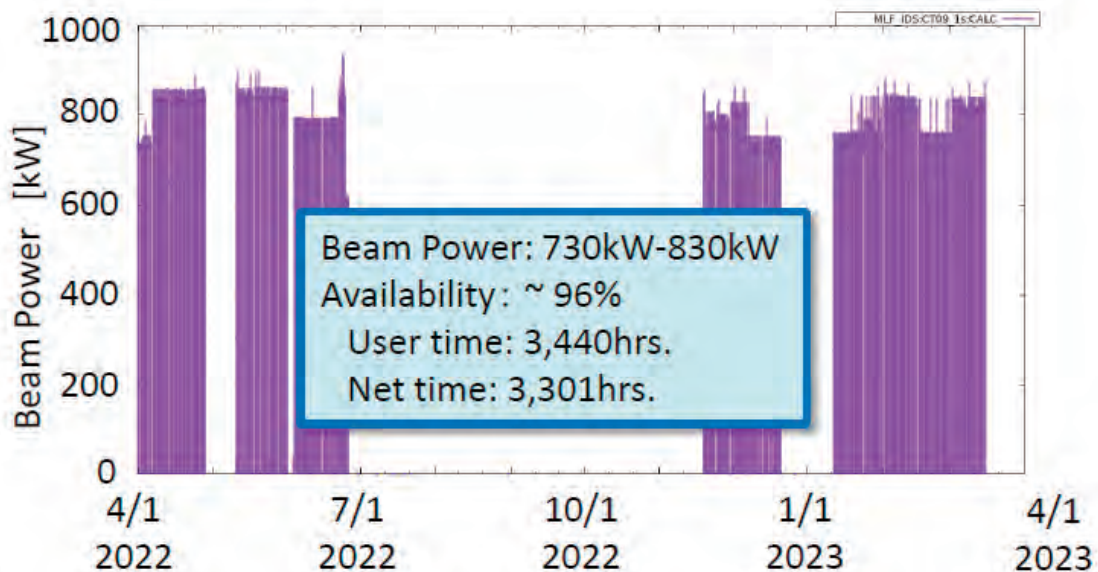


Fig. 2. Beam power and operation statistics in hours for the MLF user operation in JFY2022.

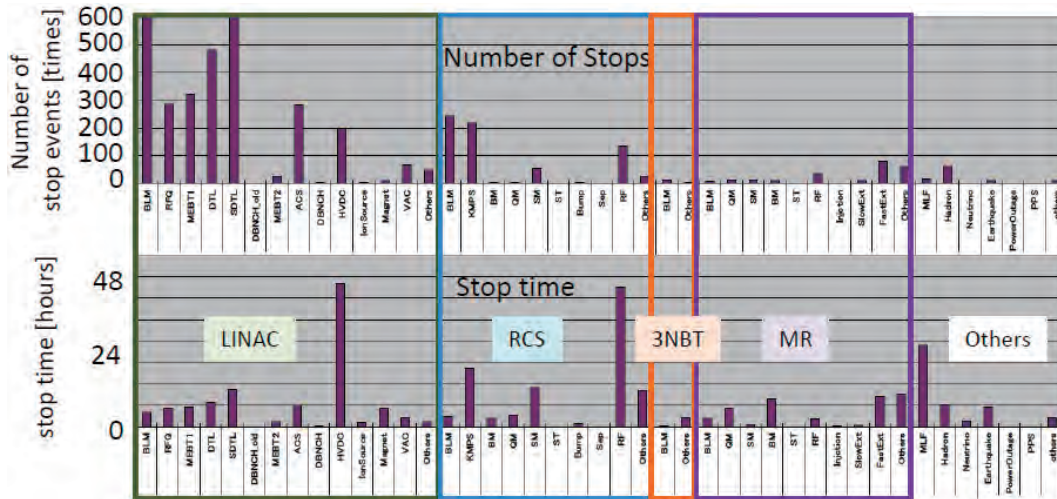


Fig. 3. Number of stop events and stop time by components in JFY2022.

Linac

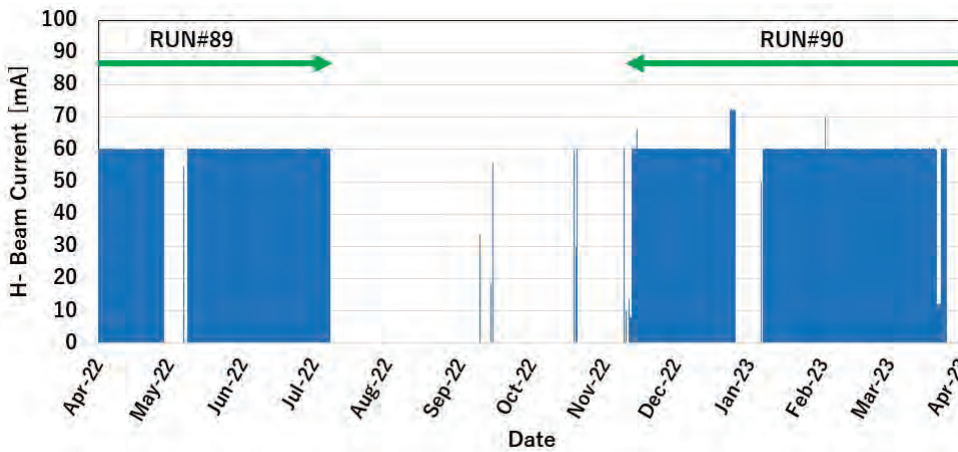


Fig. 4. Operation history of the ion source in FY2022.

Overview

The J-PARC linac has been operated with a nominal peak beam current of 50 mA. High availability of more than 95% (to the MLF), the same as in FY2021, was also kept during FY2022 at the linac. The beam studies have been conducted to resolve some issues, such as the beam loss mitigation and confirmation of feasibility for further high intensity operation due to the demand of downstream facilities.

Accelerator components status

The operation history of the ion source in FY 2022 is shown in Fig. 4. Presently, the ion source is being operated at the H- beam with a peak current of 60 mA for the user operation. Before the winter shutdown, the ion source extracted more than 72 mA beams for high-intensity beam study. Figure 5 shows the history of the continuous operation time and the beam current increase of the RF ion source (from 2014). The

replacement cycle has been gradually extended with increased operational experience. In RUN#89 (January 2022 – July 2022), the continuous operation time of the ion source has been extended to 4,001 hours (5.5 months), which was 350 hours longer than the previous record (3,651 hours in the RUN#86). As the lifetime of the ion source is mainly limited by the failure of the

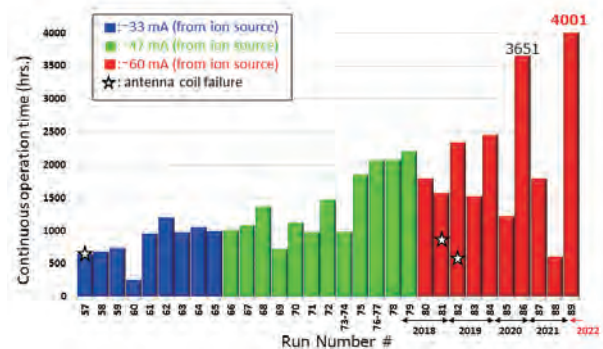


Fig. 5. History of the continuous operation time of the RF ion source.

RF antenna coil installed in the source chamber, dimension measurements and SEM/EDS analyses were applied to understand the surface discoloration of the antenna. No cracks, no pinholes and little variation in the enamel coating thickness on the antenna surface were observed. The discoloration after the long-term continuous operation is due to the deposition of injected cesium and compositions of stainless steels (Fe, Cr, Ni) used for the ion source components sputtered by plasma. The results show that the enamel coating of the antenna has not been worn out in the continuous operation for several months and that the ion source's continuous operation period can be extended more. On the other hand, the sputtering of the stainless steel is a serious issue for the stable plasma operation. The development of a new plasma chamber is proceeding to prevent the sputtering rate. The final goal is to achieve continuous operation over 7 months, approaching the full J-PARC user operation period in one year.

The RFQ trip rate has been approximately 10 times per day at 25 Hz beam operation to the MLF in FY2022. This situation is almost the same as before. An auto-restart system for the RFQ trip has been running for three years. The system resumes the beam at the next macro-pulse after the RFQ trip. Also, the beam stop associated with the RFQ trips (e.g., MPS by the beam loss downstream) occurs approximately once every 2 days.

RF trips due to the discharge have frequently occurred in DTL3 since the summer maintenance in 2022. The vacuum pressure in the cavity deteriorated when tripped, and a CCD camera attached to the viewport in front of the RF coupler confirmed that light was emitted near the ceramic window of the RF coupler. This indicates that the cause of the DTL3 trip is the discharge at the vacuum-side surface of the ceramic window. High-power conditioning was conducted at first and recovery was observed, however, it was temporary. Therefore, the ceramic window of DTL3 was replaced with a new one during the spring maintenance period at the end of March 2023. Multiple paired discharge marks were observed on the surface of the removed ceramic window and on the vacuum seal. After the replacement, almost no DTL3 trips due to the discharge were observed.

After the Great East Japan Earthquake in 2011, we could not operate with the design rf power in some SDTL cavities due to the multipactor effect. To solve the problem, we performed acetone or acid cleaning on these cavities several times. In the 2021 summer maintenance, the SDTL05A cavity was cleaned by dilute hydrochloric acid. Since then, the unstable region

disappeared for more than a year. Also, SDTL04A and SDTL04B were unstable near the operating power region, therefore acid cleaning was performed on these cavities in the 2022 summer maintenance period. Increase in the RF reflections due to multipactor has not been observed in these two cavities since then. After the 2022 summer maintenance, all SDTL cavities are operating at the designed operating power stably.

The operation of the ACS cavities was more stable than that of the other accelerator sections. The number of trips of all the ACS cavities was less than once per day.

RF system status

We have been handling two types of klystrons, such as a 324-MHz klystron and a 972-MHz one. Due to decrease in electric breakdown voltage, one 972-MHz klystron was replaced in March 2023. The operation time of the klystrons as of the end of March 2023 is shown in Fig. 6. Among a total of twenty 324-MHz klystrons, six of them reached more than 87,000 hours of operation, which corresponds to the entire period since the linac operation was started. Most of the 972-MHz klystrons reached more than 56,000 hours of operation.

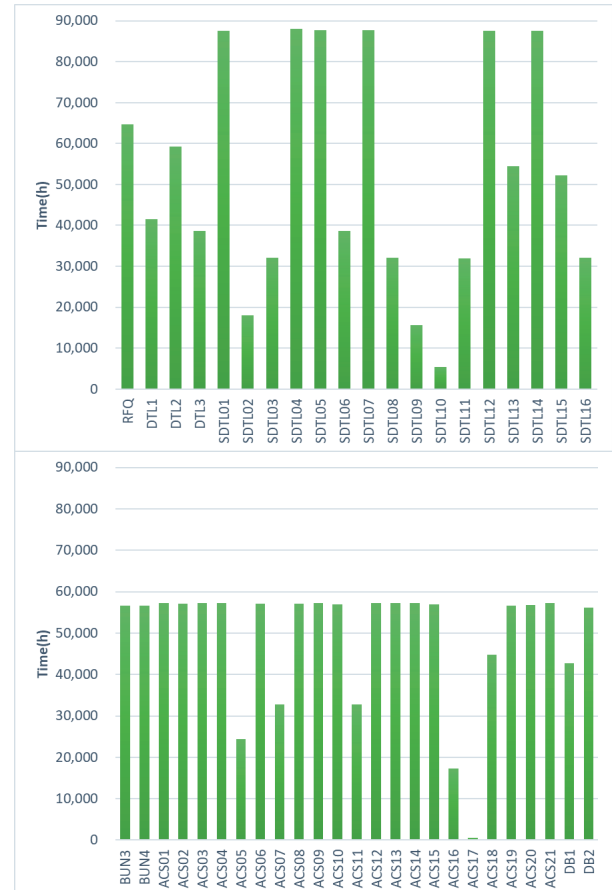


Fig. 6. The operation time of the 324-MHz klystron (top) and 972-MHz klystron (bottom) as of the end of March 2023.

Beam monitor status

It is important to measure and adjust the beam profile not only in the transverse direction but also in the longitudinal one to produce a stable beam with minimal beam loss. We have been developing a bunch shape monitor (BSM), which measures a longitudinal beam profile. Several BSMs have been installed in the Linac. The BSM at MEBT1 uses a highly oriented pyrolytic graphite (HOPG) as the secondary electron emission target. The HOPG-BSM enables a longitudinal profile measurement of a 3 MeV beam without breaking the target due to its high thermal conductivity. The longitudinal profile measurement of high-power beams, such as peak current of 55 mA and macrobunch length of 100 μ s, has been continuously performed. The longitudinal beam parameters evaluated offline from the BSM data agreed with the simulation results of a three-dimensional particle-in-cell code. We will improve the analysis method to estimate the beam parameters in a short time to use the BSM data for online beam commissioning.

Another BSM is installed in the MEBT2. This BSM played an important role in identifying the origin of a large beam loss at L3BT in beam commissioning. That beam loss was not caused by the transverse beam profile problem. The BSM showed the distortion at the beginning of the macrobunch as shown in Fig. 7. This beam abnormality was found to have originated from the inadequate feedforward setting. The BSM has been effectively used to detect beam anomalies.

Another progress of the beam monitor is the momentum correction system with beam position monitor (BPM), which has been successfully operated for years. The beam loss occurred at the dispersion peak point of the RCS and 3-50 BT during the user operation. This was caused by the drift of the beam momentum, whose origin was the dependence of the accuracy of the LLRF control devices on the humidity fluctuations.

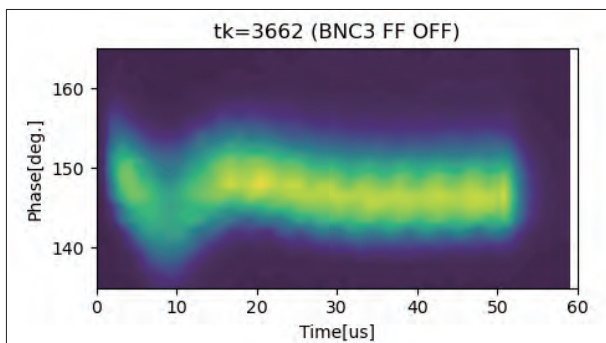


Fig. 7. The longitudinal beam profile measured by the BSM in MEBT2. Distortion in the beginning of the macrobunch was observed.

Therefore, a feedback system was constructed to constantly monitor the momentum using the BPM and to correct the phase of the end-stage of the acceleration cavity to eliminate the momentum drift when it occurred. The beam momentum has been very stable since this monitoring-correction system was introduced and later, the LLRF devices were placed in the chambers with constant temperature and humidity.

Beam study

In JFY2022, our work focuses on improving the understanding of beam property and exploring linac output beam stability. Machine learning (ML) is introduced in J-PARC to improve the accelerator performance.

As a first trial example in the J-PARC linac, a DNN (Deep-Learning Neural Network) model is trained with sufficient simulation data for the beam phase response to the RF cavity errors, as shown in the upper part of Fig. 8, which can successfully surrogate the physics process. The DNN model calibrated with the measured data shown in the lower part of Fig. 8 will be applied for compensating the RF errors.

Preliminary studies have shown that a DNN-based correction scheme can improve the linac output momentum stability by several times from the present rate of 0.01% according to the present RF design tolerance into less than $\pm 0.001\%$. Further beam study is planned to verify this result.

A subsequent study aimed at understanding and improving beam properties involved beam measurements at the most upstream beam transport line, MEBT1. This is essential since an increase in emittance has been observed during the operation of the DTL

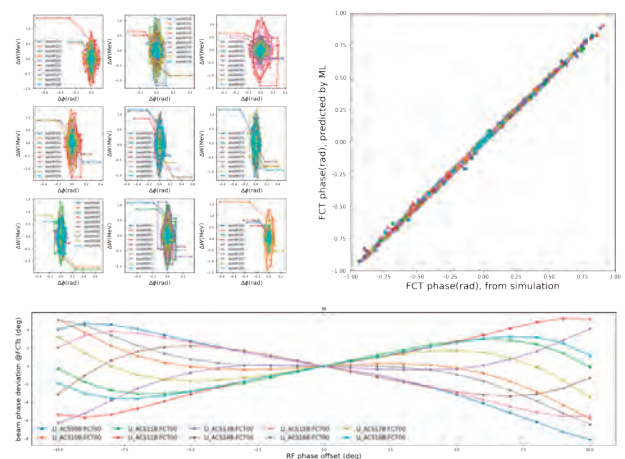


Fig. 8. Preparation and training result of ML-DNN model of RF error and beam phase response (upper), and measured data (lower).

accelerator, which is installed post-MEBT1. The beam phase space was measured using the so-called Q-scan method using a wire scanner monitor and a quadrupole magnet located in MEBT1. Figure 9 presents both the measured and simulated results in the x-direction (left) and y-direction (right). The measured profile width aligns well with the simulation, and the observed emittances are consistent within the anticipated parameters. Moreover, the beam emittance showed stability, varying by only a few percent during the measurement period. Based on these findings, the beam dynamics within the DTL are currently under investigation.

Considerable efforts have been dedicated to loss mitigation. Besides the loss in the linac, the beam outside the RCS RF bucket (called extinction) has been

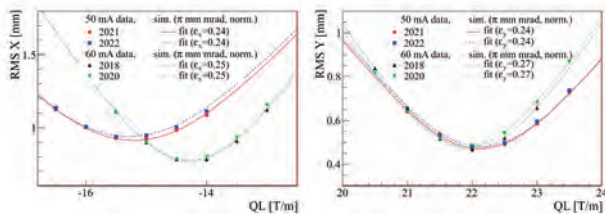


Fig. 9. Measured and simulated beam profile width.

identified as one of the primary sources of loss at RCS, which necessitates investigation prior to injecting beam to RCS. A measurement method for the extinction was developed, utilizing a stopper in the 2nd medium beam transport line (MEBT2) within the linac. Here, the corresponding beam is halted by the stopper, allowing for the measurement of the ensuing loss signal. This loss signal has been calibrated with the actual loss at RCS (see Fig. 10, left), revealing a strong correlation between them. Additionally, the dependence of the extinction on the buncher strength installed at MEBT1 was assessed, as shown in Fig. 10 (right). This analysis indicates that the extinction can be adjusted to meet the requirements by modulating the buncher strength.

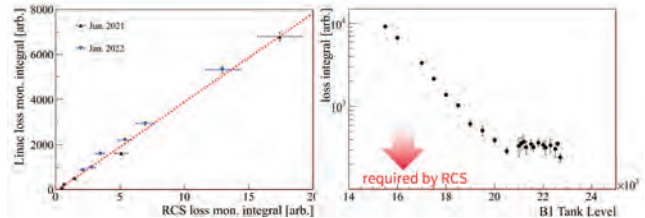


Fig. 10. Loss signal due to the stopper in linac vs loss signal in RCS (left). dependence of the extinction to the buncher strength (right).

RCS

Operational status

The MLF user operation started at a beam power of 700 kW in JFY 2022, which was increased to 800 kW in April 2022. Thereafter, the beam current was maintained, but the total number of protons on the neutron target was effectively reduced due to the shortened cycle of the MR operation. To increase the beam power in MR, the power supplies of the MR magnet system were replaced and the MR operation cycle for the fast extraction mode was reduced from 2.48 to 1.36 s. This shorter MR cycle reduced the operation duty of the MLF from 58/62 (~93.5%) to 30/34 (~88.2%), and thus, the number of protons on the neutron target was practically reduced by this factor. Finally, the beam power of the MLF has been maintained at 800 kW up until JFY 2023.

As a matter of fact, one of the transformer-rectifier assemblies of the RF system ceased operation in June 2022. Subsequently, only 11 RF cavities have been operated and 800 kW beams were still achievable under this condition. Conversely, the maximum output beam power

has been limited due to this failure. Figure 11 shows the changes in the RCS output power with respect to time.

The operation status of the RCS was sufficiently stable in JFY 2022. The availability of the RCS is summarized in Table 1. In JFY 2022, the operation time for the MLF was ~3301 h, excluding the commissioning time, and the downtime due to the RCS was ~52 h. The

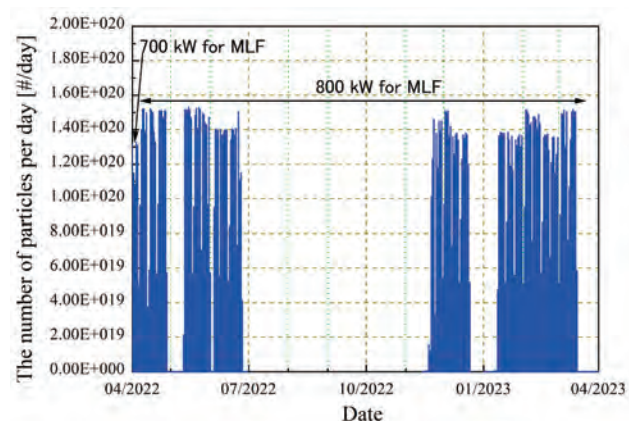


Fig. 11. Changes in the RCS output particles over time.

Table 1. Summary of availability

Facility	User time (h:m)	Trouble in RCS (h)	Availability of RCS (%)
MLF	3301:28	52:08	98.4

availability of the MLF was evaluated using these values and found to be 98.4%. In JFY 2022, RCS delivered beams only to the MLF due to the MR upgrade activity, and thus there was no operation time for Neutrino and Hadron users.

Hardware issues

- Capacity of the cooling water system

The trial of the 1-MW continuous operation in JFY2020 revealed a critical issue in achieving a stable operation. When the outside temperature and humidity increased, the temperature of the cooling water also increased and became uncontrollable. This phenomenon induced the temperature interlock of the vacuum tube in the RF final-stage amplifier. Thus, the cooling water system had to be improved to ensure a stable 1-MW operation in all seasons. In the summer shutdown period of 2021, performance recovery activity of the cooling water system was under-taken. This activity revealed that the low performance was due to the contamination of the heat exchange unit. Therefore, the unit was disassembled and washed during the summer shutdown period. After the recovery activity, the cooling water temperature was reduced despite using a higher beam power.

To confirm the effect of the recovery activity on the cooling water system, a high-power beam trial was conducted from June 24 to 26, 2022. Figure 12 shows the temperature and output beam power trends during the trial. Continuous operation commenced with 910 kW from 11:14; however, it halted at 13:33 due to

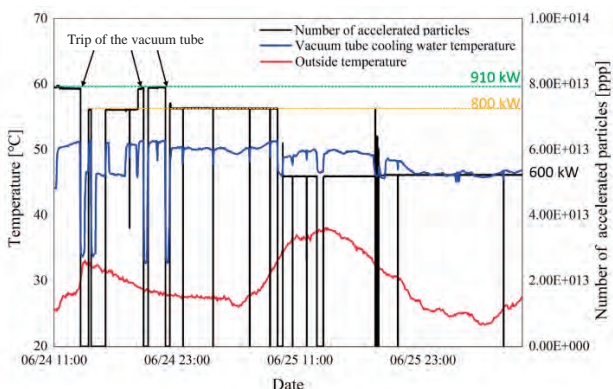


Fig. 12. Trends in beam power, cooling water temperature, and outside temperature.

the interlock of the vacuum tube temperature. At that instant, the outside temperature was rapidly increasing and reached more than 32 °C. This indicated that the capacity of the cooling water system was insufficient to cool the vacuum tube of the RF system even after the recovery of its original performance. Thereafter, beam power was reduced to 800 kW and resumed at 14:21; however, the temperature of the vacuum tube frequently increased close to the threshold. Therefore, we had to halt the trial each time and wait till the temperature decreased, but the outside temperature was kept at ~30 °C; the cooling water temperature did not decrease sufficiently even by midnight. Subsequently, the trial at 910 kW was aborted, and instead, the trial was performed at 800 kW until the next morning. However, the temperature of the vacuum tube increased close to the threshold again in the morning, and the beam power was further reduced to 600 kW. Finally, at 12:38, a failure occurred at RF #10 system. As immediate recovery was not possible, we continued the trial at 600 kW till the next morning.

Notably, the temperature in June 2022 was an extraordinary case. Figure 13 shows the temperature in June 2022 and the average values for June from 1990 to 2020. The graph reveals that the temperature at the end of June 2022 was at least 10 °C higher than average. Previous results indicated that a 1-MW beam could be accelerated if the temperature was maintained under the usual conditions. Furthermore, the user operation typically ends in the second half of June; therefore, 1-MW operation is possible when the weather is cooler than that in June 2022.

- Failure of the transformer - rectifier assembly

As mentioned above, the failure occurred at RF #10 system during the 1-MW trial in June of JFY2022. The RF

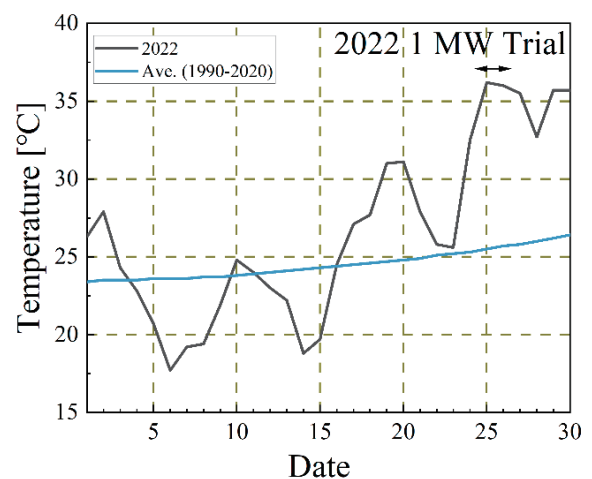


Fig. 13. Trends of the outside temperature in Mito city.

system was tripped due to an over current of the transformer-rectifier assembly, and could not be restored immediately. Figure 14 shows the transformer-rectifier assemblies of the RF system.

We replaced the failed assembly to a spare one at the end of March 2022, but the spare assembly also had problems and did not work. We have started to produce a new assembly and it will be installed at the end of JFY2023.



Fig. 14. The transformer - rectifier assemblies of the RF system.

Beam study results

We have continued the beam study to achieve further reduction of the beam loss. One of the remaining sources of the beam loss is the intrinsic sextupole field component in the injection chicane bumps (SBs). The sextupole field drives the $3\nu_x = 19$ resonance. This resonance is not so strong and does not cause immediate beam loss, but when the accelerating particle stays longer on this resonance, the horizontal emittance grows up and the particle would be lost. We have three sets of sextupole magnet systems, but these are used for chromaticity correction and suppression of the instability and no additional sextupoles exist for correction of this resonance. To reduce the effect of the intrinsic sextupole field by SBs, we studied the operation parameters with reduced SB fields for partial mitigation. Figure 15

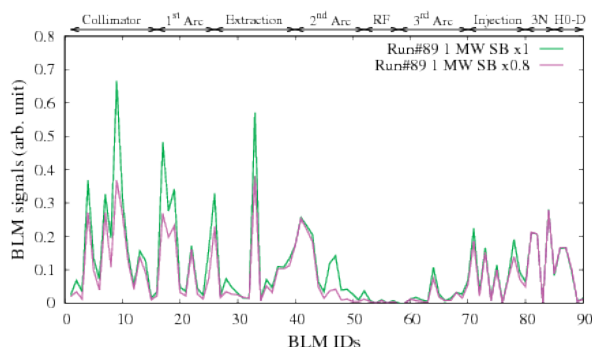


Fig. 15. Study results with/without reduced SB fields. The green line shows the loss signals at the original SB field strength, and the purple line indicates the loss signals with 80% SB field strength.

shows the study results with/without reduced SB fields.

The study results indicated that the beam loss at the collimator was approximately 50% reduced, and the horizontal beam emittance was also reduced to 90% of the original parameter case. We implemented this parameter to the operation from the autumn of 2022.

We also optimized some other parameters (transverse and longitudinal painting pattern, betatron tunes and so on), and we have achieved more than 80% beam loss mitigation at 1 MW beam operation as compared with the operation in 2020. Now the residual beam loss is less than 0.05% even at the 1-MW beam power and dominated by the foil scattering. We will try to further reduce the foil size.

In this year, MR was not operated due to its upgrade work. However, we carried out the beam tuning for MR. We tried the lower SB field strength parameter, but there was no significant improvement in the MR case. In fact, the transverse painting area in the MR operation is smaller than that of the MLF case, and this situation makes foil scattering a major cause of the loss. Therefore, the lower SB field operation is not effective for the MR case, but this guarantees that the lower SB operation does not conflict with the beam operation to the MR, while it has a significant benefit for the operation to the MLF. We also tried to extend the transverse painting area from 50 to 100 $\mu\text{mm}\cdot\text{mrad}$. with a new painting pattern. The results showed that it is possible to increase the paint area without affecting the beam emittance of MR. The number of the foil hits will be reduced by 50% for the MR operation if this new painting pattern is adopted. We will continue to optimize these MR operation parameters.

Summary

RCS is almost continuing a stable user operation with an 800-kW beam. Even after the recovery of the cooling water performance, the present system cannot accelerate a 1-MW beam under high temperature and humid condition like in the summer. However, the user operation ends in the second half of June, in the usual season, thus the 1-MW operation is possible if the weather is not as hot as it was in the last year.

For the MLF operation, optimization of the transverse and longitudinal painting, betatron tune and resonance correction were performed. The residual beam loss at 1 MW is even less than 0.05%, mitigated by more than 80% from that of the 2020 operation. The residual beam loss is mostly caused by the unavoidable foil scattering of the circulating beam. A smaller size

foil will be tested. We will also try to correct other resonances near the present operating point.

We have maintained a smaller emittance beam for the MR. A slightly larger painting area for the MR gives

a significant beam loss reduction as well as 50% foil hit reduction, while keeping the rms emittances the same. We will try to implement a larger painting area for the beam operation to the MR.

MR

Overview

MR has been operated with the beam power of 515 kW by 2021 for the fast extraction (FX) mode to the neutrino facility with the cycle time of 2.48 s. The number of accelerated protons was 2.66×10^{14} which was the world record for synchrotrons. The beam power for the slow extraction (SX) mode was 64.5 kW for the hadron experimental hall with the cycle time of 5.2 s. The extraction efficiency was 99.5% which was also a world record. To achieve higher beam power, we have upgraded the magnet power supplies, RF system, collimators, injection and extraction system. The hardware upgrade has been performed to introduce the faster cycle operation by JFY2021. We intended to shorten the cycle time to 1.36 s for the FX mode. In JFY2022, we started the tuning of the hardware and beam for the faster cycle operation. We have delivered an 8 GeV SX beam to the COMET experiment through the new Hadron C beam line.

Upgrade works for the faster operation

We have completed the construction of the power supplies for the main magnets and the rearrangement of reused power supplies in JFY2021. The rearrangement included the configuration change of five quadrupole magnet families. Each of these families was divided into two families by half a circumference each. Therefore, the number of the quadrupole families were increased from 11 to 16. We have started tuning of the power supplies in JFY2022. It has been a challenging project, because the tuning involves many new components, various types of power supplies and many patterns for the accelerator operation modes.

Seven fundamental RF cavities and two second harmonic RF cavities were used for the FX operation of the 2.48 s cycle in JFY2021. We have installed two new cavities and power amplifiers by JFY2022 (Fig. 16). Since only one of two new anode power supplies was ready for the operation in JFY2022, there were eight available RF cavities for fundamental and two for second harmonic.

The injection and extraction devices have been prepared for the faster cycling. The extraction system consists of two low field septum magnets and four high field septum magnets. Eddy current type magnets were constructed for the low field septum magnets. Three out of four high field magnets were constructed (Fig. 17) and one of them was reused from the abort side extraction magnets which had relatively larger apertures. The power supplies were also reused. To achieve the faster



Fig. 16. Two RF cavities and power amplifiers installed in the insertion A.

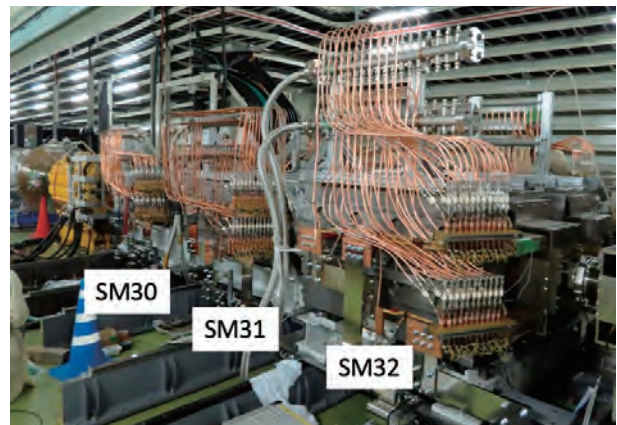


Fig. 17. High field septum magnets SM30, SM31, SM32 installed in insertion C.

cycling, the magnets were designed to have smaller inductances. They were also designed to have larger apertures and smaller leak magnetic fields to the circular orbit with magnetic field shields.

MR has a feature of beam loss localization with collimators. The number of collimators used to be four. We installed two more in 2022 (Fig. 18). We have a plan to install another one in 2023. The total number will be seven and the beam loss capacity will be from 2.0 kW to 3.5 kW. The beam loss localization will be improved.



Fig. 18. Collimator C (left) and D (right, installed in 2022) in insertion A.

Initial failures of the upgraded equipment and recovery

During the test operation of the upgraded equipment, several failures occurred. We, then, took effective measures to solve the problems.

For the main magnet power supply, the following failures occurred in 2022: a contactor failure in the BM6 power supply, a number of blown fuses due to optical fiber cable disconnection for the QFN and QDN power supplies, a power supply shutdown due to noise in the high-speed interlock system, and an IGBT unit failure in the BM4 power supply. We have taken effective measures to rectify all of the problems.

From the incident of the optical fiber cable disconnection for the timing signal, many fuses of the power supplies were blown. Clock signals such as 12 MHz are sent to the power supplies from the master timing system by optical fiber cables. If the clock signal is interrupted, the switching state of the IGBTs is fixed at that point, resulting in an overcurrent that causes the fuses to blow. We made the modification for each power supply to have an internal clock signal generator, and if the external signal is interrupted, it is switched to use the clock signal from the internal clock signal generator, and the power supply is then safely shut down.

For the newly fabricated FX septum magnets, there was poor soldering in the area where the coils make

electrical contact with each other to form turns, and the hollow conductors melted during the test operation, causing water leakage. Therefore, the soldering was reinforced, and the support was improved. In addition, the coils themselves are being re-produced, and some of them have been completed, and there are plans to manufacture and replace the remaining coils in the future.

Beam test and operation

From June to July 2022, the beam tuning was performed at 3 GeV DC without acceleration. From January to March 2023, the beam tuning was done with acceleration to 8 GeV. In addition, SX tuning and beam delivery were performed at 8 GeV for the COMET experiment. The beam power was 240 W with extraction every 9.6 s. The extraction efficiency was 99% and the spill duty was 76%.

From April 2023, we plan for beam tuning with acceleration to 30 GeV and user operation of both FX and SX mode.

Injection tuning, optical measurements and tuning were performed for the new FX mode. Using the newly installed LLRF system, voltage feedback was provided for the harmonics of 6 - 12 to suppress longitudinal oscillations with high intensity eight bunch beam (Fig. 19).

The previous FX septum magnets had a leakage field to the orbit, and vertical beta function modulation of up to 10% was observed. The new magnets have a reduced leakage field and correspondingly the beta function modulation was improved to be 1/10 (Fig. 20).

Optical correction turned out to be more difficult with the increase in the number of quadrupole magnet families from 11 to 16 and the division of five of these families by half a circumference each. In particular,

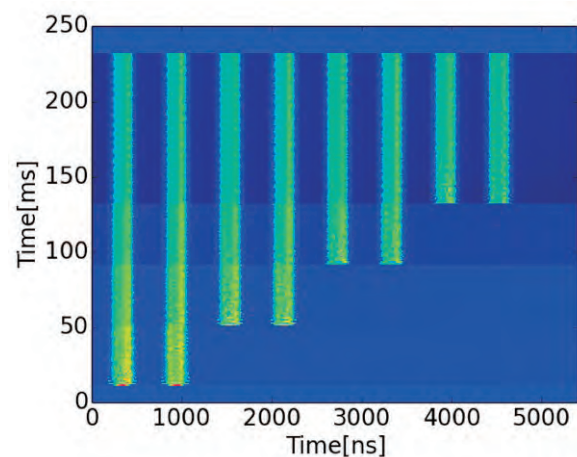


Fig. 19. Longitudinal beam oscillation observed in the mountain plot with a wall current monitor for 8 bunch injection.

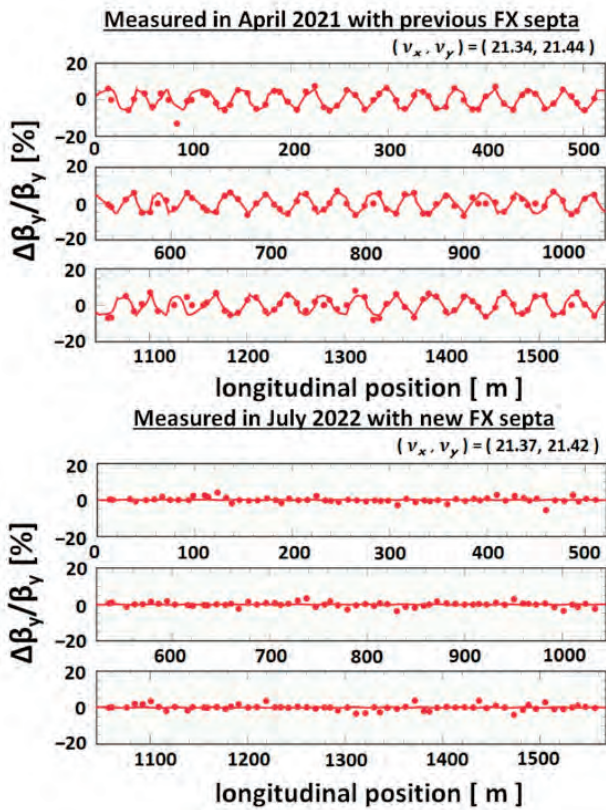


Fig. 20. Vertical beta modulation. Top figure shows the measurement in April 2021. Bottom figure shows the measurement in July 2022.

the betatron phase advances of the three arcs were aligned during the injection period. In addition, as in the previous beam tunings by 2021, the currents in the correction coils of the four sextupole magnets were adjusted to correct multiple third-order resonances. With these beam tunings, we were able to accumulate protons equivalent to a beam power of 740 kW, which was close to the original target of the J-PARC MR, with a good beam loss localization, even though only for the injection period (Fig. 21).

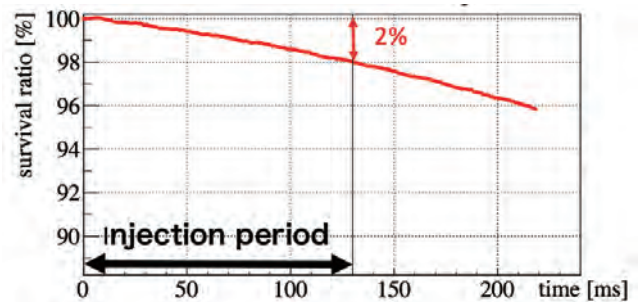
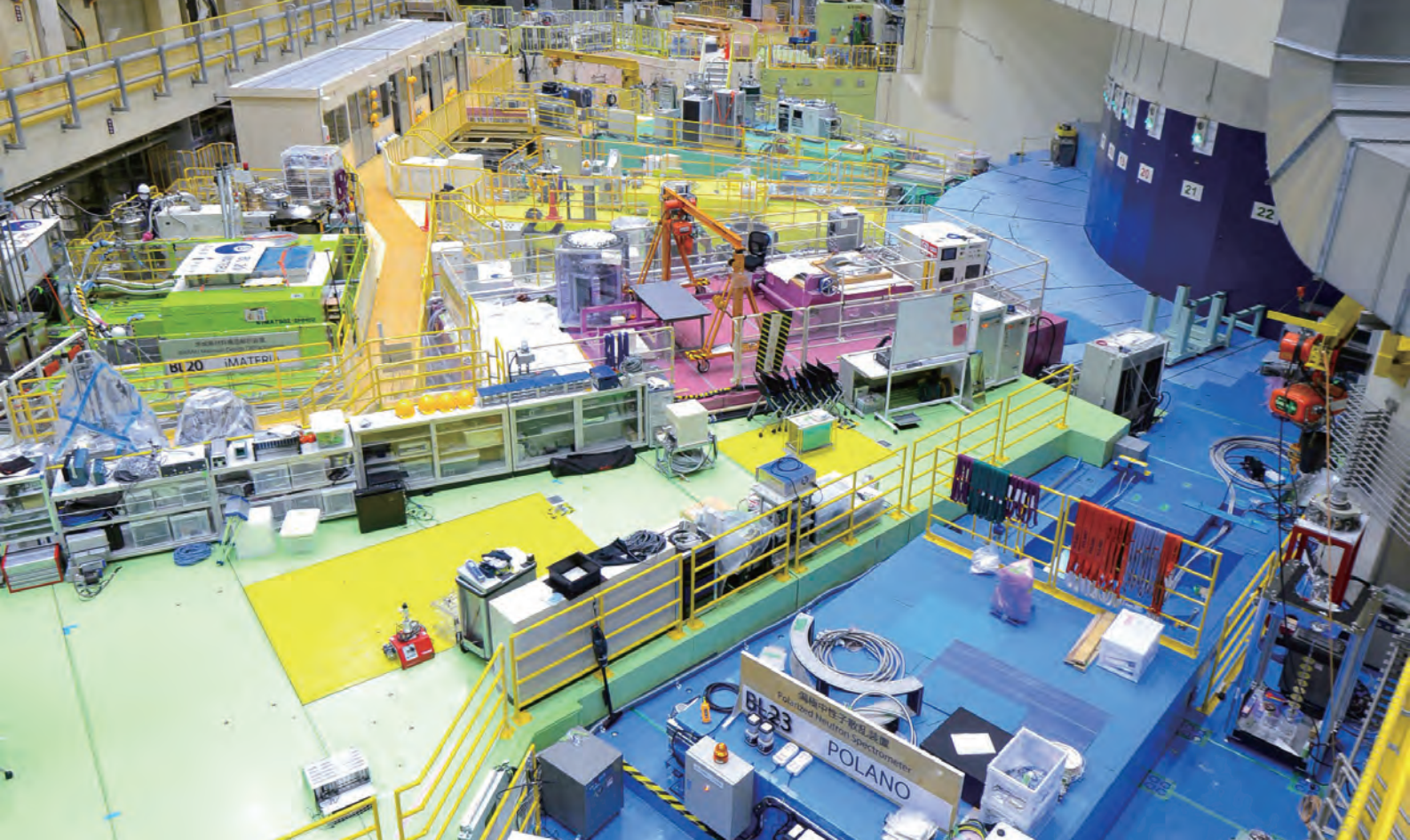


Fig. 21. Beam survival measured with DCCT.



Materials and Life Science Experimental Facility

Overview

In 2022, beam power of 830 kW with high operational efficiency of over 90% was reached for the first time in the user program. 21 neutron beamlines and 7 muon areas were operated. Despite that, the soaring electricity costs affected the beam time, J-PARC reviewed the operation schedule upon the approval of a supplementary budget and decided to elongate the MLF user operation until March 14. The user program was operated for a total of 146 days, although 159 days were originally planned, and 418 general user proposals were conducted.

Over 250 papers were published, such as a structural study of new flexible and tough super elastic Alloy with promising use in Biomedical Applications, asteroid explorer Hayabusa2, initial analysis revealing the formation and evolution of the carbonaceous asteroid Ryugu, nondestructive two-dimensional quantitative analysis of degradation of the charging capacity of Lithium-ion

secondary batteries and discovering the hidden order of the Mo and Nb atoms in disordered $Ba_7Nb_4MoO_{20}$ crystals.

As part of the process to establish a stable operation, the target vessel replacement process was re-examined, and the tritium release was successfully reduced. Also, the preparation of the spare muon target (the 3rd muon rotating target) advanced, and will be completed in 2023.

The SEOP system as a spin polarizer on BL23 has been set and finally the on-beam commissioning with a polarized neutron beam has begun. Constructing the world's first muon accelerator on the H2 area of H-line was approved by the Nuclear Regulatory Authority ("GENSHIRYOKU-KISEI-CHOU"). The RFQ and IH-DTL, by which ultra-slow muons are accelerated to 4.3 MeV, will be installed in the H2 area. They act as the front stage of the 212-MeV linear accelerators.

Events in 2022 were held in a hybrid mode of in-person and internet meetings: one of them was the Annual meeting of neutron industrial application at Akihabara with 300 participants. This annual meeting was held to merge the outcomes from the MLF and Japan Research Reactor - 3 (JRR-3) of JAEA. The 11th International Workshop on Sample Environment at Scattering Facilities (ISSE) was held at Nasu and the 6th Neutron and Muon School (NM-school) was held as KEK-IINAS

(Inter-Institution Network for Accelerator Science) School at Tokai (<https://mlfinfo.jp/sp/school/6th-nms/>).

In November 2022, the border control of Japan returned almost completely to the rules from the time before COVID-19. The number of foreign users is gradually reaching the previous level and various activities now take place as before.

Neutron Source Section

At the beginning of fiscal year 2022, the beam power at the MLF was raised from 730 kW to 830 kW on April 7, which was the highest level of beam power on record for the long-term user program. Since the proton beam pulses at the 3GeV rapid cycle synchrotron (RCS) outlet are shared between the MLF and the 30GeV main ring (MR), the beam power at the MLF becomes lower than that at the RCS outlet and is changed in accordance with the operation mode of MR. The share of MR is 3.1% in slow extraction mode and 11.8% in fast extraction mode. 830 kW at the MLF was attained when the power at the RCS outlet was raised from 760 kW to 860 kW with a slow extraction mode of MR, but due to the mode change to fast extraction, the power at the MLF was reduced to 770kW from June 4, even though the power at the RCS outlet was raised to the highest record of 870 kW. The stable operation continued, and the beam operation of the MLF ended on June 26 after a two-day operation for beam study and the maintenance works during the long outage started.

Here, some important remote-handling operations in the hot cell are highlighted. One was the replacement of the used proton beam window and volume reduction. The proton beam window is mounted on the shielding plug and integrated into one unit as shown in Fig. 1 left photo. When the operation of the proton beam window reaches the material lifetime, which is ca.10000 MWh, the unit is replaced with a new one with a new proton beam window mounted on it, and the used unit is temporarily moved to the storage space. Then, usually in later years, the used proton beam window is dismantled from the unit and replaced in the hot cell by remote handling to reuse the shielding plug. In 2022, the used proton beam window, which ended its operation in 2020, was replaced and the utility pipes were cut into pieces by the cutting machine shown in

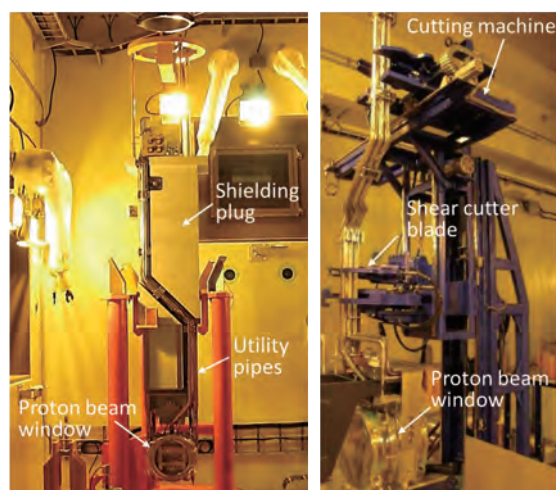


Fig. 1. Unit of proton beam window and the cutting machine.

Fig.1 right photo for volume reduction by remote handling operation. The operations were successfully done, and the new unit was ready to be used as a spare proton beam window.

Another notable operation was the remote handling test of the moderator & reflector assembly carried out using a spare assembly. An assembly consists of three moderators, a reflector, and a shielding plug, and only the used moderators and reflector are replaced while the shielding plug is reused just like the proton beam window. Because the operating lifetime of a moderator and reflector assembly is comparatively long, 30000 MWh corresponding to 8 years at 1MW, the last remote handling operation was done during the commissioning period before the beam operation of MLF started more than 10 years ago, so the inheritance of skills and experiences is very important. The remote handling procedures were checked carefully to handle the actual radioactive assembly in the near future.

On September 26, specimens were cut out from the

forefront wall of the used target vessel, which was operated with 836 kW at maximum. This time, the specimen of the inner wall of the mercury vessel, which was protected against the pitting damage by micro-bubble injection into mercury flow, could not be obtained, because the specimen fell into the mercury vessel. But the damage on the specimen of the outer wall of the mercury vessel, the mercury boundary wall, was negligibly small, which was a promising result for the stable beam operation with greater beam power. On October 11, the used mercury target vessel was replaced with a new one which had the same structure as the former one.

On November 21, the beam operation of the user program started with 780 kW, which was a little bit less than that before the long outage due to the trouble with the accelerator component. The beam power at the MLF was changed several times between 730 kW and 810 kW due to the change of the beam operation

mode of MR for beam study. The beam operation of the MLF had continued very well with the excellent availability of more than 95% and ended on March 15 as scheduled.

There were three international collaboration workshops. One was held from October 10 to 11 with European Spallation Source (ESS) on-site at Lund in Sweden with online capability. Main topics were commissioning works in every aspect of the project. The others were held on-site at J-PARC. One was held from February 27 to March 1 with ISIS of Rutherford Appleton Laboratory. Information exchange in the field of the accelerator system and neutron/muon target system was the primal scope. Another workshop was held from March 22 to 24 with the Spallation Neutron Source (SNS) of Oak Ridge National Laboratory to discuss the neutron source system issues. Many fruitful discussions were held at all workshops.

Neutron Science Section

1. User program

COVID-19 as a global health emergency has been toned down in 2022. After nearly 7 million deaths, WHO Director-General Tedros has declared the crisis is over. The user operation in Materials and Life Science Experimental Facility (MLF) was also back to normal as Japan opened its borders with cautious measures. Particularly, vaccinations could save people from severe spreading of infections and lockdown. Still, we maintained strict conditions for immigration, the MLF kept concentrating on stable operation and prudent infection control. As a result, MLF achieved 830 kW power operation in the first half of the year and over 95% operating rate, both are the best performance ever in MLF.

303 and 291 in general proposals (involving one-year proposal and new-user proposal) were submitted for the operation period of 2022A and 2022B, respectively. The number of applied proposals has kept almost stable in recent years, and 266 were approved for the year of 2022. In addition, 4 of the long-term proposals out of 5, have been approved.

2. Instruments up to date

We are continuously making efforts to upgrade the instruments for realizing much more effective and fruitful experiments. One of key items that can ensure our success are the so-called sample environment (SE)

devices, that can control external physical parameters on samples, like temperature, magnetic field, pressure, electric field, and so on. And such physical parameters are essential to investigate new phenomena, properties or even new fields of sciences. We report a couple of examples below.

Newly designed Paris-Edinburgh high-pressure apparatus has been used for investigating properties of quantum harmonic oscillator of metal hydrides under pressure. Hydrogen vibration excitations of fluorite-type $ZrH_{1.8}$ and $TiH_{1.84}$ were investigated at pressures up to 21 GPa by incoherent inelastic neutron scattering experiments. From the pressure dependence of lattice parameters determined by diffraction experiments, the relations between metal-hydrogen distance and the first excitation energy E_1 of $ZrH_{1.8}$ and $TiH_{1.84}$ at high-pressures are found [1].

Most of the neutron experiments are facing the background (BG) issues, in particular the BG from sample container/cavity. It sometimes causes distorted interpretation of the obtained data. A group of BL02 developed a low-BG sample cell specific to aqueous protein solution samples, conducted with a neutron back-scattering spectrometer. It was found that the scattering intensity of an aluminum sample cell coated with boehmite using D_2O was lower than that of a sample cell coated with regular water (H_2O). Meticulous

attention to cells with small individual weight differences and the positional reproducibility of the sample cell relative to the spectrometer neutron beam position enabled the accurate subtraction of the scattering profiles of the D₂O buffer and the sample container. Consequently, high-quality information on protein dynamics could be extracted from diluted protein solutions [2].

3. Other activities

As the pandemic situation is improving, the first in-person international workshop after COVID took place, hosted by J-PARC MLF. The 11th International Workshop on Sample Environment at Scattering Facilities (ISSE-WS) was successfully held at Resort Hotel Laforet Nasu, Tochigi, Japan, from August 28th to September 1st. This workshop series takes place every 2 years under the patronage of the International Society for Sample Environment (ISSE). Engineers, technicians and scientists working on sample environment at the neutron/synchrotron facilities in the world and industrial partners participate in this workshop to present

various topics related to sample environment and to discuss new techniques, collaboration among facilities and so on. There were 87 participants, including five online participants, gathered in Japan from 11 countries. Also, some of other activities are as follows: The Commissioning Workshop of ESS & J-PARC collaboration (October 10, 2022); The 6th Neutron Muon School (December 12 to 16, 2022); Quantum Beam Science Festa 2022 in Tsukuba (March 13 to 15, 2023).

4. Award

The JSNS (Japanese Society for Neutron Science) Encouragement Award has been given to Dr. Wu Gong for “Studies on Microstructure Evolution and Mechanical Properties in Structural Metallic Materials by *in-situ* Neutron Diffraction”. Also, the JSNS Poster Award, given to Dr. Wenqi Mao for “Effect of Grain Refinement on Deformation-induced Martensitic Transformation”.

Reference

- [1] T. Hattori, *et al.*, Phys. Rev. B **106** 134309 (2022).
- [2] T. Tominaga, *et al.*, Life **12**(5) 675 (2022).

Neutron Instrumentation Section

The neutron instrumentation section has been developing position-sensitive neutron detectors (PSND) for upgrading of the neutron scatterings instruments in the MLF.

As for the ³He gas-based neutron detectors, their performances have been simulated by using GEANT4 by the KEK detector team. Geant4 is a toolkit for simulating the physics interaction of particles passing through matter and can be used to evaluate detector performance [1]. Figure 2 shows the amount of energy loss that occurred in the ³He(n,p)³H reaction within a

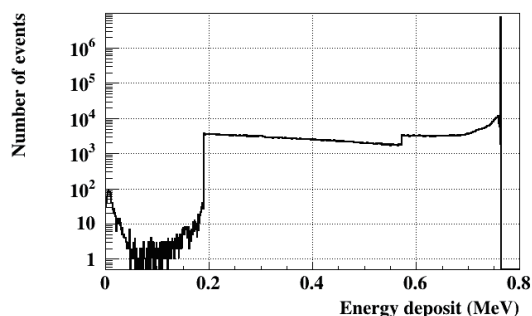


Fig. 2. Amount of energy loss within a ³He-gas based PSND in the ³He(n,p)³H reaction with a 25-meV incident neutron.

³He-gas based PSND when a 25 meV neutron is vertically incident on the detector. One characteristic shape is that the events lower than 0.05 MeV are contributions from electrons not mediated by the ³He(n,p)³H reaction. These electrons are produced by the γ -rays emitted by the absorption reaction between the incident neutrons and the SUS that is the detector housing. Events due to wall effects are widely distributed from 0.19 MeV to the total absorption peak at 0.76 MeV. The edges at 0.57 MeV and 0.19 MeV correspond to the initial energies of proton and triton, respectively. For events contained in the 0.05 MeV to 0.19 MeV region, the reaction point of the ³He(n,p)³H reaction is extremely close to the detector housing, so proton and triton lose little energy in the sensitive area. This information is difficult to obtain from actual measurements and is one of the benefits of simulations that provide support in the evaluation of detector performance.

As for scintillation detectors, a new large area detector has been successfully developed for the SENJU instrument. SENJU is a time-of-flight Laue single crystal neutron diffractometer. To scan a wide reciprocal space as efficiently as possible, SENJU has been equipped with

41 original detector modules. Although these detectors contribute to the increase of a solid angle coverage, physical gaps between detectors cause missing diffraction peaks inherently. Hence, a large area detector has been requested for a long time. With the preceding feasibility study and careful long-term stability test [2], the large area detector was developed and produced in

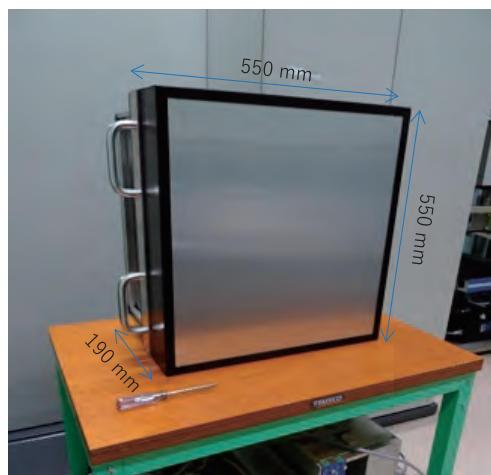


Fig. 3. Photograph of the new large area position-sensitive scintillation neutron detector for the SENJU instrument.

2022 for SENJU (Fig. 3). Like in the case of the original detectors, a scintillator and wavelength-shifting fiber detector technology has been employed. The detector has a neutron-sensitive area of 512 x 512 mm, which is four-fold compared to the original one with a detector pixel size of 4 x 4 mm, which is like that of the original SENJU detector. In order to fit in the limited installation space, the detector depth has been designed as thin as possible to ~190 mm, which is 63% of the original one. The detector exhibited detection efficiency of 50% for 2-Å neutrons, ^{60}Co gamma-ray sensitivities of $\sim 1 \times 10^{-6}$, neutron count uniformity of 5~9% (1σ). All of these parameters exceeded those of the original ones, and they are acceptable for use in the beam line. The detector has been installed under the new vacuum vessel in SENJU and has been in service since 2022.

References

- [1] S. Agostinelli, *et al.*, Nucl. Instr.& Meth. A **506** 250 (2013), H. Ohshita, *et al.*, to be published.
- [2] T. Nakamura, *et al.*, 2019 IEEE NSS/MIC Conference Records, N19-236.
DOI: 10.1109/NSS/MIC42101.2019.9059981

Muon Section

1. Development of the D2 instrument

In recent years, elemental analysis with muonic X-rays is becoming popular in the D line. A lot of elemental analyses were conducted on archaeological objects, meteorites, and lithium-ion batteries. To obtain the data in a shorter time, the sample environment and the detectors were refurbished. The major change was in the sample chamber, the newly installed hemispherical chamber has 11 ports to mount the detectors (Fig. 4).

2. Progress of the laser system for ultra-slow muon generation

The ultra-slow muons are generated by ionizing the evaporated muonium from the muon-stopping target by irradiating coherent lights. To realize efficient ionization of muonium, vacuum ultraviolet (VUV) light (122.09 nm Lyman- α) and coherent light with wavelengths shorter than 360 nm are required. So far, over 10 μJ Lyman- α light has been successfully generated and applied to ultra-slow muon generation. To generate high-power VUV light, the power of the fundamental pulses of 1062.78 nm is required to be 100 mJ,



Fig. 4. Picture of the Hemispheric chamber in the view from downstream of the beam. Gold coins are set at a sample position. The Ge detectors and multi-pixel detectors are equipped at Port 1 - 7, and Port 8 - 9, respectively. Ports 10 -11 can be used for decay counters and other detectors.

and specially produced Nd:YAG and Nd:YAG ceramics rods ($\phi 4$ mm, 80 mm long) are used in diode-pumped amplifiers as a gain medium. However, when using such a long rod, it was difficult to eliminate the optical wavefront distortion caused by the inhomogeneity in the medium. Thus, we decided to change the pumping configuration from a conventional side pump to an end pump geometry to reduce the optical path length in the gain medium (Fig. 5). The pump light from laser diodes (LDs), which used to be injected from the side of the rod, will be injected coaxially. The new pumping geometry requires spatial profile shaping for the pump light beam from LDs, but the wavefront distortion can be dramatically reduced by shortening the crystal length. In the new method, sapphire substrates are bonded to the light input and output surfaces of Nd:YAG for efficient cooling and end-face protection. The amplifier module is composed of 9.3 mm cubic Nd:YAG ceramic, sapphire plates ($\phi 25.4$, $t=2$ mm) bonded on the ceramic, and a water-cooling holder (Fig. 6).

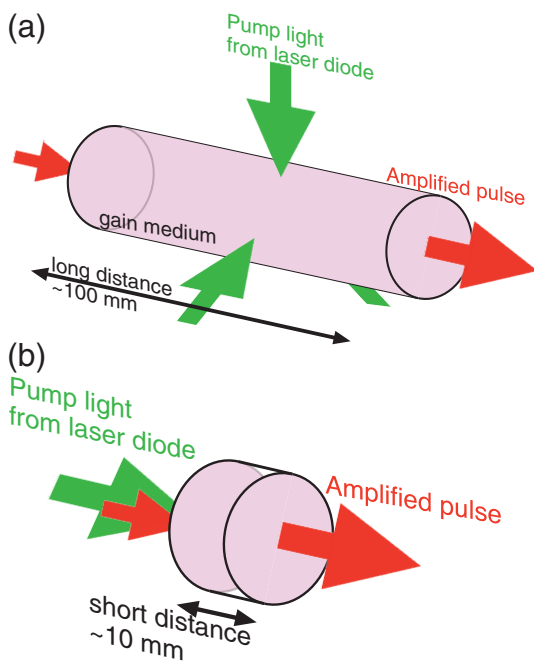


Fig. 5. Schematic of pumping geometry. (a) conventional side pump for long laser rod and (b) end pump for short laser disk

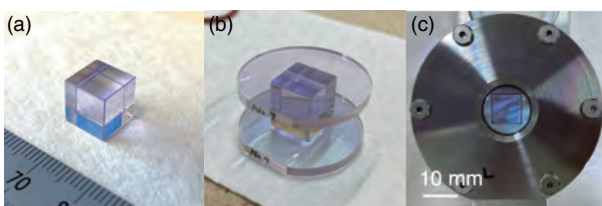


Fig. 6. Nd:YAG ceramic for power amplifier. (a) polished ceramic cube, (b) bonded ceramic cube with sapphire plates and (c) set in a water-cooling holder

3. The kicker system of the S line

The kicker is essential for the simultaneous single-pulse operation of the S1 and S2 areas. However, as shown in Fig. 7, the number of failures has increased in last few years. This could be due to MOS-FET degradation in the kicker power supply. Therefore, just before the start of the 2022B period, we replaced some MARX boards preventively by measuring the MOS-FET leakage current. However, many boards judged healthy in the preventive diagnosis failed in the 2022B period. As



Fig. 7. Number of MARX board failures that occurred in each operating period. Gray (yellow) bars represent the number of failures in the circuit that kicks the beam toward S1 (S2), respectively.

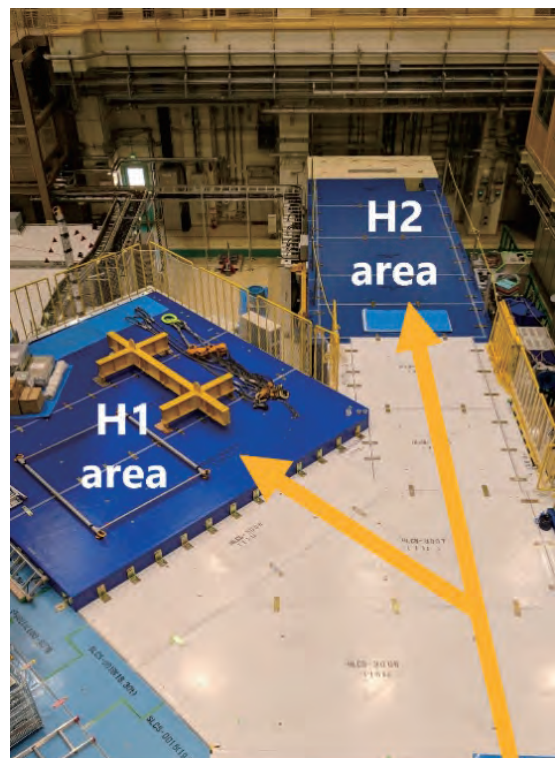


Fig. 8. Picture of the H-line after the H2 area construction.

a next countermeasure, we plan to replace the MOS-FET devices with modern SiC devices; we have already selected SiC devices and verified the operation of the power supplies alone. The replacement work will be done after clearing the technical issue of mixing the use of the SiC device with the existing MOS-FET.

4. The H2 area construction

The first branch of the H-line named the H1 area was completed in January 2022, and then the commissioning was performed. The intensity of the surface muons was measured and was almost the same as its design value (10^8 muons/s), despite the absence of a DC separator (or Wien filter) and the failure of the power supplies of the capture solenoids. Currently, the H1 area is open for users. In the second branch of the H line, the

H2 area, applying the technique developed in the U line, ultra-slow muons are produced and re-accelerated up to 4 MeV and will be the frontstage of the world's first muon accelerator. The beamline is planned to be extended further to produce a novel low-emittance muon beam by accelerating up to 212 MeV. The beam will be used in the measurement of the muon $g-2$ and electric dipole moment and the transmission muon microscope ($T\mu M$). A new building on the east side of the MLF is necessary to extend the beamline. The engineering design of the extension building will be finalized in the next fiscal year. The H2 area construction was completed in March 2023 and the self-radiation inspection was done in April (Fig. 8). The commissioning will be performed in the subsequent periods.

Technology Development Section

The technology development section has been developing a pulsed magnet system higher than 30 Tesla. After the high-intensity pulsed neutron beam became available at the MLF, we received requests from users to introduce pulsed-type high magnetic field equipment at the MLF. In order to make the equipment usable at several beamlines, we made it compact and movable [1]. Figure 9 shows the cross-section of the developed pulsed magnet equipment. It comprises a vacuum chamber, a closed-cycle refrigerator for sample cooling down to 4 K, and a nitrogen bath made of a rectangular cross-section stainless-steel (SUS) tube.

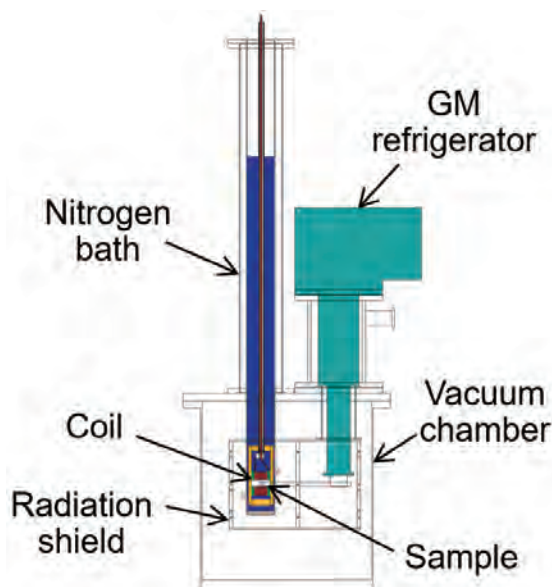


Fig. 9. Cross-section of the pulsed magnet equipment.

The coil is inserted in the nitrogen bath. It is immersed in liquid nitrogen to reduce the resistance and quickly remove the Joule heat generated by the pulsed current of the coil. Figure 10 depicts a photograph of the coil. A high-tensile strength Cu–Ag alloy with 1 mm ϕ (CA10-OPIWC-7, SWCC Showa Cable System Co., Ltd.) for the wire is used. The sum of the turns is approximately 200. The coil inductance and resistance at 100 Hz are 670 μ H and 100 m Ω at 77 K, respectively. The sample is attached to a 7 mm ϕ single-crystalline sapphire rod that is connected to the GM refrigerator and cooled down to 4 K through heat conduction. The sample is placed in the center of the coil. The scattering angle, 2θ , is 42 $^\circ$.

The pulsed magnet system was commissioned on NOBORU (BL10) as a demonstration [2]. A single-crystalline multiferroic $TbMnO_3$ [3] was used as a test sample. The change in the TOF spectrum of the Mn moments with and without a magnetic field was experimentally

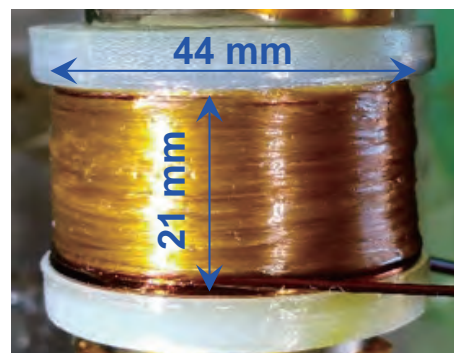


Fig. 10. Photograph of the coil.

validated. As shown in Fig. 11, the TOF spectra of the red and blue points are 0 and 30 Tesla, respectively. There are Bragg peak signals in Fig. 11 that correspond to the propagation wave vector (0, 0.28, 1) of the Mn moments at 0 T and (0, 0.25, 1) of it at 30 T. The TOF of the Bragg peaks are estimated to be approximately 10.25 ms and 10.4 ms using the Gaussian function, respectively. This result means that the magnetic field dependence of the diffraction peaks with and without a magnetic field was clearly observed using the pulsed magnet system.

References

- [1] M. Watanabe, H. Nojiri, J. Neutron Res. **21** 39 (2019).
- [2] M. Watanabe, T. Kihara, H. Nojiri, Quantum Beam Sci. **7** 1 (2022).
- [3] S. Quezel, F. Tcheou, J. Rossat-Mignod, G. Quezel, E. Roudaut, Physica B+C **86-88** 916 (1977).

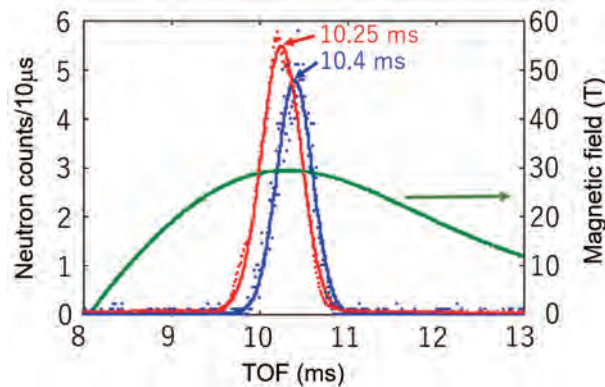
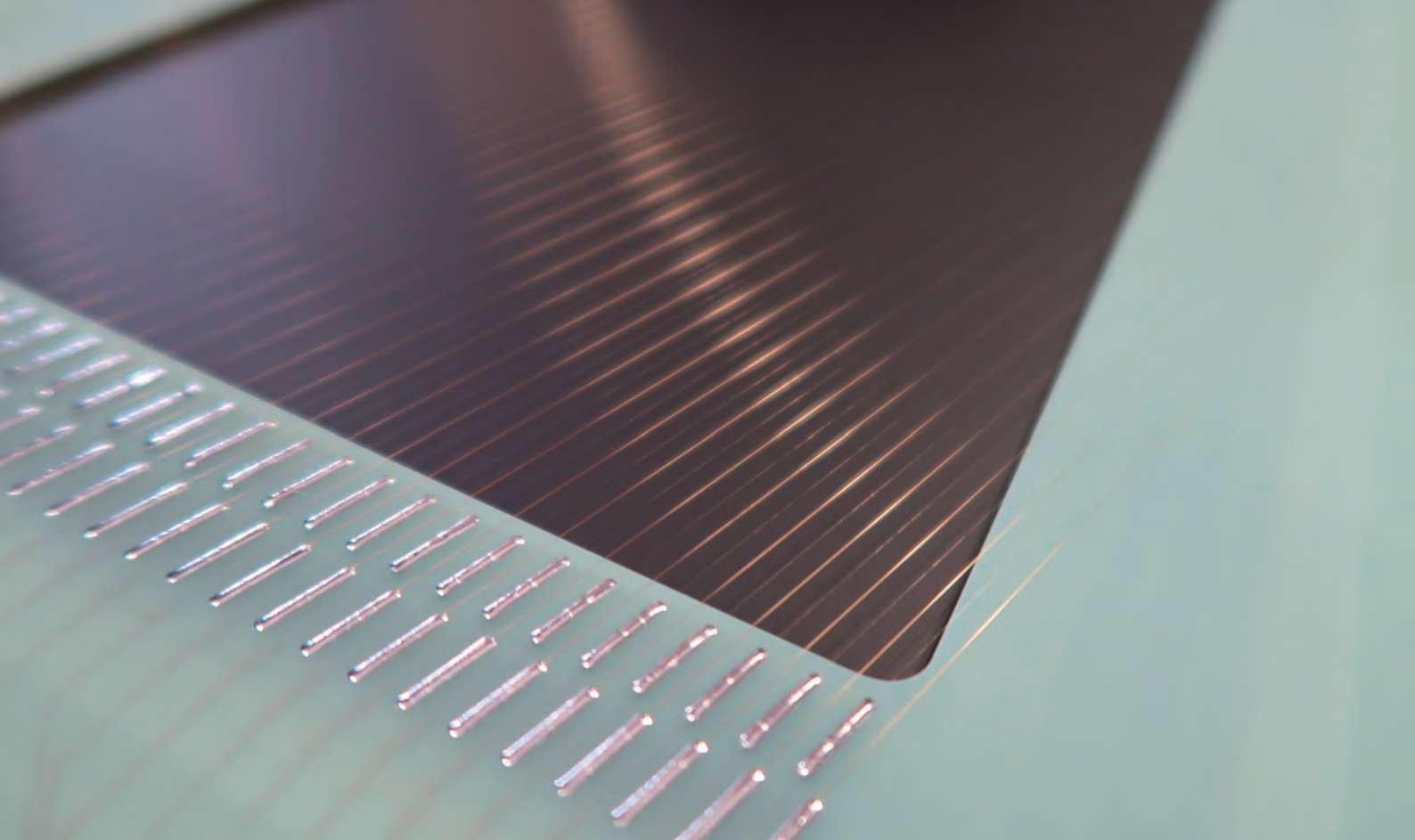


Fig. 11. TOF spectrum applied to the sample.



Particle and Nuclear Physics

Neutrino Experimental Facility

In FY2022, the Neutrino Experimental Facility continued to carry out maintenance and upgrade work started in FY2021. Although the upgraded neutrino beam was originally supposed to restart operation in the fall of 2022, the start date was delayed to early FY2023 due to the MR accelerator commissioning.

Various neutrino beamline upgrades towards accepting 750kW beam power were completed. Two of the three electro-magnetic focusing horns on the beamline were successfully replaced with new ones. The new horn 2 has an improved cooling scheme, and all horns are now compatible with an operation at a proton beam power of >1.3 MW. A new horn power supply, which was installed in FY2021, also allows the horns to run at a current of 320 kA, which improves the horn focusing power

by $\sim 5\sim 10\%$. An upgraded target cooling system was also installed, which allows the neutrino production target to withstand 750kW proton beam power. A new target designed to withstand >1.3 MW is also under development at Rutherford Appleton Laboratory in the UK.

Major upgrade work was also carried out for the near and far detectors of the T2K experiment during FY2022. For the near detector upgrade, a new tracking detector, SuperFGD, was assembled at J-PARC by a dedicated team of experts and shift people, as shown in Fig. 1.

The detector consists of ~ 2 million $1 \times 1 \times 1$ cm³ scintillator cubes read out in three dimensions by wavelength shifting fibers coupled to ~ 56 k photosensors. Two new High-Angle TPCs, as well as six new Time-of-Flight panels, were also assembled and tested at CERN and will be

shipped to J-PARC in FY2023. These new detectors will all be installed inside of the T2K ND280 near detector in FY2023.

The Super-Kamiokande detector was successfully doped with additional Gd, increasing the Gd concentration from 0.01% to 0.03%. This improved the neutron capture efficiency of the detector from 50% to 75%, without negative impact to the other detector measurement capabilities or parameters.

The Hyper-Kamiokande project is proceeding, as tunnel excavation for the far detector is progressing well and slightly ahead of schedule.

The quality of about 3,700 newly developed 50-inch photomultiplier tubes (PMTs), which are key components of the Hyper-Kamiokande detector, were inspected for mass production by the beginning of FY2022. PMT delivery will be re-started in early FY2023,



Fig. 1. SuperFGD during assembly.

and a total of 50-inch 20,000 PMTs will be installed in the tank by FY2026. Investigation of the Intermediate Water Cherenkov Detector candidate site, civil construction methods, and cost estimation is ongoing.

Hadron Experimental Facility (HEF)

Hadron Experimental Facility (HEF) was developed for the fixed-target experiments for particle and nuclear physics using secondary particle beams produced by slowly extracted (SX) high-intensity proton beam through the A-line from Main Ring (MR) synchrotron as well as the 30-GeV primary proton beam at the B-line. In FY2022, a new beam line (C-line) for COMET started its operation.

Technical paper on the currently using indirect water-cooled production target at the A-line which can accommodate 95 kW beam was published [1].

COMET Experiment

COMET aims to identify muon-to-electron conversion with a sensitivity higher than 10^{-14} . Intensive research and development were conducted in FY2022.

The C-line is the third primary beam line branched off from the B-line in the Hadron Experimental Hall. The 8 GeV proton beam is delivered through the C-line to a production target made of a thin graphite in the primary beam line area of the Hadron South Building (Fig.2 Left). Muons, decay products of pions produced backward are delivered to the experimental area (MU experimental area) through the transport system which currently comprises of a superconducting solenoid magnet called muon transport solenoid (MTS) and vacuum ducts.

The first beam of the 8-GeV protons was delivered to the C-line on February 8 (Fig. 2 Right). The commissioning

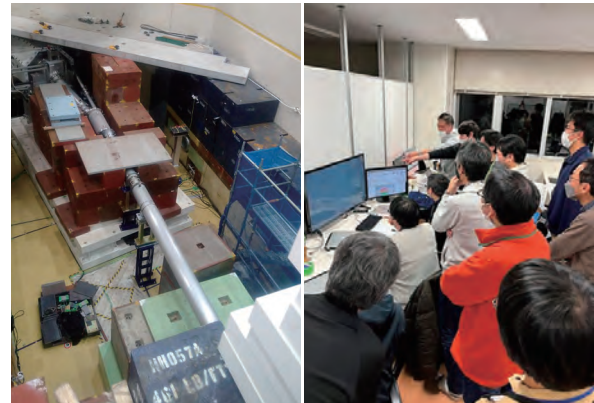


Fig. 2. (Left) C-line in the primary beam area in Hadron South Building. The 8-GeV proton beam is injected to the production target from the top. (Right) Researchers in the counting room at the first beam shot.

of the C-line and COMET engineering run were carried out on in February and March 2023 for 301 hours in total. After the facility inspection by a third-party organization on March 14, the change of the license as a radiation facility was officially approved on March 15.

Strangeness / Hadron Physics Experiments

Installation of detectors of a new particle spectrometer, S-2S, is in progress at K1.8. Reaction spectroscopy of the double-strangeness Ξ hypernucleus, $^{12}_{\Xi}\text{Be}$, (E70) and X-ray spectroscopy of Ξ^- -C atom (E96) are planned to be conducted using S-2S after S-2S commissioning in FY2023. Maintenance and reinforcement of detector

modules are also in progress at the high-p beam line (B-line) for the E16 experiment which aims to study in-medium mass modification of vector mesons and the generation mechanism of hadron mass.

Several results from the experiments were published in FY2022. The $\bar{K}N$ pole position of $\Lambda(1405)$ was newly determined by the E31 group conducted at K1.8BR in 2016 and 2017 [2] (see the highlight article for details). Commissioning of electron identification detectors for E16 was reported [3].

E40 conducted at K1.8 from 2018 to 2020 reported differential cross section for Σ^+p elastic scattering and the first trial to evaluate phase shifts of the 3S_1 and 1P_1 channels [4]. In the 3S_1 channel, a large repulsive core is predicted owing to the Pauli effect between quarks. The evaluated interaction in this channel is moderately repulsive.

The result of Ξ^- atomic X-ray spectroscopy was reported by E07 which aims to study the double strangeness system by stopping Ξ^- particles in the nuclear emulsion at K1.8 in 2015 to 2017 [5]. In this analysis, X-rays from Ξ^- -Ag and Ξ^- -Br atoms were measured in coincidence with the Ξ^- stop identification by the emulsion scanning. No clear peak was observed mainly due to statistics. However, they reduced successfully backgrounds by a factor of 1/170 by employing the Ξ^- stop identification.

KOTO Experiment

The KOTO experiment studies the decay of a long-lived neutral kaon into a neutral pion (π^0) and a pair of neutrinos. The process breaks CP symmetry directly and its branching fraction is theoretically well predicted in the Standard Model as $(3.0 \pm 0.3) \times 10^{-11}$. The detection of this decay is challenging because only two photons from π^0 are observable, and the decay mode has not been observed. By examining this ultra-rare decay, a new source of CP symmetry breaking that can explain

the matter-antimatter asymmetry in the universe may be revealed.

In FY2022, the analysis of the data taken in 2021 was intensively processed. In parallel, a search for pair-production of dark particles in a K_L decay, $K_L \rightarrow XX$ with $X \rightarrow \gamma\gamma$, was performed by using data taken in 2018, and the result was published [6]. For preparation of the next run, development of the new data acquisition that can accommodate a higher beam power and fabrication of a new charged particle detector with a better background rejection were carried out.

Future Plans of HEF

After the discussion at KEK Science Advisory Committee (SAC), the future plans of HEF, namely, the HEF Extension Project, was regarded as the first priority project to request new budget in the KEK Project Implementation Plan 2022.

The 3rd HEF-ex workshop on the HEF extension project was conducted at Tokai from March 14 to 16, using a hybrid style. The event featured 89 talks addressing both experimental and theoretical aspects of the latest physics research. Among the 188 participants, 59 were international, with 60 attending in-person, including 10 from abroad. This marked the first major in-person international workshop post-COVID-19, emphasizing the active and ongoing research in the HEF extension project across both experimental and theoretical domains.

References

- [1] M. Saito *et al.*, *Phys. Rev. Accel. Beams* 25, 063001 (2022).
- [2] S. Akikawa *et al.*, *Phys. Lett. B* 837, 137637 (2023).
- [3] S. Nakasuga *et al.*, *Nucl. Instr. Meth. A* 1041, 167335 (2022).
- [4] T. Nanamura *et al.*, *Prog. Theor. Exp. Phys.* 2022 093D01 (2022).
- [5] M. Fujita *et al.*, *Prog. Theor. Exp. Phys.* 2022 123D01 (2022).
- [6] C. Lin *et al.*, *Phys. Rev. Lett.* **130**, 111801 (2023).

Particle and Nuclear Physics Experiments at MLF

The JSNS2 experiment to search for sterile neutrinos had its second long-term data taking period, from January to June 2022, running with 800kW beam power. Also, the second phase of the experiment, JSNS2-II, received stage-2 approval from KEK/J-PARC. A new detector at 48 m from the target, outside of the MLF experimental hall, is under construction as shown in Fig. 3.

The IPNS muon and neutron group focuses on precision measurements using muons and neutrons. In 2022, they launched the KEK-PSI workshop on muon and neutron technology, with the inaugural workshop held virtually in April. The group is preparing to measure the anomalous magnet moment (g-2) and electric dipole moment (EDM) of muons at J-PARC MLF. They have successfully directed the surface muon beam to

the H1 area, with its commissioning confirmed through beam characteristics. Infrastructure changes, like radiation shielding and assembly of the H2 experimental area, are in progress for the muon $g-2$ /EDM experiments. Additionally, preparatory works outside the MLF building, including relocation of cables and water piping, have been completed. The building's area plan is being fine-tuned under the J-PARC working group.

The vacuum chamber, equipped with electrodes for the initial acceleration and transport of muons, and the IH-DTL acceleration cavity for the low-energy part of the RF accelerator were fabricated. The collaboration set up an experiment to demonstrate muon cooling by means of the resonant laser ionization of muonium atoms at the MLF S2 area. This experiment took data successfully until mid-March 2022. Developments of muon LINAC, injection system, storage magnet, magnetic field monitors, and positron detector has been carried out. The group published two technical papers about their work [1, 2]



Fig. 3. PPMT installation in the new JSNS² detector.

References

- [1] "Modeling the diffusion of muonium in silica aerogel and its application to a novel design of multi-layer target for thermal muon generation", C. Zhang *et al.*, NIM A 1042 167443 (2022).
- [2] "High-power test of an interdigital H-mode drift tube linac", Y. Nakazawa *et al.*, PRAB 25, 110101 (2022).

Theory Group

The mission of the theory group at the J-PARC branch is to investigate the theoretical aspects of particle and nuclear physics, in collaboration with the experimental groups at IPNS and J-PARC. At the same

time, it serves as a hub for gathering theorists and experimentalists in these fields. Several workshops on hadron physics were organized in FY2022.

Technical Support Group (Esys-Tokai)

The electronic systems group constructs electronic systems for IPNS/J-PARC and collaborates with other institutes through a framework, "Open-It." A variety of wide-bandgap semiconductors are intensively studied for applying to the COMET experiment at J-PARC.

The data streaming type high-resolution TDC (Str-HRTDC) was developed and implemented to the general-purpose FPGA module, AMANEQ. It was realized by several techniques, that is, the tapped-delay-line based FPGA HR-TDC, the heartbeat method defining the global time frame, and the clock distribution system,

MIKUMARI. The TDC can provide unique time stamp with 30 ps precision over 2.4 hours and continuously send the data to a PC with 10 Gbps using SiTCP-XG.

We developed the next generation DAQ software for the trigger-less data acquisition called NestDAQ. Its feature is the semi-automatic process connection topology. The complex multi-end topology can be generated with a small description in the configuration file. The load balancing is natively supported. We tested them at the RCNP Grand Raiden.

— Research Highlight —

Mass and Width of the $\Lambda(1405)$ Hyperon Resonance

Hadrons are composite particles constituted of quarks. They are classified into baryons and mesons. In the naïve quark model that preceded the standard model, a baryon is a bound state of three valence quarks while a meson is a bound state of a pair of a quark and an antiquark. Protons and neutrons (generally called nucleons) are the lightest baryons, from which various atomic nuclei are synthesized, which in turn form elements.

The ordinary visible matter that makes us up and surrounds us is made of the elements. Research on hadrons is challenging, especially the question of how hadrons are formed from quarks, which is the basis of the formation and evolution of matter in the universe (Fig. 4).

$\Lambda(1405)$ is one of well-known baryons as the first excited state of a Lambda (Λ) hyperon. It is an unstable (a very short-lived) resonance state that upon creation immediately decays into a π meson and a Sigma (Σ) hyperon. On the other hand, it has been argued for many years that $\Lambda(1405)$ is not an excited state of the simple orbital motion of quarks in a baryon, but a bound state of an anti- K (\bar{K}) meson and a nucleon (N). In the latter case, $\Lambda(1405)$ is regarded as a so-called exotic state, which contains an anti-quark in a baryonic system that does not fit the conventional hadron classification mentioned above. In this regard, $\Lambda(1405)$ has attracted the attention of researchers around the world for many years.

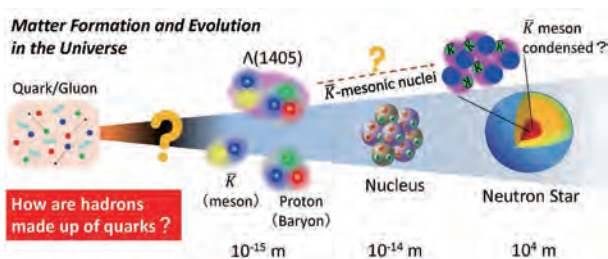


Fig. 4. Schematic illustration of matter evolution in the universe. “How are hadrons constituted of quarks?” is an important question sitting on the basis of the formation and evolution of matter in the universe. A better understanding of $\Lambda(1405)$ can improve our understanding of how ordinary visible matter has evolved since the Big Bang.

If we can directly synthesize $\Lambda(1405)$ by fusing \bar{K} and N , we should be able to obtain useful information on the $\bar{K}N$ interaction and the properties of $\Lambda(1405)$. However, since $\Lambda(1405)$ is lighter than the sum of \bar{K} and N masses, it cannot be synthesized by the direct fusion of \bar{K} and N in free space. This was a barrier to study the properties of $\Lambda(1405)$.

Using an intense, negatively-charged K -meson (K^-) beam provided at the K1.8BR beam line in the J-PARC Hadron Experimental Facility, we have carried out an experiment and succeeded in measuring the series of reaction processes to form $\Lambda(1405)$ [1], in which a deuteron, that is the bound system of a proton and a neutron, is impacted by K^- to knock out a neutron, and a recoil \bar{K} meson is slowed down and reacts with a residual N , as shown in Fig. 5. The recoil \bar{K} is a so-called off-shell kaon, whose mass differs from and can be lower than that in free space. Thus, we could produce $\Lambda(1405)$ via a fusion reaction of the off-shell \bar{K} and the residual N which is also off-shell.



Fig. 5. Schematic illustration of the reaction to form $\Lambda(1405)$. An incident K^- knocks out a neutron from a deuteron at a forward angle and a recoil off-shell \bar{K} (green circle) reacts with a residual off-shell N (thick blue circle) forming $\Lambda(1405)$.

We measured the $\pi\Sigma$ production cross section in the $K^-d \rightarrow n\pi\Sigma$ reaction as a function of the invariant mass of the final π and Σ state, as shown in Fig. 6 (a). The spectrum contains the scattering amplitude of the $\bar{K}N \rightarrow \pi\Sigma$ reaction. As a result of analyzing this reaction process according to the scattering theory in the $\bar{K}N$ and $\pi\Sigma$ coupled system, we were able to deduce $\bar{K}N \rightarrow \bar{K}N$ scattering amplitude and determine the mass and width of $\Lambda(1405)$, as shown in Fig. 6 (b). We found the mass of $1417.7^{+6.0}_{-7.4}(\text{fit})^{+1.1}_{-1.0}(\text{syst.}) \text{ MeV}/c^2$ and the half width of $-26.1^{+6.0}_{-7.9}(\text{fit})^{+1.7}_{-2.0}(\text{syst.}) \text{ MeV}/c^2$. This mass estimate is $13 \text{ MeV}/c^2$ heavier than $1405 \text{ MeV}/c^2$ which has been referred as the mass of $\Lambda(1405)$ so far.

Furthermore, we have shown that $\Lambda(1405)$ has a larger component of $\bar{K}N$ than that of $\pi\Sigma$. The latest theories suggest that there are two resonances coupled to $\bar{K}N$ and $\pi\Sigma$ at around the $\Lambda(1405)$ mass region. The $\Lambda(1405)$ observed so far might be superposition of the two resonances. The present result is consistent with the resonance coupled to $\bar{K}N$.

The results of the present research directly provide basic information on the interactions between \bar{K} and N as well as for understanding the properties of the recently discovered novel \bar{K} mesonic nucleus [2, 3]. The strength of the attraction between \bar{K} and N /nucleus affects the description of ultra-high-density nuclear matter, such as whether \bar{K} mesons are condensed in the core of a neutron star.

Reference

[1] S. Aikawa *et al.*, Phys. Lett. B 837, 137637 (2023).

[2] S. Ajimura *et al.*, Phys. Lett. B 789, 620 (2019).

[3] T. Yamaga *et al.*, Phys. Rev. C **102**, 044002 (2020).

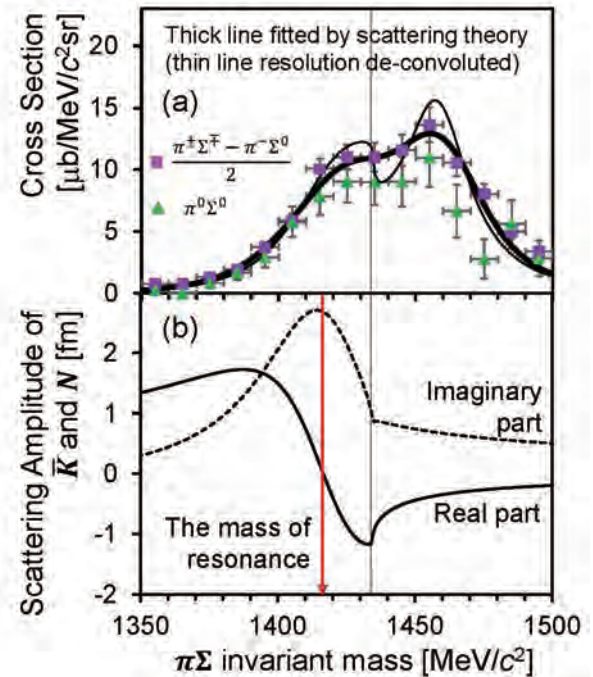


Fig. 6. (a) Measured $\pi\Sigma$ production cross section in the $\bar{K}d \rightarrow N\pi\Sigma$ reaction as a function of the invariant mass of $\pi\Sigma$. Squares and triangles were obtained from different charge states of π and Σ . The vertical line indicates the location of the sum of \bar{K} and N masses. The measured spectrum was reproduced by scattering theory (solid lines, see description in the figure). (b) Deduced $\bar{K}N \rightarrow \bar{K}N$ scattering amplitude. When the real part (solid line) crosses 0, the imaginary part (dashed line) reaches its maximum value. These are typical line shapes in the case that a resonance state exists. The arrow indicates the location of the mass of the resonance state.



Cryogenics Section

Overview

The Cryogenics Section supports scientific activities in applied superconductivity and cryogenic engineering, carried out at J-PARC. It also supplies cryogen of liquid helium and liquid nitrogen. The support work includes maintenance and operation of the superconducting magnet systems for the T2K neutrino beamline and

the muon beamlines at the Materials and Life Science Experimental Facility (MLF) and construction of the magnet systems at the Hadron Experimental Facility (HEF). It also actively conducts R&D works for future projects at J-PARC.

Cryogen Supply and Technical Support

The Cryogenics Section provides liquid helium cryogen for physics experiments at J-PARC. The used helium is recycled by the helium gas recovery facility at the Cryogenics Section. Figure 1 summarizes the liquid helium supply in FY2022.

Liquid nitrogen was also supplied to the users for

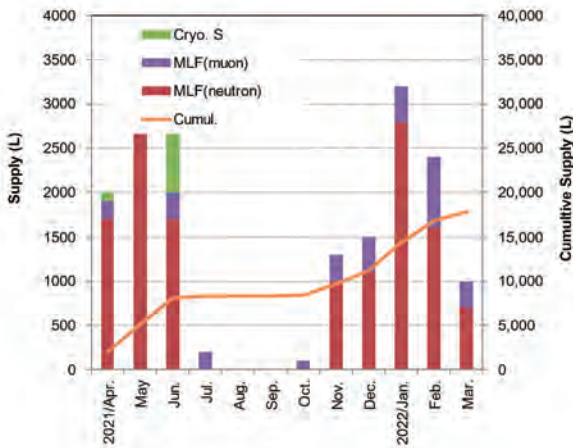


Fig. 1. Liquid helium supply at J-PARC from April 2022 to March 2023.

their convenience. Its amount in FY2022 is summarized in Fig. 2. The MR has been shut down until the end of 2022, but the heavy user of cryogen is MLF user, therefore the amount of cryogen usage did not change that much compared with the last year.

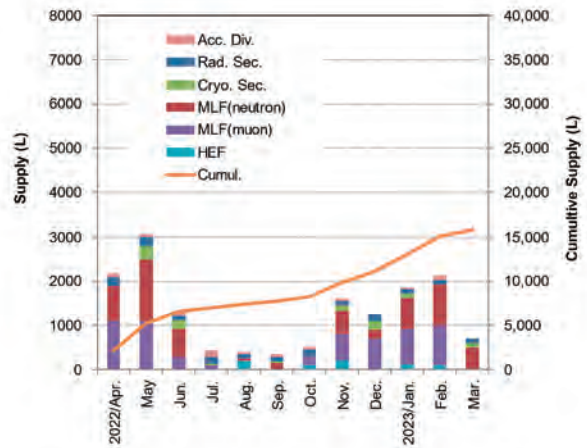


Fig. 2. Liquid nitrogen supply at J-PARC from April 2022 to March 2023.

Superconducting Magnet System for T2K

Table 1. Operation history of the T2K superconducting magnet system.

	2022								2023				
	April	May	June	July	Aug.	Sept.	Oct.	Nov.	Dec.	Jan.	Feb.	Mar	April
Operation									↔				↔
Maintenance						↔			12/12-12/28				4/3-4/27

The superconducting magnet system for the T2K experiment operated during the periods shown in Table 1. The system worked well without disturbing the beam time. The operation time was only 16 days in December and regular maintenance works were carried out in the autumn. Figure 3 summarizes the incidents in the refrigeration system from FY2009, which shows that the magnet system has been quite stable.

Table 1. Operation history of the T2K superconducting magnet system.

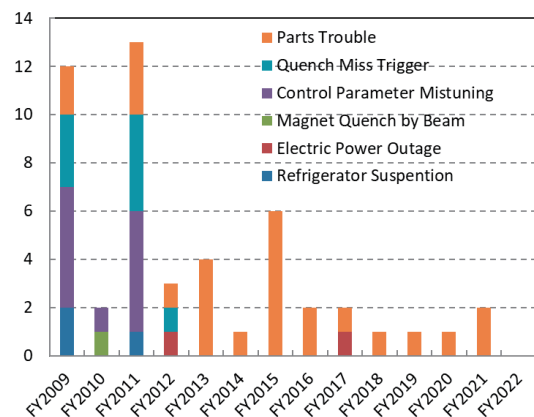


Fig. 3. Summary of incidents in the Refrigerator system for T2K.

Superconducting Magnet Systems at the MLF

The Cryogenic Section contributes to the operation and maintenance of the superconducting magnet systems at the Muon Science Facility (MUSE) in the MLF. The superconducting solenoid in the Decay Muon Line (D-line) was operated from January 11 to July 4 2022. Annual maintenance, such as exchange of the second oil separation filter, safety valve maintenance and so on, was performed from July to the end of October.



Fig. 4. Exchange work of the second oil separation filter.

Superconducting Magnet Systems at the HEF

The COMET experiment is under construction in the Hadron South Experimental Hall (HDS) of the Hadron Experimental Facility (HEF). The Cryogenics Section was involved in the construction of the superconducting magnets and cryogenic system. The COMET magnet system consists of a pion capture solenoid (PCS), a muon transport solenoid (MTS), a bridge solenoid (BS), and a detector solenoid (DS). The MTS and BS magnets have already been delivered to J-PARC. The PCS and DS magnets are under construction at their respective factories. In the winter of 2022, the J-PARC accelerator provided a beam for the COMET experiment with a simple secondary beamline configuration using only MTS called Phase- α .

The MTS completed the connection of the current lead box and cold box via the transfer tube in FY2021, and commissioning have been performed to confirm the soundness of the system and magnetic field measurement. During the first commissioning, the circuit was shut down due to the movement of the coils and the instability of the power supply, finally, the staff succeeded in realizing current transport up to 130 A for solenoid and 175 A for dipole without quench. The magnetic field maps of the solenoid and dipole were measured using three-axis Hall probes on a cart. Figure 5 shows a photograph of the cart with the Hall probe mounted and Figure 6 shows a comparison between the measurement result and the simulation by OPERA of the solenoid field at the center of the muon beam axis in case of the transport current of 105 A.

Measured data at the center of the muon beam axis are in good agreement with a field calculated by OPERA.

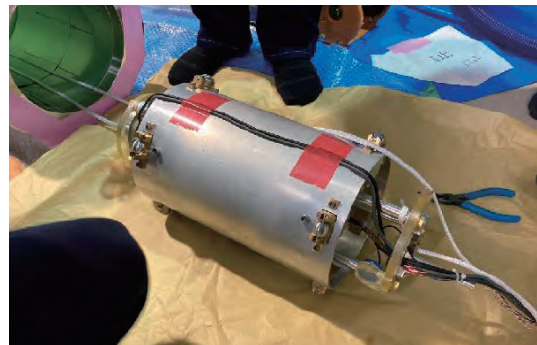


Fig. 5. A photograph of the cart with the Hall probe mounted.

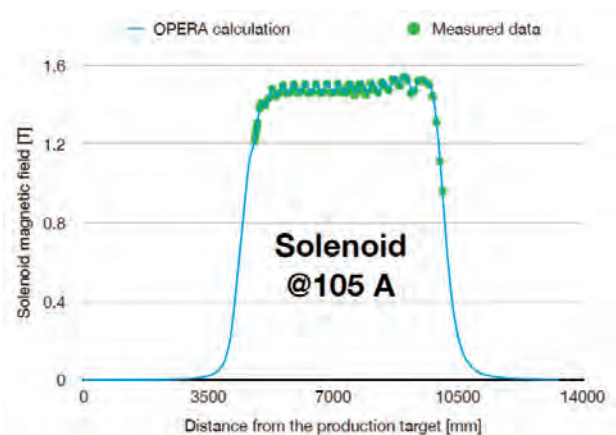


Fig. 6. A comparison between the measurement and the simulation of the solenoid field in case of the transport current of 105 A.

The MTS was operated for the COMET Phase- α experiment. The large eddy current and force had current rating of 105 A limited to half for solenoid corresponding to a magnetic field of 1.5 T due to unconfirmed additional support soundness. During the beamtime, MTS kept the excitation for a total of 319 hours without shutdown.

The commissioning of MTS aimed at generating a 3 T solenoid field was performed after the beam time for Phase- α . We succeeded in the combined current transport for Phase-I experiments of 210 A for solenoid (3 T), ± 175 A for dipole (± 70 mT), and -21 A for suspension using TS3 coil.

The PCS and MTS magnets are conductively cooled to around 4 K by two-phase flow helium supplied from a helium refrigerator having two turbines. We conducted a cooling and excitation test of the transport magnet system until the first half of the fiscal year. The transport solenoid reached a steady cryogenic state 21 days after the start of precooling. Figure 7 shows the precooling curves of the transport magnet system. TS-3 and TS-2a are the magnets farthest from the helium cooling pipe, and TS-3 has a larger cold mass than the other magnets, therefore TS-3 takes a longer time to reach a steady state. After the magnet reached a steady state, various interlock tests were conducted to confirm

the soundness of the control system. After that, excitation and shutdown tests were carried out. An automatic control system for various operations, such as precooling, warm-up, quench recovery and re-cooling was established through a series of the cooling and excitation tests. After local construction for Phase- α and completion inspection based on high pressure gas regulation, cooling operation for the Phase- α started in mid-December 2022. The cooling system, including the transport solenoid, operated without any trouble for about three months until the end of the experiment in mid-March.

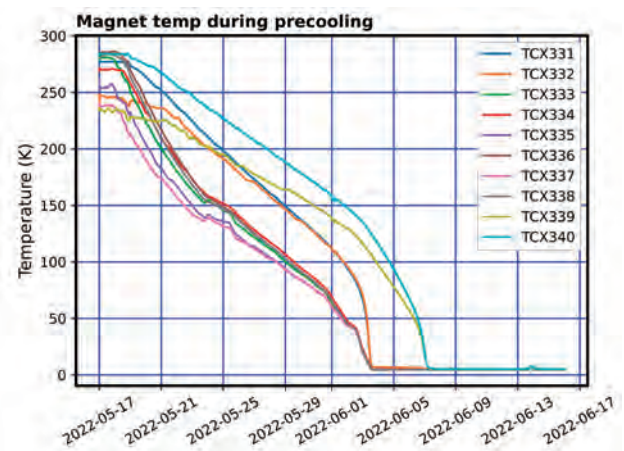


Fig. 7. Precooling trend of the transport solenoids

R&D for the Future Projects at J-PARC

The g-2/EDM project aims for the precise measurement of the anomalous magnetic moment and the electric dipole moment of muons. This experiment was proposed at the MUSE H-Line. A superconducting solenoid with a high field homogeneity, better than 1 ppm locally, plays a very important role as a muon storage ring. The kicker coil is installed inside the magnet bore to store the muon beam around the magnet center.

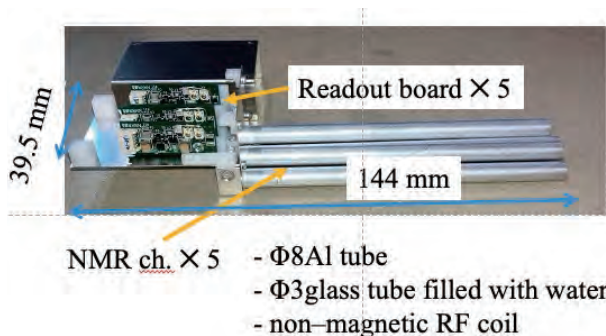


Fig. 8. Prototype of magnetic field distribution measurement system for g-2/EDM experiment.

The study of kicker coil showed to require Cu busbars for supplying current, meaning that vertically straight holes in the bottom iron yoke plate are necessary. The yoke design is now being optimized in terms of magnetic field homogeneity even in the vertical asymmetry of yoke structure.

The prototype of magnetic field distribution measurement system has been developed. Figure 8 shows the prototype of the system.

Applied research based on REBCO (rare-earth barium copper oxide) exhibiting high temperature superconductivity is underway to realize the future pion capture system for the muon beamline of MLF second target station (TS2-PCS). The TS2-PCS magnet will be required to operate in extremely high radiation environments where the absorbed dose reaches 130 MGy. In such an environment, conventional organic insulating methods, such as epoxy resin, will not be

applicable. Therefore, we have been developing the mineral insulated HTS coils to which ceramic coating and ceramic bonding technology are applied. As a result of research and development so far, we succeeded in molding a ceramic insulating layer of about 20 μm thickness on both sides of a tape-shaped conductor with a thickness of 0.1 mm and a width of 4 mm over a length of 40 m using a continuous spray and drying method. The about 20 μm thick-insulating layer composed of a one-to-one ratio of aluminum oxide and silicon dioxide has been confirmed to have a withstand voltage of 2 kV. In FY2022, three seamless double pancake type racetrack coils with a straight section length of 300 mm and a width of 20 mm were wound based

on a coated 4 mm wide tape conductor by a so-called wet winding method using a ceramic adhesive. Figure 9 shows a picture of wound mineral insulated racetrack coil based on REBCO coated conductor. These coils will be assembled with external supports for reinforcement and copper stabilizers with ceramic adhesive, and will be fitted with voltage taps and Hall sensors. As part of U.S.-Japan Science and Technology Cooperation Program in High Energy Physics, they will then be sent to Brookhaven National Laboratory in the United States for performance evaluation tests in a liquid helium immersion-cooled test stand with a back-up field of approximately 10 T.

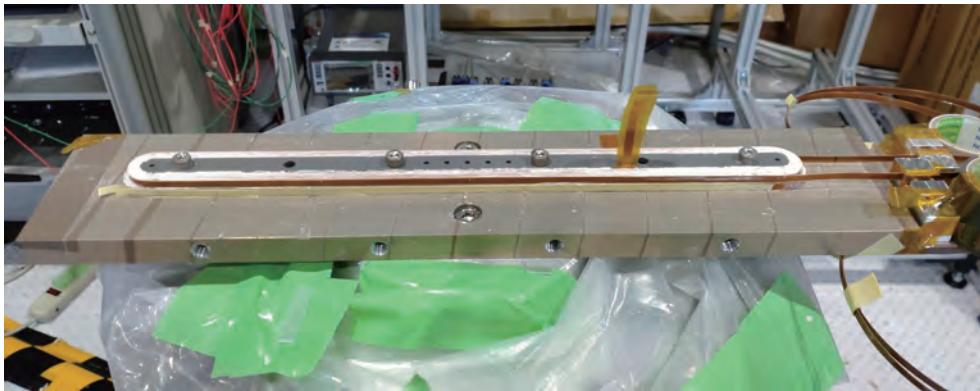


Fig. 9. A picture of wound mineral insulated racetrack coil based on REBCO coated conductor.



Information System

Overview

The Information System Section plans, designs, manages, and operates the network infrastructure of J-PARC and also provides support to ensure its information security. In terms of computing, until now, J-PARC has owed its major computer resource for analyzing

and storing data from neutrinos, nuclear physics and MLF experiments to the KEK central computer system. The section connects the J-PARC network to the KEK central computing system directory and helps the users to utilize the system effectively.

Status of Networking

Since 2002, the J-PARC network infrastructure, called JLAN, has been operated independently from KEK LAN and JAEA LAN in terms of logical structure and operational policy. In 2022, the total number of hosts on JLAN exceeded 5,800, which has increased by 36 hosts in this year. The growth curve of edge switches,

wireless LAN access points and hosts (servers and PCs) connected to JLAN are shown in Fig. 1.

In April 2022, the National Institute of Informatics (NII) upgraded SINET (Japan Science Information Network <https://www.sinet.ad.jp>) from version 5 to 6. SINET is not only a gateway from JLAN to the internet

but also an important connection between the Tokai and the KEK Tsukuba sites in J-PARC.

Figures 2 and 3 show the network utilization of the internet from/to JLAN. Since the bandwidth capacity for the internet through the SINET is 10 Gbps (Giga-bits per second), it is clear that there is enough space for

additional activity. Figures 4 and 5 show the statistics of data transfer between the Tokai and Tsukuba sites. The network bandwidth capacity between the two sites is 20 Gbps. This shows that the usage level has been approaching half of its capacity, especially during the period when the Hadron and g-2 facilities were running.

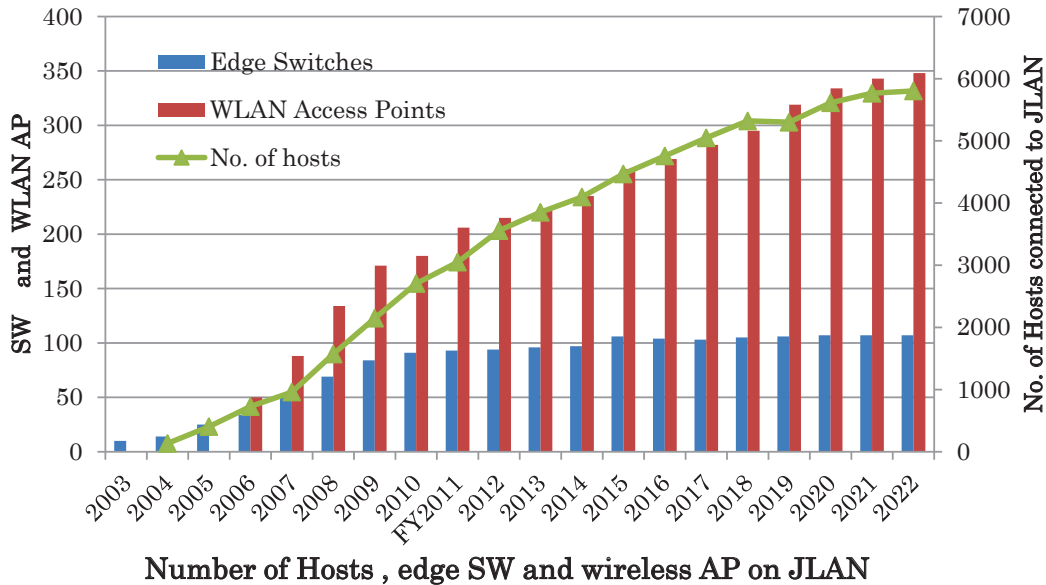


Fig. 1. Number of hosts, edge SW and wireless AP on JLAN.

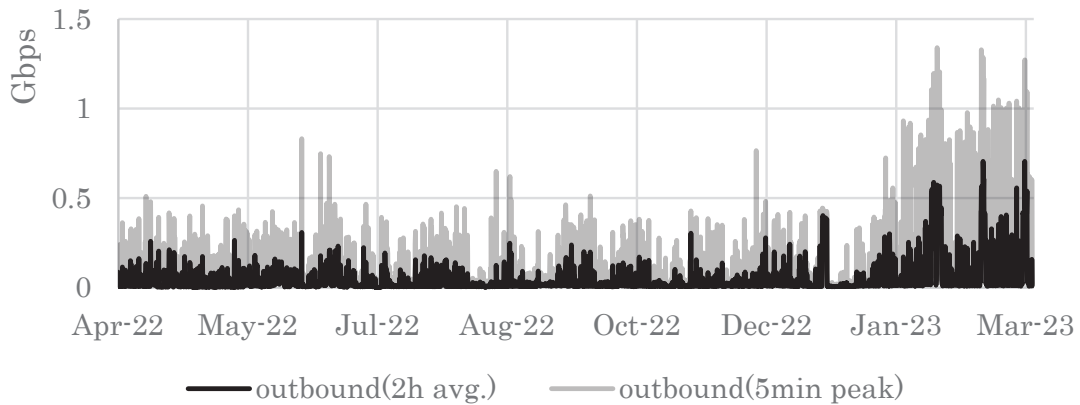


Fig. 2. Network traffic from JLAN to the internet. (1 hour average and 5 minutes peak value)

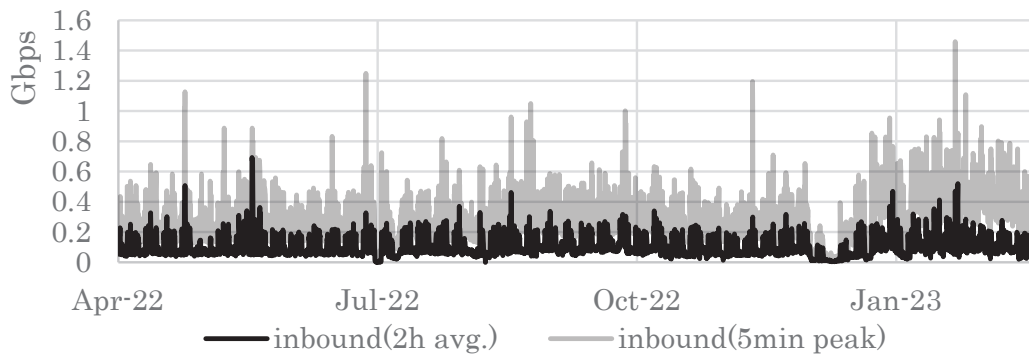


Fig. 3. Network traffic from the internet to JLAN.

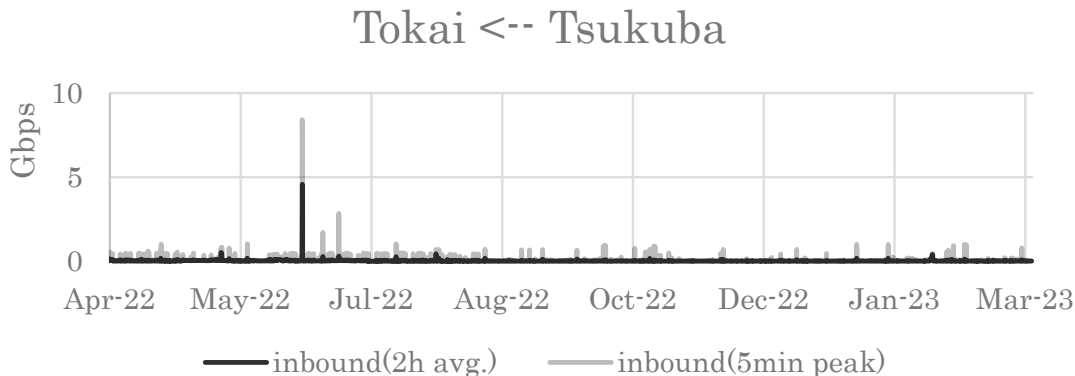


Fig. 4. Network traffic from the Tsukuba to Tokai sites.

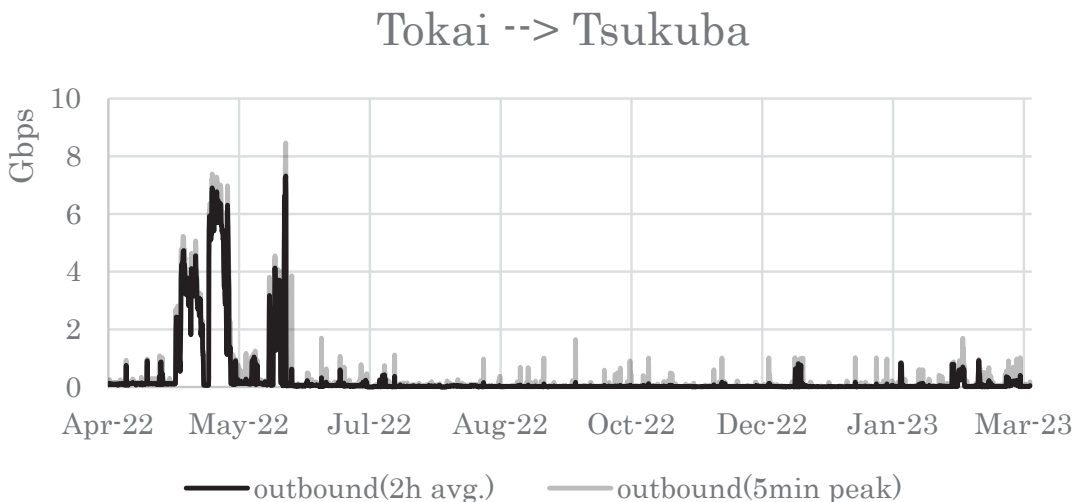


Fig. 5. Network traffic from the Tokai to Tsukuba sites.

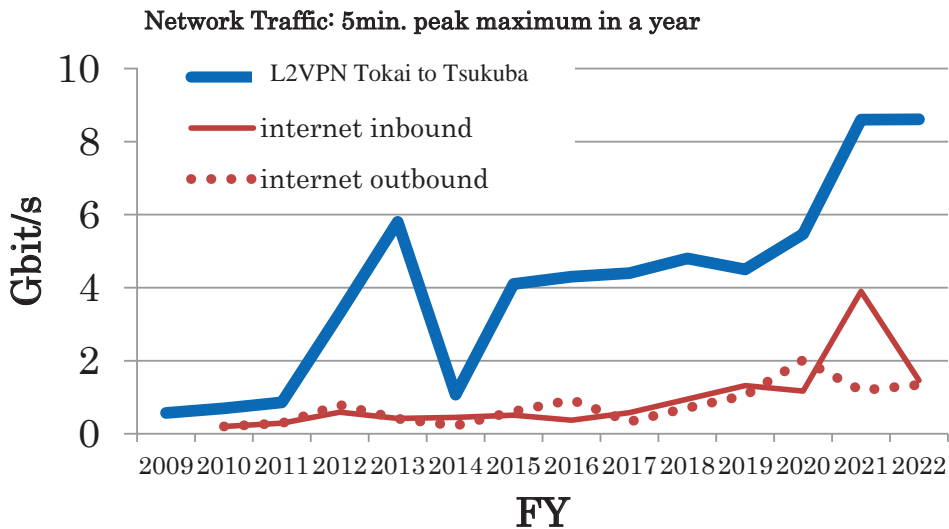


Fig. 6. Peak network traffic for the recent years.

Internet Connection Services for Visitors and Public Users of J-PARC

Since 2009, J-PARC had offered a Guest Network (GWLAN) service, which is a wireless internet connection service for short-term visitors, available in almost all J-PARC buildings. In the end of 2014, additional network service called User LAN had started. To use the GWLAN, users are required to receive a password at the J-PARC Users Office beforehand, while in the User LAN, they are authenticated by the same ID and password for the User Support System, which is also used for dormitory reservation and so on. From March 2016, a new

service called “eduroam” had been started. The eduroam (<https://www.eduroam.org/>) is a secure roaming access service developed for the international research and education community and mutually used among a huge number of research institutes, universities, and other institutions around the world. The eduroam service will be a convenient third option of internet connection service for J-PARC visitors. Figure 7 shows this fiscal year’s usage statistics of GWLAN, User LAN and eduroam services.

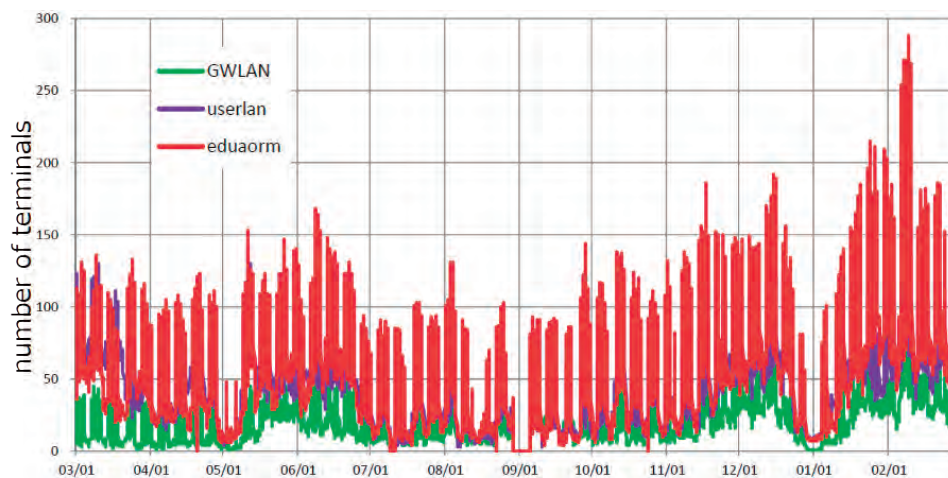


Fig. 7. Usage trends of GWLAN, User LAN and eduroam.

Status of Computing

Table 1. Computing resources in the KEKCC.

CPU (Intel Xeon Gold 6230)	15000 cores
RAID Disk (GPFS)	25.5 Peta Bytes
Tape Library (HSM)	100 Peta Bytes

Since J-PARC does not have computing resources for physics analysis, starting from 2009, the KEK central computing system (KEKCC) at the KEK Tsukuba campus has been mainly used for that purpose. KEKCC is shared by most of the research groups of KEK, including J-PARC. At the Neutrino (T2K), Hadron and Neutron (MLF) experiments, the data taken in J-PARC are temporarily saved at their facilities and then promptly transferred, stored, and analyzed at the system in Tsukuba. The storage of

the system is also utilized as a permanent data archive for their data. The third upgrade of the system was completed in 2020, and the computing resources are shown in Table 1. Figures 8-10 show the utilization statistics of the computing resources in FY2022. The main users who used the CPU and storage constantly were from the Hadron and Neutrino experiment groups. The MLF group also started to store data to tapes on the system.

CPU Utilization

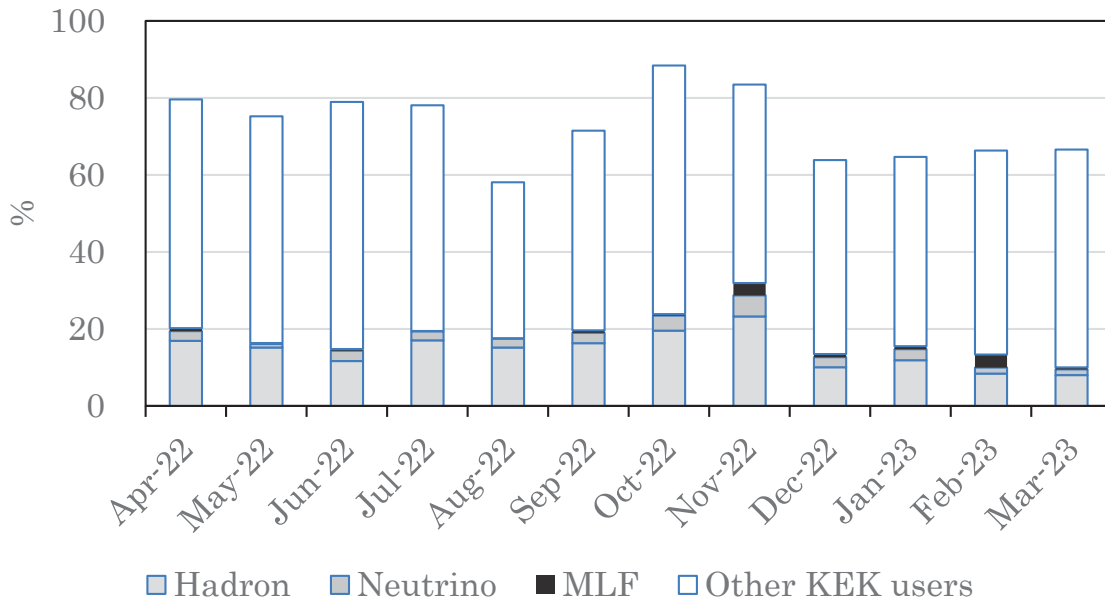


Fig. 8. CPU usage statistics of KEKCC in FY2022.

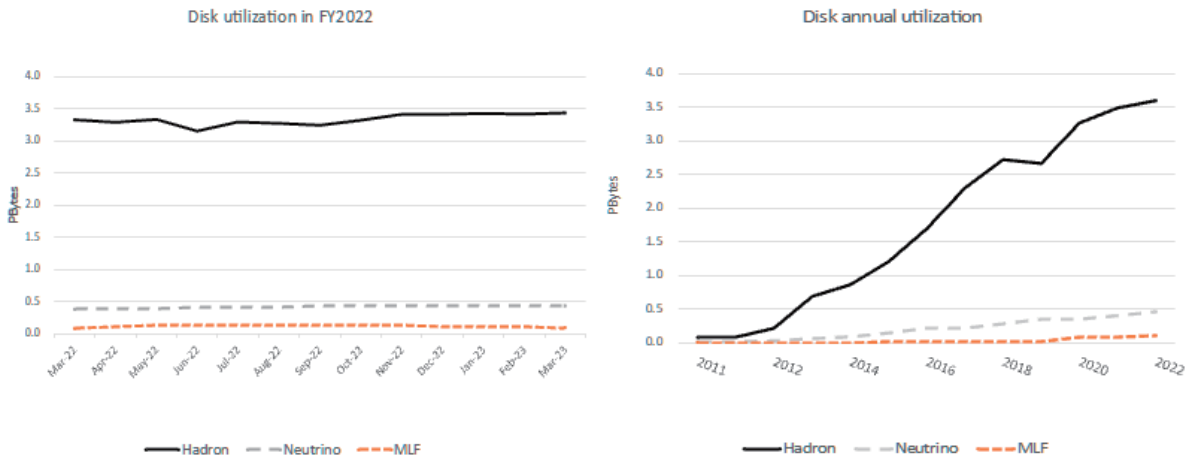


Fig. 9. Disk usage statistics (left: trend of FY2022; right: annual trend)

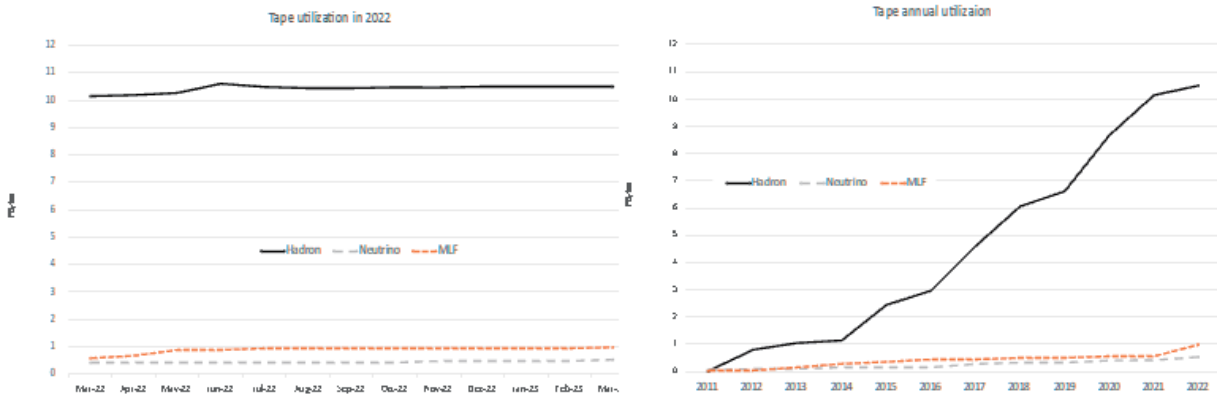


Fig. 10. Tape library usage statistics (left: trend for FY2020, right: annual trend)



Transmutation Studies

Overview

We are developing nuclear transmutation technology with accelerator-driven systems (ADS) using the J-PARC's research resources and expertise in high-power accelerator and target technologies. The ADS is an effective nuclear system for volume reduction and mitigation of harm caused by high-level radioactive waste produced in nuclear power reactors. We believe that the ADS is one of the most beneficial applications of high-power accelerators for contributing to human society such as the carbon neutrality and SDGs.

We have developed the J-PARC Transmutation Experimental Facility (TEF). One of the two individual facilities of TEF is the ADS Target Test Facility (TEF-T) for irradiation of beam window materials in a flowing high-temperature lead bismuth eutectic (LBE) alloy target. The baseline design of TEF-T is available in the design report JAEA-Technology 2017-003. The future direction of TEF

was discussed in the Partitioning and Transmutation Technology Evaluation Task Force (TF) established by the Ministry of Education, Culture, Sports, Science and Technology (MEXT) in 2021. In accordance with the TF's conclusion, the future policy of TEF planning was stated in the JAEA's mid- to long-term plan (MLTP) as follows; "Regarding the J-PARC TEF program, JAEA reframes the facility plan based on the results of related R&D and versatile needs to the facility in addition to nuclear transmutation research." Now we are building up the facility concept to comply with the MLTP.

On July 28, 2022, a workshop on "J-PARC Proton Beam Irradiation Facility Plan and Establishment of Its User Community" was held. There were 133 participants, with 14 in-person and 119 online. After addressing the importance of nuclear transmutation and the current status of the facility planning, needs of the potential

users of the facility were presented from four areas, i.e., material damage, semiconductor soft error testing, radioisotope production for medical applications, and proton beam applications. Then, a user community of the facility was launched. A questionnaire survey of participants' areas of interest revealed that they have high expectations for the proton beams available in the facility in many areas in addition to the nuclear transmutation research. As a part of the initial activities of the user community, users' expectations from the facility in the four areas have been summarized in a document of six pages, and the user community submitted it to J-PARC in April 2023. The latest facility concept with incorporating the users' needs is shown in Fig. 1.

As for the R&D activities on the lead-bismuth target technology, the third campaign of materials corrosion

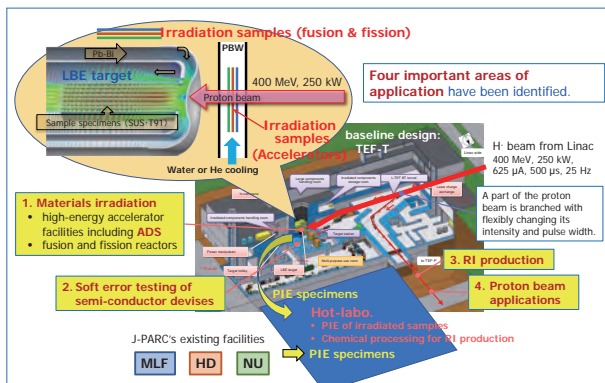


Fig. 1. The latest facility concepts.



Fig. 2. From left, Drs. Yosuke Iwamoto, Hiroki Iwamoto, Shin-ichiro Meigo and Daiki Satoh.

test for 7,000 hours under oxygen concentration controlled high-temperature lead-bismuth flowing using the OLLOCHI loop was completed successfully in October 2022. Sample steel specimens are under examination.

As for the R&D activities on the proton beam technology, a series of measurements of neutron production yields from iron, lead and bismuth targets bombarded by a 107-MeV proton beam provided by the fixed-field alternating gradient accelerator at Kyoto University was completed. A research paper describing the measured data in comparison with theoretical simulation calculation results published in Journal of Nuclear Science and Technology [1] has been awarded the paper prize by the Atomic Energy Society of Japan in March 2023 (Fig. 2).

In addition, the basic design of a super-conducting linac for ADS with introducing the fault tolerant capability has been completed. Assembling of a super-conducting spoke cavity for ADS's linac by electron beam welding has progressed.

In February 3, 2023, the ninth TEF Technical Advisory Committee (T-TAC) was held online. J-PARC staff reported the progress in the facility planning and their R&D activities on the ADS development. The main conclusion for the facility planning was as follows: "T-TAC encourages to further capture on a regular base the needs of potential user's communities also at an international level as well as to involve these communities in the progress of the realization of the whole facility while continuously analyzing the complementarity of the facility regarding other existing or projected infrastructures."

Reference

- [1] H. Iwamoto, *et al.*, Measurement of 107-MeV proton-induced double-differential thick target neutron yields for Fe, Pb, and Bi using a fixed-field alternating gradient accelerator at Kyoto University, *J. Nucl. Sci. Technol.* 60 (4) (2023) 435–449. doi:10.1080/00223131.2022.2115423.

Research and development

Lead-bismuth target technology development

Management of the Lead-bismuth eutectic (LBE) is one of the key issues of the ADS. At J-PARC, various research activities, such as operation of a corrosion test loop "OLLOCHI", operation of a spallation target mockup loop "IMMORTAL", and development of various sensors for LBE are underway.

1. OLLOCHI

The third campaign of long-term corrosion test in OLLOCHI (Oxygen-controlled LBE LOop Corrosion tests in High-temperature) [1] for 7,000 hours, which corresponds to the yearly operating hours of the ADS, started in October 2021 and completed in October 2022. Test conditions of the third campaign were as follows: the

maximum temperature and the temperature difference were 450°C and 100°C, respectively. The flow rate was about 1 m/s at the specimens' position. The oxygen concentration (OC) was kept at 1×10^{-6} wt%. The tested specimens were taken out from the specimen holders and are being observed.

After the third campaign of the corrosion test, we started the fourth one in March 2023. The total operation period was about 2,000 hours. Prior to testing, pre-oxidation operation was conducted at 500°C for 168 hours in LBE at near saturated OC. The OC was then adjusted to 1×10^{-6} wt%. The maximum temperature and temperature difference were 500°C and 100°C, respectively. The flow rate was about 1 m/s at the specimen position.

Observation and analysis for specimens of the first campaign have progressed. Test conditions of the first campaign were as follows: the maximum temperature and the temperature difference were 450°C and 100°C, respectively. The flow rate was about 1 m/s at the specimens' position. The OC was kept at 1×10^{-6} wt% and the test duration was 2,000 hours. As an example, SEM images for cross sectional observation after the

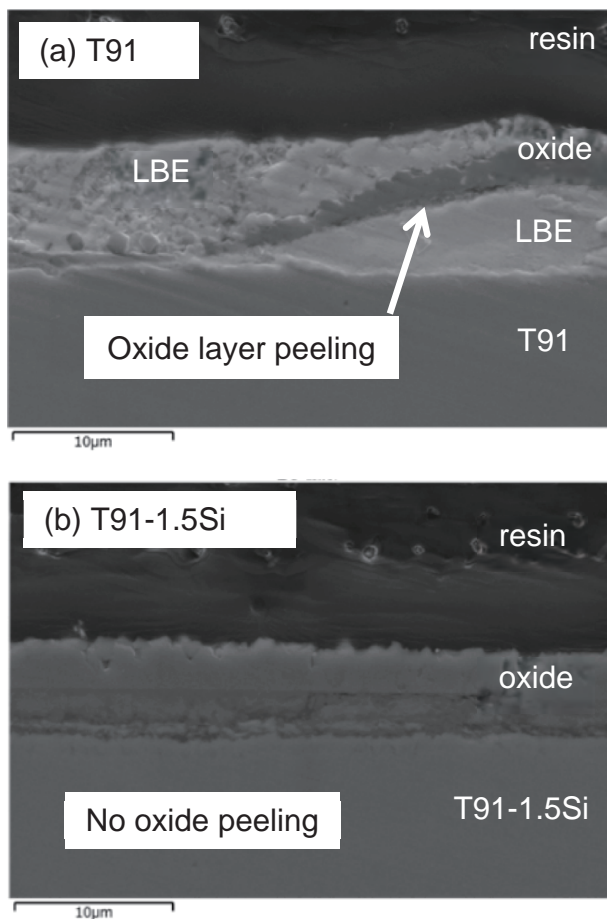


Fig. 3. SEM images for cross sectional observation of (a) T91 and (b) Si-added T91 after the corrosion test.

corrosion tests for (a) T91 (Mod.9Cr-1Mo steel) and (b) Si-added T91 are shown in Fig. 3. For the T91 specimen, the oxide layer is peeled off and Pb and Bi are revealed under the oxide layer. For Si-added T91, no oxide peeling and no Pb and Bi under oxide layer are observed. These results indicate that Si addition could suppress the Pb/Bi penetration and oxide peeling.

2. IMMORTAL

IMMORTAL [2] is a mockup loop of the LBE spallation target in TEF-T. In the loop, LBE, pressurized water, and air were employed as coolants for primary, secondary, and ternary systems, respectively. LBE, a low Prandtl number fluid, shows different heat transfer behavior in comparison with common fluids, such as water. However, experimental data to evaluate its heat transfer are scarce due to the difficulty of experimental measurement. Therefore, we have measured the turbulent heat transfer of lead-bismuth in a circular flow channel with pressurized water as the secondary coolant using a heat exchanger of IMMORTAL.

Figure 4 represents the relationship between the Nusselt number and Peclet number, which are commonly used to evaluate heat transfer. Two recommended correlations for LBE given in the literature [3] are presented in the figure. Originally, these correlations have been proposed for the sodium heat transfer. In our experiments, the provided heat input into LBE was set to 21 kW. The obtained experimental data showed a correlation close to the equation proposed by Seban-Shimazaki. In FY2023, we plan to extend the experimental data and propose a heat transfer correlation dedicated to LBE flow in a circular channel. subsequently, we are also planning to perform experiments on transient phenomena, such as a loss of flow accident.

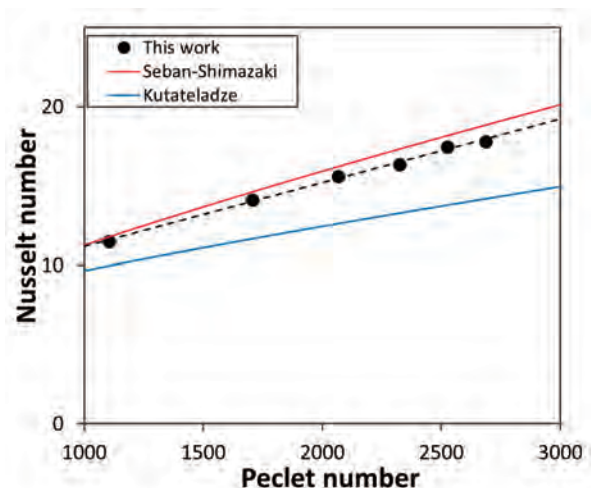


Fig. 4. Relationship between the Nusselt number and Peclet number

References

- [1] S. Saito, *et al.*, Development of High Temperature LBE Corrosion Test Loop "OLLOCHI", JAEA-Technology 2021-034, (2022), 94p. DOI:10.11484/jaea-technology-2021-034
- [2] H. Obayashi, *et al.*, Development of Mock-up Test Loop (IMMORTAL) for LBE Spallation Target, JAEA-Technology 2021-035, (2022), 66p. DOI:10.11484/jaea-technology-2021-035
- [3] Handbook on Lead-bismuth Eutectic Alloy and Lead Properties, Materials Compatibility, Thermal-hydraulics and Technologies – 2015 Edition, (2015), 950p. NEA. No. 7268,

Super-conducting linac development for ADS

1. Extraction system for the ion source

The ion source is necessary for particle accelerators since it provides the particles that are accelerated downstream. In general, the ion sources consist of two components, namely, a plasma generator and an extraction system. The plasma generator provides the required ions, and the extraction system shapes the beam with the required size and orientation for the next section. As a first step to complete the ion source design, we concentrated on the extraction system.

To ensure optimal functioning of ADS linacs, high availability is mandatory. Thus, a triode configuration consisting of plasma (35 kV), suppressor (-2 kV), and ground (0 kV) electrodes was chosen for the extraction system. This scheme strikes a balance between beam efficiency and simplicity. Additionally, the model keeps the electric field strength between the electrodes below 6 kV/mm to reduce the risk of arc discharge.

The optimization of the extraction system was done through a series of steps using AXCEL-INP 2-D program. Initially, the design geometry was parametrized, followed by sequential scans. Finally, the beam performance was evaluated to guarantee optimal results. During the process the input values were rectified to achieve the desired beam performance.

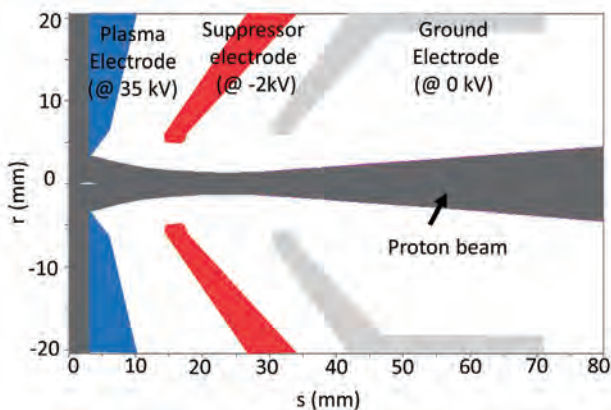


Fig. 5. Beam trajectory for the optimized triode extraction system for the JAEA-ADS linac.

Figure 5 presents the JAEA-ADS triode extraction system that has been optimized to control the proton beam divergence. The proton beam has a current of 25 mA, an energy level of 35 keV, and normalized rms transverse emittances of 0.08π mm mrad. These beam values fulfill the specifications required for the JAEA-ADS linac.

2. Fabrication progress of the prototype spoke cavity for the JAEA-ADS linac

In preparation for the actual design of the continuous wave (CW) proton linac for the JAEA-ADS, we are now prototyping a low-beta single-spoke cavity. This prototyping will provide us with various insights on the development of superconducting (SC) cavities with transverse electromagnetic (TEM) mode resonance.

We have started welding together the shaped cavity parts in 2021. The prototype spoke cavity is made of pure niobium (Nb) except for the niobium-titanium alloy (Nb-Ti) flanges for the radio frequency (RF) ports and the beam ports. Before welding the actual cavity parts, the electron beam welding (EBW) beam parameters for each welding condition were carefully investigated using mock-up test pieces (Nb and Nb-Ti). Furthermore, all welding grooves were acid cleaned (chemically polished) to remove impurities prior to each EBW. Consequently, each cavity part was joined together with smooth welding beads. The beam port sections were successfully fabricated in fiscal year 2022 in addition to the body section fabricated in fiscal year 2021. So far, no obvious welding defects, such as unpenetrated welds and welding holes, have been found.

We have temporarily assembled the prototype spoke cavity and measured its resonant frequency. The cavity was assembled from the body section, two beam ports, and two lids. Since the difference between the measured and simulated frequencies was well within

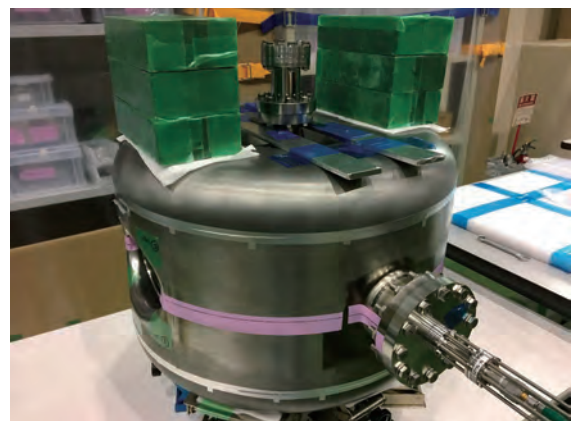


Fig. 6. Setup for the frequency measurement.

the adjustment range in the final assembly process, it was confirmed that there were no significant problems with the cavity fabrication.

Study for nuclear technology

From fiscal year 2019 to 2022, we conducted an experimental program on nuclear data for the research and development of ADS, entrusted by MEXT. A series of experiments within this program were conducted using the fixed-field alternating gradient (FFAG) accelerator at Kyoto University. The program comprised two subprograms: neutron energy spectrum measurement and high-energy fission measurement. For both subprograms, we utilized 107-MeV proton beams generated with the FFAG accelerator.

In the first subprogram, we measured energy spectra of neutrons from proton-induced reactions using a scintillation spectrometer system with the time-of-flight technique. This allowed us to obtain nuclear data for Fe, Pb, and Bi, which are crucial materials for ADS. Furthermore, we successfully measured the fission rate of ^{237}Np induced by spallation neutrons.

In the second subprogram, we measured the mass distribution of fission fragments and fission neutrons

from ^{208}Pb and ^{209}Bi produced in proton-induced reactions, utilizing a combination of multi-wire proportional counters (MWPCs) and a neutron detector system (Fig. 7).

As of March 2023, we have successfully completed all measurements in this experimental program, obtaining valuable nuclear data that will significantly contribute to the ADS design. These data are expected to enhance the prediction accuracy of neutronic design, benefiting not only ADS research but also the design of accelerator facilities that utilize proton beams.

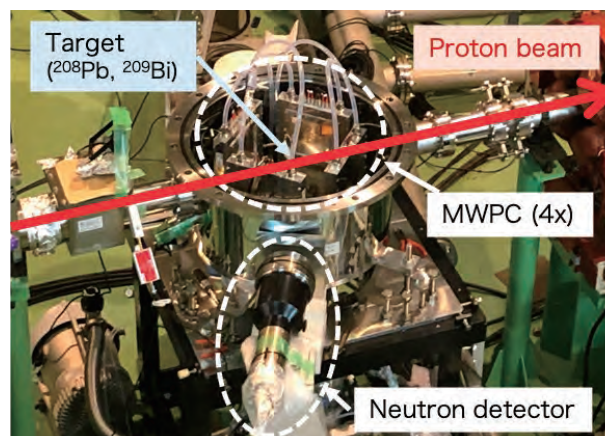


Fig. 7. Experimental setup of high-energy fission measurement

International and Domestic Cooperation

We are collaborating with the Belgian Nuclear Research Centre (SCK CEN) for the ADS development under the collaboration arrangement between SCK CEN and JAEA. SCK CEN is promoting the MYRRHA (Multi-purpose hYbrid Research Reactor for High-tech Application) project, which is the world's first large scale ADS project at power levels scalable to industrial systems. We frequently discussed with the MYRRHA accelerator team for the super-conducting Linac development. An on-line workshop, mainly for neutronics, was held in January 2023.

We continued the collaboration with Karlsruhe Institute of Technology in Germany on the LBE technology. We exchanged information about the LBE loop operation.

We are participating with the eighth Spallation Target Irradiation Program (STIP-8) at Paul Scherrer Institute in Switzerland, and a proton-beam irradiation program of steel samples including JAEA's ones has been completed. Sample specimens were taken out of

the target vessel for PIE.

We are also collaborating with domestic universities and institutes. One of the collaborations is with the University of Fukui on behavior of spallation and corrosion products in LBE. We are developing the Transport of Radionuclides In Liquid metal systems (TRAIL) code. We continued the experimental study on the evaporation behavior of volatile elements from LBE.

Another collaboration is with the Tokyo Institute of Technology (TIT). Several steel specimens were provided by TIT, and these specimens were served for the materials corrosion test with using the OLLOCHI loop.

In December 2022, we visited the National Institute for Fusion Science (NIFS) in Gifu prefecture. They are operating a high-temperature Pb-Li loop "Orosshi". We have common interests in the high-temperature liquid metal technology. We discussed the operation of both NIFS's and J-PARC's liquid metal loops, i.e., Pb-Li, LBE and Hg, and recovery of tritium from liquid metal, and so on.



Safety

Safety

1. Major events on safety culture and safety activities in the J-PARC

Through our experiences of the various accidents and incidents, J-PARC has reaffirmed that “The safety of the facility is achieved by the efforts of every person involved”, and we actively implement safety culture development activities to upgrade the safety awareness and skills of each person. Our efforts to enforce the safety culture in J-PARC include sharing safety information, enhancement of safety awareness, education and training, etc. For these purposes, new approaches are being introduced sequentially. In addition, these activities are being reviewed internally and by external experts to ensure continuous improvement.

In FY2022, we established a safety policy of “Follow safety rules and make potential risks shared”. Workers were expected to improve their “sensitivity to risk” and “on-site capabilities” by engaging in the following activities: 1) knowing the rules, complying with them, and understanding their significance and principles; 2) carefully identifying latent risks and problems and sharing them; 3) if having any questions or concerns, speaking out and thinking about it together. Table 1 lists the major events on safety culture and safety activities in the J-PARC.

In order not to forget the radioactive material leak incident that occurred on May 23, 2013, the J-PARC exchanges safety information between each section and has a workshop for fostering safety culture around May 23 every year. The Safety Day in FY2022 was held on May 23 via an online meeting. Some good practices were awarded by the director. Following that, the main talk entitled “Improving on-site capabilities through manuals - The concept of safe ergonomics” was given by Prof. Akinori Komatsubara, Waseda University. In the afternoon session, safety initiatives at each facility were introduced. Further, an updated video material on the radioactive material leak incident in 2013 was presented.

An emergency drill was conducted on October 25 at the Materials and Life Science Facility. It was assumed that the neutron beam shutter was opened when a worker was left in the neutron beam line BL22 and was exposed to radiation. The drill included transportation and decontamination of the exposed worker, estimation of exposure doses, setup of the command post and communication with the accident site, report to the headquarters via TV conference, and a press release.

The fiscal 2022 J-PARC safety audit was conducted by two auditors on November 28. They reviewed the following points: 1) organizational structure for safety management, 2) safety management in works, 3) emergency response, 4) safety education and fostering safety culture. The auditors reported that a safety management system for keeping steady operation with minimum trouble is being created. And they recommended that 1) in order to establish these achievements as J-PARC’s culture, we should repeatedly discuss what J-PARC should do for the future, reviewing what was pointed out at past audits in the viewpoints of a long-term period, 2) making sure to pass on the design concepts of J-PARC to the next generation, and develop human resources through active participation in expansion and new construction projects.

2. Radiological license update and facility inspection

Applications to update the radiological license were submitted to the Nuclear Regulation Authority on February 16, 2022. Table 2 lists the main changes in the applications. The permit for the applications was issued on August 24, 2022.

On January 11, 2022, “The new construction plans” for new and additional facilities for the Materials and Life Science Experimental Facility, Hadron Experimental Facility, and Neutrino Experimental Facility were submitted to the Ibaraki prefecture for prior approval by the local government in accordance with the Ibaraki Prefecture Nuclear Safety Agreement.

The facility inspection for the new primary beam line (C-line) of the Hadron Experimental Facility, permitted above, was conducted by Radiation Management Research Institute, Inc., registered inspection agency, on March 14, 2023.

3. Meeting of the committee on the radiation safety matter

The J-PARC Radiation Safety Committee is organized as an advisory committee to both JAEA and KEK to discuss policy on radiation safety in J-PARC. Meanwhile, the Radiation Safety Review Committee has been established to discuss specific subjects of radiation safety in the J-PARC.

In FY2022, the J-PARC Radiation Safety Committee met twice, and the Radiation Safety Review Committee met three times. Table 3 lists the major issues for the committees.

4. Radiation exposure of radiation workers

The number of persons subject to annual measurement of external exposure in FY2022 was 3111.

Table 4 lists the distribution of annual exposed doses for each category of workers. There was no exposure exceeding the dose limit specified in the local

radiation protection rule for J-PARC and the administrative dose limits (7 mSv/year) specified in the detailed rule of local radiation protection rule for J-PARC. The total annual effective dose was 26.8 person·mSv, and the maximum effective dose was 1.6 mSv.

Table 1. List of major events on safety in FY2022.

Day	Events
May 23, 2022	Safety Day (Meeting to exchange safety information between each section, Workshop for fostering safety culture)
July 1, 2022	Liaison committee on safety and health for contractors
October-December	Refresher course on radiation safety for in-house staff (e-learning)
October 25, 2022	Emergency drill assuming, while a worker was in the neutron beam line BL22 of the Materials and Life Science Facility, the beam shutter was opened, causing massive exposure
November 28, 2022	FY2022 J-PARC Safety Audit

Table 2. Major application items of the radiological license

Facility	Items of an application
Li	<ul style="list-style-type: none"> • Change in the maximum number of accelerated particles • Appropriateness of description
RCS	<ul style="list-style-type: none"> • Change in the maximum number of accelerated particles • Appropriateness of description
MR	<ul style="list-style-type: none"> • Change in the maximum number of accelerated particles • Appropriateness of description
MLF	<ul style="list-style-type: none"> • Installation of the Muon accelerator • Modification of exhaust purification system (a gas waste treatment facility) • Appropriateness of description
HD	<ul style="list-style-type: none"> • Change in the maximum number of accelerated particles • Expansion of the room for radiation generator use (installation of a new primary beamline (C-line)) • Modification of the exhaust system, addition of exhaust and drainage facilities • Appropriateness of description
NU	<ul style="list-style-type: none"> • Change in the maximum number of accelerated particles • Addition of entrance for the radiation-controlled area • Modification of the air exhauster

Table 3. Radiation Safety Committee (RSC) and Radiation Safety Review Committee (RSRC) in FY2022

No.	Date	Major Issues
The Radiation Safety Committee		
39 th	July 19, 2022	• Report on the progress status of change permission application, personal exposure situation, amount of radioactive waste released in FY2021
40 th	March 16, 2023	• Report on the response to legal revisions (ensuring measurement reliability)
The Radiation Safety Review Committee		
34 th	August 25, 2022	• Revision of the transportation rule for radioactive materials in J-PARC site
35 th	January 11, 2023	• Revision of the operation manual for J-PARC (MLF, HD)
36 th	March 30, 2023	• Revision of the guidelines for accident countermeasure activities • Revision of the operation manual for J-PARC (MLF)

Table 4. Annual exposure doses in FY2022

	# of workers	Dose range x (mSv)				Collective dose (person · mSv)	Maximum dose (mSv)
		ND	$0.1 \leq x \leq 1.0$	$1.0 < x \leq 5.0$	$5.0 < x$		
In-house staff	691	672	19	0	0	5.7	0.7
Users	1117	1116	1	0	0	0.1	0.1
Contractors	1306	1249	54	3	0	21.0	1.6
Total	3111	3034	74	3	0	26.8	1.6

*If the same worker changed the worker classification during the fiscal year, the worker was counted as one worker per the classification. Therefore, the total number does not match the sum of the respective classification.



User Service

Users Office (UO)

Outline

The J-PARC Users Office (UO) was established in 2007. It opened an office on the first floor of the IBARAKI Quantum Beam Research Center in Tokai-mura, in December 2008. UO maintains the Tokai Dormitory for the J-PARC users. UO provides on-site and WEB support with one-stop service for the utilization of the J-PARC. As of March 31, 2023, UO had 11 staffs and 5 WEB Support SE staffs in the Users Affairs Section. The J-PARC Users, after the approval of their experiment, follow the administrative procedures outlined on the Users Office (UO) WEB Portal Site, related to the regis-

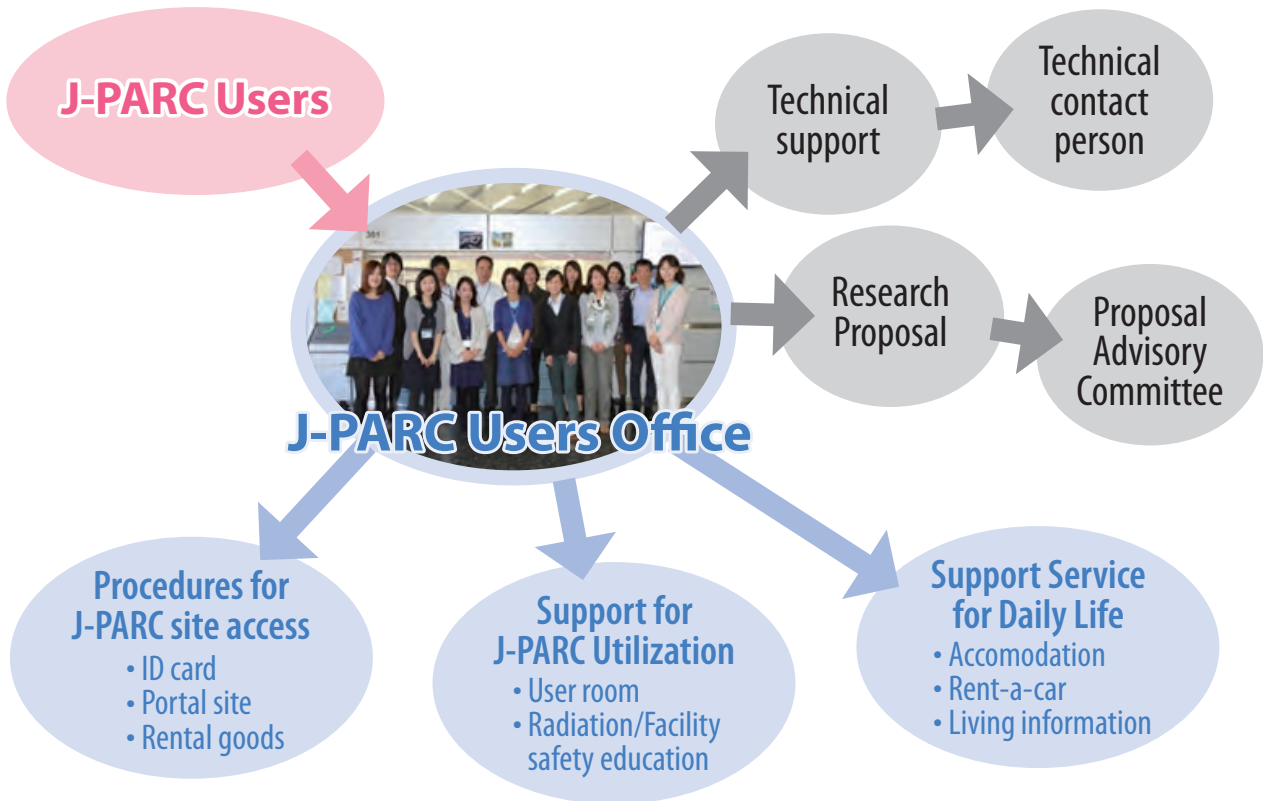
tration as a J-PARC User, radiation worker registration, safety education, accommodation, invitation letter for visa and other requirements. Then, the UO staffs provide them with support by e-mail. After their arrival at the J-PARC, UO gives on-site assistance to the J-PARC Users, like receiving the J-PARC ID, glass badge, and safety education. Since 2015, UO had been doing its part to improve the J-PARC online experiment system and make it more user-friendly.

After the experiments UO may return the experiment samples at User's cost after cooling the radioactive activities.



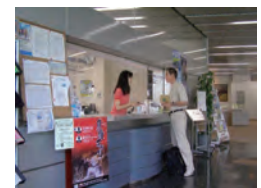
Map to J-PARC Users Office

Activities of UO



One stop service for J-PARC users

on the web	on-site support
<p>Step 1 User registration</p> <p>New user: Getting user ID Registered user: Annual registration, specifying of the visit</p> <p style="text-align: center;">Approval of UO</p>	<p>Step 3</p> <p> Procedures upon arrival at the first day</p> <p> Recieve J-Parc User ID card</p> <p> Vehicle Permission pass</p> <p>Safety education and dosimeter</p>
<p>Step 2-1 Obligatory application</p> <p>Application form to visit J-PARC Visit proposal (foreign nationality) Reservation of safety training On-line education video</p>	<p style="text-align: right;">Rental goods</p> <div style="border: 1px solid black; padding: 5px; background-color: #fff9c4;"> <p>Bicycle PHS Cafeteria card Locker key Office key</p> </div>
<p>Step 2-2 Optional application</p> <p>J-PARC Card for facility access Network registration Radiation worker registration Reservation of Dormitory Invitation letter for Visa</p>	<p>Step 4 J-PARC Experiment and meeting</p> <p>Step 5 Leaving procedures</p> <p>Return all cards, keys, rental goods UO (office hours) or return box!</p>



Users Office at IQBRC
Office hours(9:00-17:00, Mon.-Fri.)



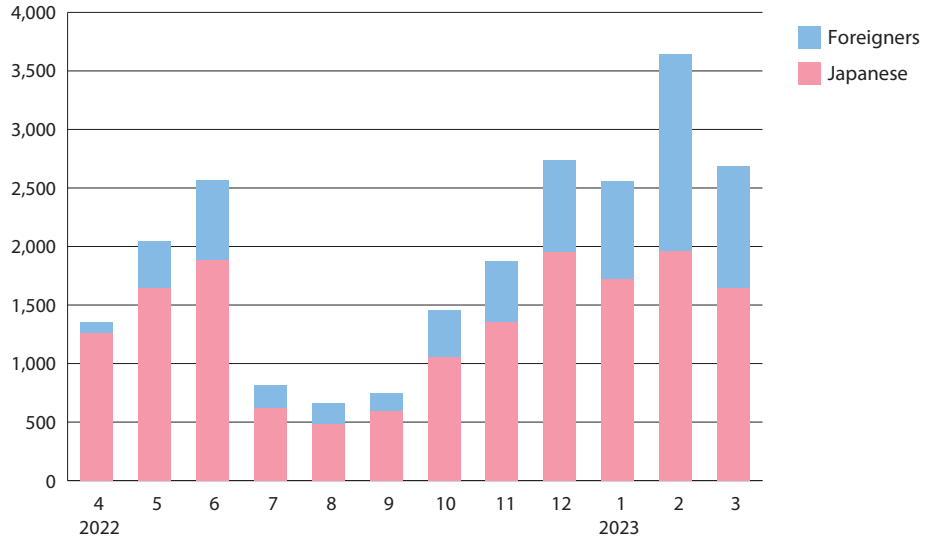
Rental bicycle



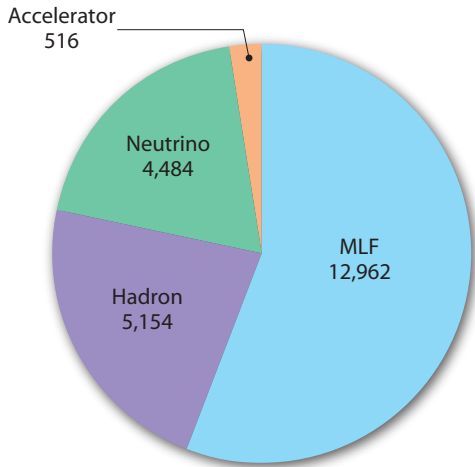
Return box at IQBRC

User Statistics

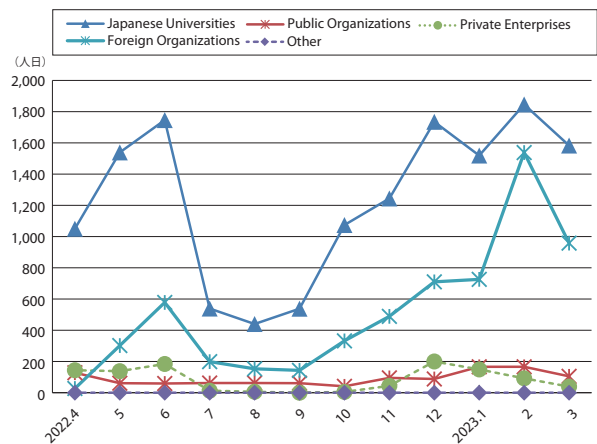
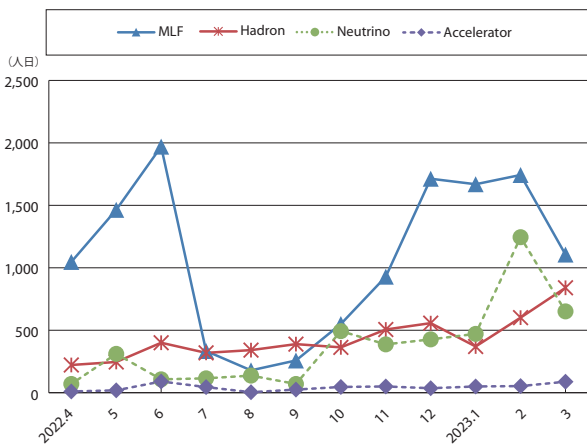
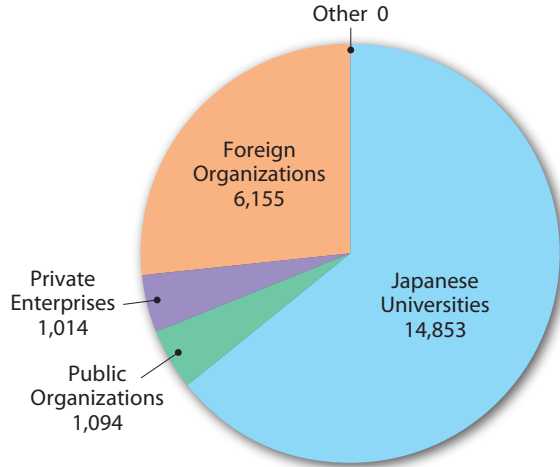
Users in 2022 (Japanese/Foreigners, person-days)



Users in 2022 (according to facilities, person-days)



Users in 2022 (according to organizations, person-days)



MLF Proposals Summary - FY2022

Table 1. Number of Proposals by Beamline

Beam-line	Instrument	2022A		2022B		Full Year				
		Submitted	Approved	Submitted	Approved	Submitted		Approved		
		GU	GU	GU	GU	PU/S	IU	PU/S	IU	
BL01	4D-Space Access Neutron Spectrometer - <i>4SEASONS</i>	22(0)	8(0)	25(0)	9(0)	0	1	0	1	
BL02	Biomolecular Dynamics Spectrometer - <i>DNA</i>	18(2)	12(2)	21(1)	7(1)	2	1	2	2	
BL03	IBARAKI Biological Crystal Diffractometer - <i>IBIX</i>	(100-β) [†]	2	1	4	1	0	0	0	0
		(β) [‡]	0	0	1	1	24 [※]	0	24 [※]	0
BL04	Accurate Neutron-Nucleus Reaction Measurement Instrument - <i>ANNRI</i>	8	4	4	3	2	1	2	1	
BL05	Neutron Optics and Physics - <i>NOP</i>	8	6	7	5	1	0	1	0	
BL06	Village of Neutron Resonance Spin Echo Spectrometers - <i>VIN ROSE</i>	3	2	4	2	1	0	1	0	
BL08	Super High Resolution Powder Diffractometer - <i>SuperHRPD</i>	11	8	6	5	1	0	1	0	
BL09	Special Environment Neutron Powder Diffractometer - <i>SPICA</i>	5	5	1	1	1	0	1	0	
BL10	Neutron Beam-line for Observation and Research Use - <i>NOBORU</i>	17	3	9	10	2	1	2	1	
BL11	High-Pressure Neutron Diffractometer - <i>PLANET</i>	8(0)	7(0)	13(0)	5(0)	0	2	0	2	
BL12	High Resolution Chopper Spectrometer - <i>HRC</i>	10	6	7	5	1	0	1	0	
BL14	Cold-Neutron Disk-Chopper Spectrometer - <i>AMATERAS</i>	35	8	35	8	1	1	1	1	
BL15	Small and Wide Angle Neutron Scattering Instrument - <i>TAIKAN</i>	34(2)	13(2)	36(0)	10(0)	2	4	2	4	
BL16	Soft Interface Analyzer - <i>SOFIA</i>	21	12	21	10	1	1	1	1	
BL17	Polarized Neutron Reflectometer - <i>SHARAKU</i>	17(2)	14(2)	15(1)	7(1)	3	2	3	2	
BL18	Extreme Environment Single Crystal Neutron Diffractometer - <i>SENJU</i>	18(0)	8(0)	17(0)	7(0)	1	1	1	1	
BL19	Engineering Materials Diffractometer - <i>TAKUMI</i>	27	12	29	7	2	1	2	1	
BL20	IBARAKI Materials Design Diffractometer - <i>IMATERIA</i>	(100-β) [†]	3	3	5	5	0	0	0	0
		(β) [‡]	18	18	13	13	23	0	23	0
BL21	High Intensity Total Diffractometer - <i>NOVA</i>	21	19	14	10	1	0	1	0	
BL22	Energy Resolved Neutron Imaging System - <i>RADEN</i>	23(0)	8(0)	18(1)	8(1)	0	2	0	2	
BL23	Polarization Analysis Neutron Spectrometer - <i>POLANO</i>	5	4	6	4	1	0	1	0	
D1	Muon Spectrometer for Materials and Life Science Experiments - <i>D1</i>	12(0)	6(0)	16(0)	9(0)	0	1	0	1	
D2	Muon Spectrometer for Basic Science Experiments - <i>D2</i>	10(4)	5(3)	5(0)	1(0)	1	1	1	1	
S1	General purpose μSR spectrometer - <i>ARTEMIS</i>	28(0)	15(0)	37(1)	12(1)	1	1	1	1	
S2	Muonium Laser Physics Apparatus - <i>S2</i>	0(0)	0(0)	0(0)	0(0)	0	1	0	1	
U1A	Ultra Slow Muon Microscope - <i>U1A</i>	0	0	0	0	0	1	0	1	
U1B	Transmission Muon Microscope - <i>U1B</i>	0	0	0	0	0	0	0	0	
H1	High-intensity Muon Beam for General Use - <i>H1</i>	0	0	0	0	0	1	0	1	
Total		382	207	371	158	65	24	65	24	

GU : General Use PU : Project Use or Ibaraki Pref. Project Use S : S-type Proposals

IU : Instrument Group Use

† : Ibaraki Pref. Exclusive Use Beamtime (β = 80% in FY2022)

‡ : J-PARC Center General Use Beamtime (100-β = 20% in FY2022)

() : Number of proposals under the New User Promotion (BL01, BL02, BL11, BL15, BL17, BL18, BL22) or

P-type proposals (D1, D2, S1) in GU

※ : Operations period is held twice per year (for each of the A and B periods), with only the yearly total shown above.

The actual total number of proposals in each beamline named in the table does not match the number shown in the "Total" cell, because some proposals are submitted or approved across multiple beamlines.

Table 2. Number of Long-Term Proposals by Fiscal Year

Application FY	Submitted	Approved
2020	13	3
2021	0	0
2022	5	4

Due to the COVID-19 situation, no Long-Term Proposals were called for FY2021.

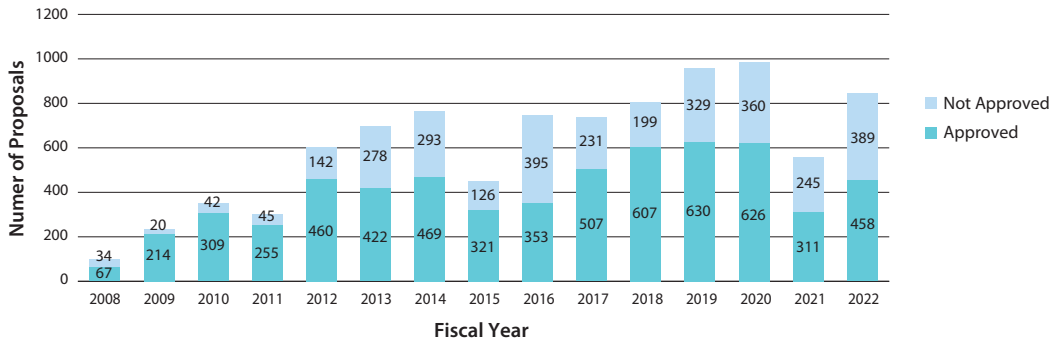


Fig. 1. Number of MLF Proposals over Time

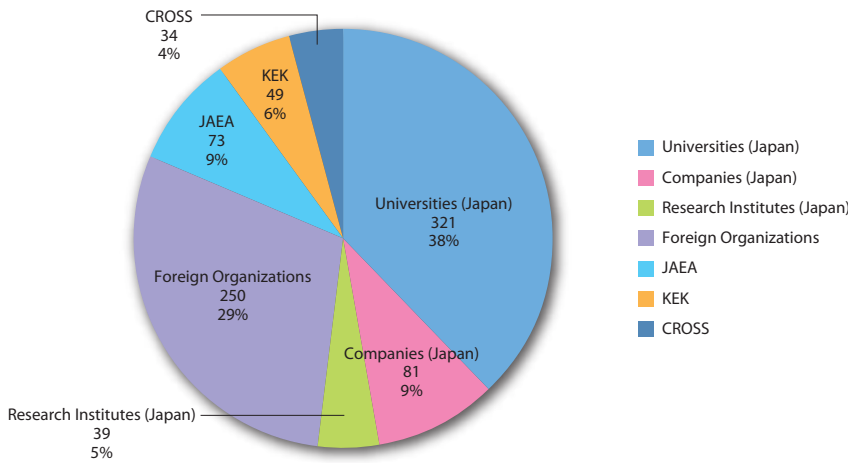


Fig. 2. Origin of Submitted Proposals by Affiliation - FY2022

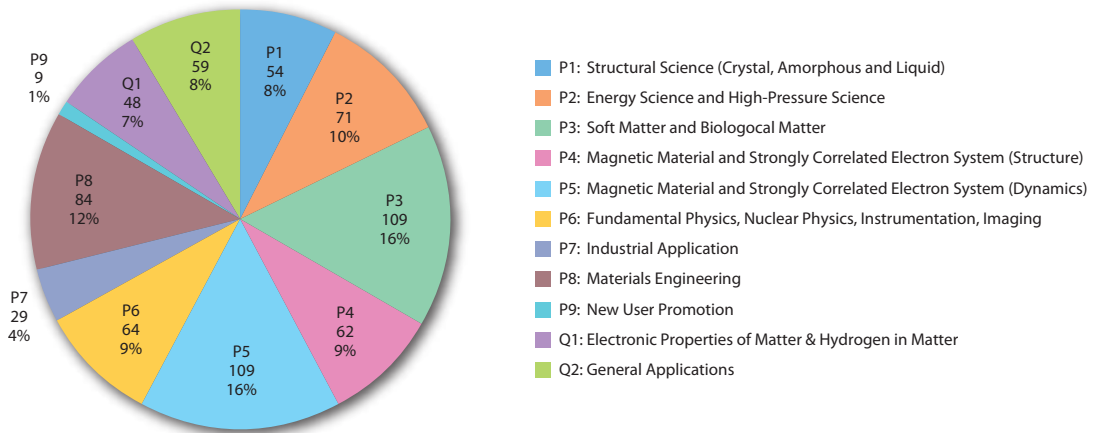


Fig. 3. Submitted Proposals by Sub-committee/Expert Panel – FY2022

J-PARC PAC Approval Summary for the 2022 Rounds

	(Co-) Spokespersons	Affiliation	Title of the experiment	Approval status (PAC recommendation)	Beamline	Status
E03	K.Tanida	JAEA	Measurement of X rays from X^- Atom	Stage 2	K1.8	Data taking
P04	J.C.Peng, S.Sawada	U of Illinois at Urbana-Champaign; KEK	Measurement of High-Mass Dimuon Production at the 50-GeV Proton Synchrotron	Deferred	Primary	
E05	T.Nagae	Kyoto U	Spectroscopic Study of X-Hypernucleus, $^{12}_X\text{Be}$, via the $^{12}\text{C}(K^-, K^+)$ Reaction	Stage 2 New experiment E70 based on the S-2S spectrometer	K1.8	Finished
E06	J.Imazato	KEK	Measurement of T-violating Transverse Muon Polarization in $K^+ \rightarrow p^0 m^+ n$ Decays	E36 as the first step	K1.1BR	
E07	K.Imai, K.Nakazawa, H.Tamura	JAEA, Gifu U, Tohoku U	Systematic Study of Double Strangeness System with an Emulsion-counter Hybrid Method	Stage 2	K1.8	Finished Data analysis
E08	A.Krutenkova	ITEP	Pion double charge exchange on oxygen at J-PARC	Stage 1	K1.8	
E10	A.Sakaguchi, T.Fukuda	Osaka U, Osaka EC U	Production of Neutron-Rich Lambda-Hypernuclei with the Double Charge-Exchange Reaction (Revised from Initial P10)	Stage 2	K1.8	Li run finished, Be target run with S-2S
E11	A.K.Ichikawa, F.Sanchez	KEK	Tokai-to-Kamioka (T2K) Long Baseline Neutrino Oscillation Experimental Proposal	Stage 2	neutrino	Data taking
E13	H.Tamura	Tohoku U	Gamma-ray spectroscopy of light hypernuclei	Stage 2	K1.8	Finished
E14	T.Yamanaka	Osaka U	Proposal for $K_L \rightarrow p^0 n \bar{n}$ Experiment at J-PARC	Stage 2	KL	Data taking
E15	M.Iwasaki, T.Nagae	RIKEN, Kyoto U	A Search for deeply-bound kaonic nuclear states by in-flight $3\text{He}(K^-, n)$ reaction	Stage 2	K1.8BR	Finished
E16	S.Yokkaichi	RIKEN	Measurements of spectral change of vector mesons in nuclei (previously "Electron pair spectrometer at the J-PARC 50-GeV PS to explore the chiral symmetry in QCD")	Stage 2 for Run 0 Deferred for Run 1. PAC recommended 101h+100h beam time for beam study & trigger study.	High p	Data taking
E17	R.Hayano, H.Outa	U Tokyo, RIKEN	Precision spectroscopy of Kaonic ^3He $3d \rightarrow 2p$ X-rays	Registered as E62 with an updated proposal	K1.8BR	
E18	H.Bhang, H.Outa, H.Park	SNU, RIKEN, KRISS	Coincidence Measurement of the Weak Decay of $^{12}_L\text{C}$ and the three-body weak interaction process	Stage 2	K1.8	
E19	M.Naruki	KEK	High-resolution Search for Q^+ Pentaquark in $p^- p \rightarrow K^+ X$ Reactions	Stage 2	K1.8	Finished
E21	Y.Kuno	Osaka U	An Experimental Search for $\mu - e$ Conversion at a Sensitivity of 10^{-16} with a Slow-Extracted Bunched Beam	Phase-I Stage 2	COMET	
E22	S.Ajimura, A.Sakaguchi	Osaka U	Exclusive Study on the Lambda-N Weak Interaction in A=4 Lambda-Hypernuclei	Stage 1	K1.8	
T25	S.Mihara	KEK	Extinction Measurement of J-PARC Proton Beam at K1.8BR	Test Experiment	K1.8BR	Finished
E26	K.Ozawa	KEK	Search for w -meson nuclear bound states in the $p + ^A_Z \rightarrow n + ^{(A-1)}_w(Z-1)$ reaction, and for w mass modification in the in-medium $w \rightarrow p^0 g$ decay	Stage 1	K1.8	
E27	T.Nagae	Kyoto U	Search for a nuclear K bar bound state $K^- pp$ in the $d(p^+, K^-)$ reaction	Stage 2	K1.8	Finished
E29	H.Ohnishi	RIKEN	Search for f -meson nuclear bound states in the $pbar + ^AZ \rightarrow f + ^{(A-1)}_f(Z-1)$ reaction	Stage 1	K1.1	
E31	H.Noumi	Osaka U	Spectroscopic study of hyperon resonances below KN threshold via the (K^-, n) reaction on Deuteron	Stage 2	K1.8BR	Finished Data analysis
T32	A.Rubbia	ETH, Zurich	Towards a Long Baseline Neutrino and Nucleon Decay Experiment with a next-generation 100 kton Liquid Argon TPC detector at Okinoshima and an intensity upgraded J-PARC Neutrino beam	Test Experiment	K1.1BR	Finished
P33	H.M.Shimizu	Nagoya U	Measurement of Neutron Electric Dipole Moment	Deferred	Linac	
E34	T.Mibe	KEK, RIKEN	An Experimental Proposal on a New Measurement of the Muon Anomalous Magnetic Moment $g-2$ and Electric Dipole Moment at J-PARC	Stage 2	MLF	

	(Co-) Spokespersons	Affiliation	Title of the experiment	Approval status (PAC recommendation)	Beamline	Status
E36	M.Kohl, S.Shimizu	Hampton U, Osaka U	Measurement of $G(K^+ \rightarrow e^+ n)/G(K^+ \rightarrow m^+ n)$ and Search for heavy sterile neutrinos using the TREK detector system	Stage 2	K1.1BR	Finished Data analysis
E40	K.Miwa	Tohoku U	Measurement of the cross sections of Σp scatterings	Stage 2	K1.8	Finished Data analysis
P41	M.Aoki	Osaka U	An Experimental Search for $\mu - e$ Conversion in Nuclear Field at a Sensitivity of 10^{-14} with Pulsed Proton Beam from RCS	Deferred	MLF	Reviewed in MLF/IMSS
E42	J.K.Ahn	Pusan National U	Search for H-Dibaryon with a Large Acceptance Hyperon Spectrometer	Stage 2	K1.8	Finished Data analysis
E45	K.H.Hicks, H.Sako	Ohio U, JAEA	3-Body Hadronic Reactions for New Aspects of Baryon Spectroscopy	Stage 2 PAC requests that the group further examine ways to reduce the total beam time requested and to find an efficient running scheme, including quick but careful beam tuning.	K1.8	
T46	K.Ozawa	KEK	EDIT2013 beam test program	Test Experiment	K1.1BR	Abandoned
T49	T.Maruyama	KEK	Test for 250L Liquid Argon TPC	Test Experiment	K1.1BR	Withdrawn
E50	H.Noumi	Osaka U	Charmed Baryon Spectroscopy via the (π, D^+) reaction	Stage 1 The FIFC, IPNS, and E50 should investigate the beam-line feasibility	High p	
T51	S.Mihara	KEK	Research Proposal for COMET(E21) Calorimeter Prototype Beam Test	Test Experiment	K1.1BR	had to be stopped
T52	Y.Sugimoto	KEK	Test of fine pixel CCDs for ILC vertex detector	Test Experiment	K1.1BR	not performed yet
T53	D.Kawama	RIKEN	Test of GEM Tracker, Hadron Blind Detector and Lead-glass EMC for the J-PARC E16 experiment	Test Experiment	K1.1BR	not performed yet
T54	K.Miwa	Tohoku U	Test experiment for a performance evaluation of a scattered proton detector system for the Σp scattering experiment E40	Test Experiment	K1.1BR	not performed yet
T55	A.Toyoda	KEK	Second Test of Aerogel Cherenkov counter for the J-PARC E36 experiment	Test Experiment	K1.1BR	had to be stopped
E56	T.Maruyama	KEK	A Search for Sterile Neutrino at J-PARC Materials and Life Science Experimental Facility	Stage 2	MLF	Data taking
E57	J. Zmeskal	Stefan Meyer Institute for Subatomic Physics	Measurement of the strong interaction induced shift and width of the $1s$ state of kaonic deuterium at J-PARC	Stage 1	K1.8BR	in preparation
P58	M. Yokoyama	U. Tokyo	A Long Baseline Neutrino Oscillation Experiment Using J-PARC Neutrino Beam and Hyper-Kamiokande	Deferred	neutrino	
T59	A. Minamino	Kyoto U	A test experiment to measure neutrino cross sections using a 3D grid-like neutrino detector with a water target at the near detector hall of J-PARC neutrino beam-line	To be arranged by IPNS and KEK-T2K	neutrino monitor bld	Finished
T60	T. Fukuda	Toho U	Proposal of an emulsion-based test experiment at J-PARC	Arranged by IPNS and KEK-T2K	neutrino monitor bld	Finished
E61	M. Wilking	Stony Brook U	NuPRISM/TITUS	Superseded. E61 has been adopted in Hyper-K as IWCD. IWCD is reviewed by HK-PAC.	neutrino	
E62	R. Hayano, S. Okada, H. Ota	U. Tokyo, RIKEN	Precision Spectroscopy of kaonic atom X-rays with TES	Stage 2	K1.8BR	Finished
E63	H. Tamura	Tohoku U	Gamma-ray spectroscopy of light hypernuclei II	Stage 2	K1.1	BL not ready yet. Exp. in preparation
T64	Y. Koshio	Okayama U	Measurement of the gamma-ray and neutron background from the T2k neutrino/anti-neutrino at J-PARC B2 Hall	Arranged by IPNS and KEK-T2K	neutrino	
E65	A.K.Ichikawa, F.Sanchez	Kyoto U	Proposal for T2K Extended Run	Stage 2	neutrino	
T66	T. Fukuda	Nagoya U	Proposal of an emulsion-based test experiment at J-PARC	Test Experiment	neutrino	

	(Co-) Spokespersons	Affiliation	Title of the experiment	Approval status (PAC recommendation)	Beamline	Status
P67	I. Meigo	JAEA	Measurement of displacement cross section of proton in energy region between 3 and 30 GeV for high-intensity proton accelerator facility	Carry out the experiment within the framework of facility development	MR	
T68	T. Fukuda	Nagoya U	Extension of T60/T66 Experiment: Proposal for the Run from 2017 Autumn	Test Experiment	neutrino	
E69	A. Minamino	Yokohama National U	Study of neutrino-nucleus interaction at around 1GeV using cuboid lattice neutrino detector, WAGASHI, muon range detectors and magnetized spectrometer, Baby MIND, at J-PARC neutrino monitor hall	Superseded. Merged with T2K.	neutrino	
E70	T. Nagae	Kyoto U	Proposal for the next E05 run with the S-2S spectrometer	Stage 2	K1.8	
E71	T. Fukuda	Nagoya U	Proposal for precise measurement of neutrino-p-water cross-section in NINJA physics run	Stage 2	neutrino	Data taking
E72	K. Tanida	JAEA	Search for a Narrow Λ^* Resonance using the $p(K, \Lambda)\eta$ Reaction with the hypTPC Detector	Stage 2	K1.8BR	
E73	Yue Ma	RIKEN	$^3_{\Lambda}H$ and $^4_{\Lambda}H$ mesonic weak decay lifetime measurement with $^3He(K, \pi^0)^3_{\Lambda}H$ reaction	Stage 2	K1.8BR	
P74	A.Feliciello	INFN, Torino	Direct measurement of the $3\Lambda H$ and $4\Lambda H$ lifetimes using the $3,4He(\pi^-, K^0)3,4\Lambda H$ reactions	Rejected	K1.1	
E75	H.Fujioka	Tokyo Inst. Tech,	Decay Pion Spectroscopy of $5\Lambda H$ Produced by Ξ -hypernuclear Decay	Stage 2	K1.8	
P76	H.M.Shimizu	Nagoya U	Searches for the Breaking of the Time Reversal Invariance in Polarized Epithermal Neutron Optics	Deferred	MLF	
T77	Yue Ma	RIKEN	Feasibility study for $3\Lambda H$ mesonic weak decay lifetime measurement with $3,4He(K, \pi^0)3,4\Lambda H$ reaction	PAC supports the continuation of T77 by an explorative run with the $3He$ target.	K1.8BR	Finished Data analysis
T78	H.Nishiguchi	KEK	8GeV Operation Test and Extinction Measurement	Test Experiment	K1.8BR	Finished
E79	T.Ishikawa	Tohoku U	Search for an $I=3$ dibaryon resonance	Stage 1	High p	
E80	F.Sakuma	RIKEN	Systematic investigation of the light kaonic nuclei	Stage 1 Deferred for Stage-2. TDR update based on FIFC comments is necessary.	K1.8BR	
T81	T.Fukuda	Nagoya U	Proposal of test experiment for technical improvements of neutrino measurements with nuclear emulsion detector	Test Experiment	neutrino	
E82	T.Maruyama	KEK	JSNS2-II	Stage 2	MLF	
E83	J. H. Yoo	Korea U	Search for sub-millicharged particles at J-PARC	Conditional to the satisfactory update of the TDR, PAC suggests Stage 2	neutrino	
P84	S. Nakamura	Tohoku U	High precision spectroscopy of Lambda hypernuclei with the (π^+, K^-) reaction at the High Intensity High Resolution beamline	Deferred This proposal is a part of the hadron extension discussion and PAC awaits the outcome of the special committee to convene in August for more information.	HIHR	
P85	K. Shirotori	Osaka U (RCNP)	Spectroscopy of Omega Baryons	Deferred This proposal is a part of the hadron extension discussion and PAC awaits the outcome of the special committee to convene in August for more information.	K10, T2 target	
E86	K. Miwa	Tohoku U	Measurement of the differential cross section and spin observables of the Λp scattering with a polarized Λ beam	Stage 1	K1.1	
P87	T. Gunji, K. Ozawa, H. Sako	Tokyo, KEK, JAEA	Proposal for dielectron measurements in heavy-ion collisions at J-PARC with E16 upgrades	Deferred PAC encourages the proponents to think about more versatile detector enabling (for example) concurrent measurement of leptonic and hadronic measurements.	HI, high-p	
E88	H. Sako	JAEA	Study of in-medium modification of phi mesons inside the nucleus with $\phi \rightarrow K^+ K^-$ measurement with the E16 spectrometer	Stage 1	high-p	

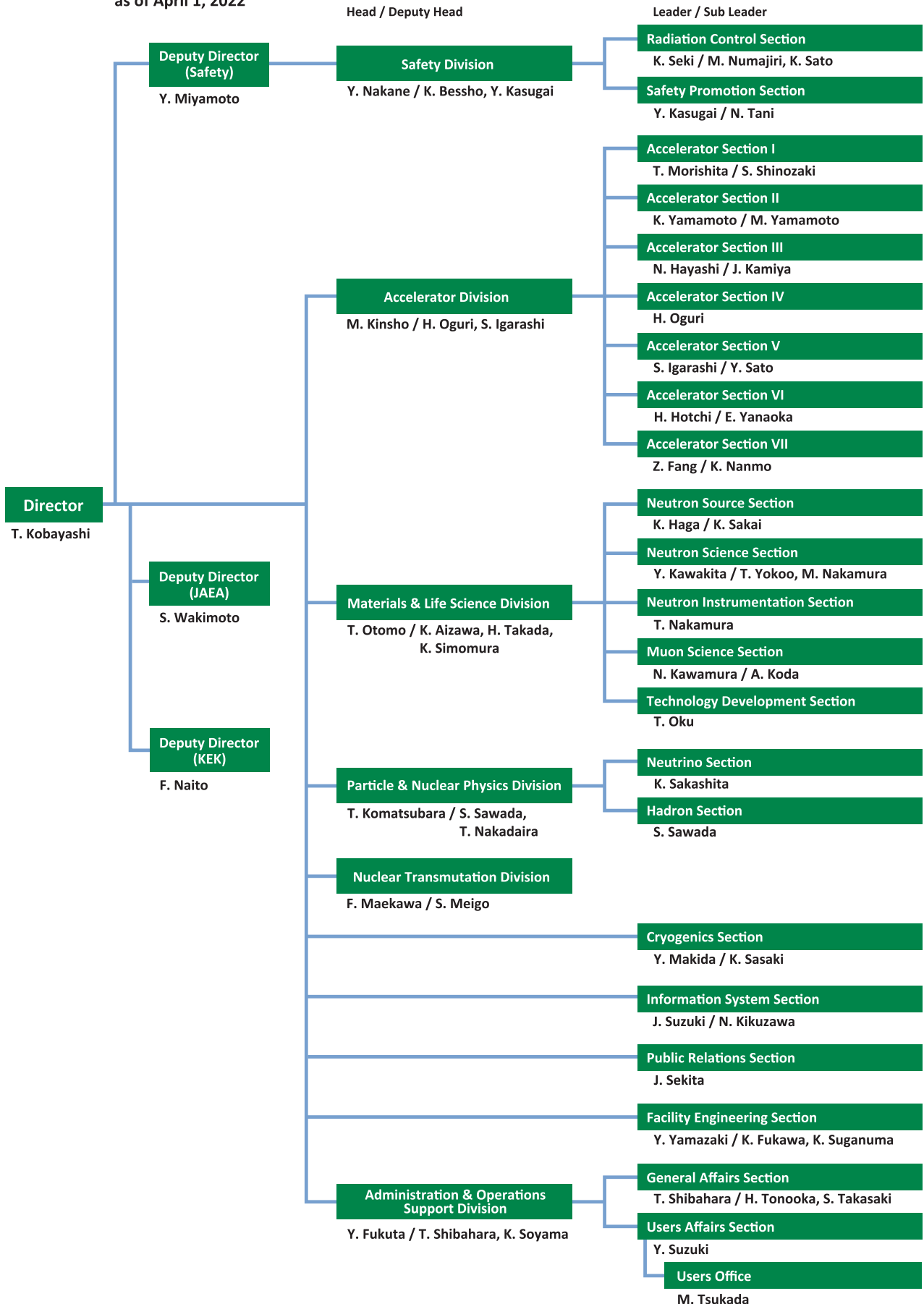
	(Co-) Spokespersons	Affiliation	Title of the experiment	Approval status (PAC recommendation)	Beamline	Status
P89	T. Yamaga	RIKEN	Investigation of fundamental properties of the KNN state	Deferred. PAC would like to see the detailed feasibility of P89 after E80's TDR.	K1.8BR	
E90	Y.Ichikawa, K.Tanida	JAEA	High resolution spectroscopy of the " Σ N cusp" by using the $d(K^+, \pi^-)$ reaction	Stage 1	K1.8	
P91	Y.Morino	KEK	Proposal for study of charm component in the nucleon via J/ψ measurement with the J-PARC E16 spectrometer	Deferred.	high-p	
P92	F.Sakuma	RIKEN	Proposal for the E80 Phase-I Experiment: Investigation of the KNNN ⁻ Bound State Focusing on the Λ d Decay	Deferred.	K1.8BR	
P93	K.Shirotori	Osaka U (RCNP)	Proposal of test experiment to evaluate performances of secondary beam mode at the high-momentum beam line	Deferred PAC requests the proponent to continue discussion with the Lab/ Facility management	high-p	
E94	T.Gogami	Kyoto U	New generation Λ hypernuclear spectroscopy with the (π^+, K^+) reaction by S-2S	Stage 1	K1.8	
P95	T.Ishikawa	Tohoku U	Pion-induced phi-meson production on the proton	Deferred	high-p	
E96	T.O.Yamamoto	JAEA	Measurement of X rays from Ξ^- -C atom with an active fiber target system	Stage 2	K1.8	
E97	M. Naruki	Kyoto U	Cascade baryon spectroscopy at J-PARC high momentum beamline	Stage 1	high-p	
T98	K. Yorita	Waseda U	Measurement of Anti-Matter Reaction in Liquid Argon Time Projection Chamber (LAR-TPC)	Test Experiment	K1.8BR	

Organization and Committees

Organization Structure

J-PARC Center Management System Chart

as of April 1, 2022



Members of the Committees Organized for J-PARC

(as of March, 20203)

1) Steering Committee

(*) Chair

Junji Haba (*)	High Energy Accelerator Research Organization (KEK), Japan
Koki Uchimaru	High Energy Accelerator Research Organization (KEK), Japan
Naohito Saito	High Energy Accelerator Research Organization (KEK), Japan
Nobuhiro Kosugi	High Energy Accelerator Research Organization (KEK), Japan
Tadashi Koseki	High Energy Accelerator Research Organization (KEK), Japan
Hiroyuki Oigawa (*)	Japan Atomic Energy Agency (JAEA), Japan
Yoshinori Horiuchi	Japan Atomic Energy Agency (JAEA), Japan
Masayasu Takeda	Japan Atomic Energy Agency (JAEA), Japan
Toshiyuki Momma	Japan Atomic Energy Agency (JAEA), Japan
Akira Endo	Japan Atomic Energy Agency (JAEA), Japan
Takashi Kobayashi	J-PARC Center, Japan

2) International Advisory Committee

(*) Chair

Thomas Prokscha	Paul Scherrer Institute (PSI), Switzerland
Yoko Sugawara	Toyota Physical and Chemical Research Institute, Japan
Paul Langan	Institut Laue-Langevin, France
Takeshi Egami	University of Tennessee, USA
Dan Alan Neumann	National Institute of Standards and Technology, USA
Robert McGreevy (*)	Science & Technology Facilities Council (STFC), UK
Jie Wei	Michigan State University, USA
John Thomason	Science & Technology Facilities Council (STFC), UK
Joachim Mnich	The European Organization for Nuclear Research(CERN), Switzerland
Dmitri Denisov	Brookhaven National Laboratory, USA
Angela Bracco	INFN, Istituto Nazionale di Fisica Nucleare, Italy
Reiner Kruecken	TRIUMF, Canada
Hamid Aït Abderrahim	Belgian Nuclear Research Centre (SCK CEN), Belgium
Akira Hasegawa	Tohoku University, Japan
Shinichi Kamei	Mitsubishi Research Institute, Japan
Hiromi Yokoyama	The University of Tokyo, Japan

3) User Consultative Committee for J-PARC

(*) Chair

Masaki Ishitsuka	Tokyo University of Science, Japan
Hajime Nanjo	Osaka University, Japan
Shoji Asai	The University of Tokyo, Japan
Takeshi Komatsubara	High Energy Accelerator Research Organization (KEK), Japan
Satoshi Nakanura	The University of Tokyo, Japan
Tomofumi Nagae	Kyoto University, Japan
Fuminori Sakuma	RIKEN, Japan
Shinya Sawada	High Energy Accelerator Research Organization (KEK), Japan
Kouji Miwa	Tohoku University, Japan
Toshio Yamaguchi (*)	Fukuoka University, Japan
Takashi Kamiyama	Hokkaido University, Japan
Takatsugu Masuda	The University of Tokyo, Japan
Kazuhisa Kakurai	Comprehensive Research Organization for Science and Society (CROSS), Japan
Toshiya Otomo	High Energy Accelerator Research Organization (KEK), Japan
Kenya Kubo	International Christian University, Japan
Tadashi Adachi	Sophia University, Japan
Koichiro Shimomura	High Energy Accelerator Research Organization (KEK), Japan
Yuko Kojima	Mitsubishi Chemical Corporation, Japan
Hiroyuki Kishimoto	Sumitomo Rubber Industries, Ltd. Japan
Hideto Imai	FC-Cubic, Japan
Kenji Ohoyama	Ibaraki University, Japan
Hideya Anzai	Ibaraki Prefecture, Japan
Mitsuhiro Fukuda	Osaka University, Japan
Cheol-Ho Pyeon	Kyoto University, Japan
Kazufumi Tsujimoto	Japan Atomic Energy Agency (JAEA), Japan

4) Accelerator Technical Advisory Committee

(*) Chair

Wolfram Fischer	Brookhaven National Laboratory (BNL), USA
Mats Lindroos	European Spallation Source, ERIC, Sweden
John Thomason	Science and Technology Facilities Council (STFC), UK
Sheng Wang	Institute of High Energy Physics, CAS, China
Toshiyuki Shirai	National Institutes for Quantum and Radiological Science and Technology, Japan
Alexander Aleksandrov	Oak Ridge National Laboratory, USA
Jie Wei (*)	Michigan State University, USA
Robert Zwaska	Fermi National Accelerator Laboratory (FNAL), USA
Simone Gilardoni	European Organization for Nuclear Research (CERN), Switzerland

5) Neutron Advisory Committee

(*) Chair

Phillip King	Rutherford Appleton Laboratory, UK
Bertrand Blau	Paul Scherrer Institut (PSI), Switzerland
Michael J Dayton	Oak Ridge National Laboratory (ORNL), USA
Guenter Muhrer	European Spallation Source(ESS), Sweden
Christiane Alba-Simionesco	Laboratoire Leon Brillouin (LLB) Saclay, France
Jamie Schulz (*)	Australian Nuclear Science and Technology Organization(ANSTO), Australia
Jon Taylor	European Spallation Source(ESS), Sweden
Sungil Park	Korea Atomic Energy Research Institute(KAERI), Korea
Yoshie Ohtake	RIKEN, Japan
Takahisa Arima	The University of Tokyo, Japan
Ken Anderson	Oak Ridge National Laboratory (ORNL), USA
Toyohiko Kinoshita	Japan Synchrotron Radiation Research Institute(JASRI), Japan

6) Muon Advisory Committee

(*) Chair

Martin Månsson	KTH Royal Institute of Technology, Sweden
Thomas Prokscha (*)	Paul Scherrer Institut (PSI), Switzerland
Andrew MacFarlane	The University of British Columbia, Canada
Klaus Kirch	ETH Zurich and Paul Scherrer Institute (PSI), Switzerland
Kenya Kubo	International Christian University, Japan
Tadayuki Takahashi	The University of Tokyo, Japan
Nori Aoi	Osaka University, Japan
Hiroshi Amitsuka	Hokkaido University, Japan

7) Radiation Safety Committee

(*) Chair

Yoshitomo Uwamino (*)	Japan Radioisotope Association, Japan
Yoshihiro Asano	High Energy Accelerator Research Organization (KEK), Japan
Hiroshi Watabe	Tohoku University, Japan
Takeshi Iimoto	The University of Tokyo, Japan
Takeshi Murakami	National Institutes for Quantum and Radiological Science and Technology (QST), Japan
Yukinori Kobayashi	High Energy Accelerator Research Organization (KEK), Japan
Toshiya Sanami	High Energy Accelerator Research Organization (KEK), Japan
Yoshihito Namito	High Energy Accelerator Research Organization (KEK), Japan
Akira Endo	Japan Atomic Energy Agency (JAEA), Japan
Takumi Nemoto	Japan Atomic Energy Agency (JAEA), Japan
Hideki Hangai	Japan Atomic Energy Agency (JAEA), Japan

8) Radiation Safety Review Committee

(*) Chair

Yukihiro Miyamoto (*)	Japan Atomic Energy Agency (JAEA), Japan
Yoshihiro Nakane	Japan Atomic Energy Agency (JAEA), Japan
Masaharu Numajiri	High Energy Accelerator Research Organization (KEK), Japan
Hidetoshi Kikunaga	Tohoku University, Japan
Hiroshi Yashima	Kyoto University, Japan
Kanenobu Tanaka	Institute of Physical and Chemical Research (RIKEN), Japan
Nobuyuki Chiga	National Institute for Quantum and Radiological Science and Technology (QST), Japan
Toshiro Itoga	Japan Synchrotron Radiation Research Institute (JASRI), Japan
Koji Kiriya	Comprehensive Research Organization for Science and Society (CROSS), Japan
Junko Matsumoto	Japan Atomic Energy Agency (JAEA), Japan
Makoto Kobayashi	Japan Atomic Energy Agency (JAEA), Japan
Kaiichi Haga	High Energy Accelerator Research Organization (KEK), Japan
Kazuyoshi Masumoto	High Energy Accelerator Research Organization (KEK), Japan
Michikazu Kinsho	Japan Atomic Energy Agency (JAEA), Japan
Takeshi Nakadaira	High Energy Accelerator Research Organization (KEK), Japan
Takeshi Komatsubara	High Energy Accelerator Research Organization (KEK), Japan
Hiroshi Takada	Japan Atomic Energy Agency (JAEA), Japan

9) MLF Advisory Board

(*) Chair

Takahisa Arima (*)	The University of Tokyo, Japan
Taku Sato	Tohoku University, Japan
Osamu Yamamuro	The University of Tokyo, Japan
Takashi Kamiyama	Hokkaido University, Japan
Yoshiharu Sakurai	Japan Synchrotron Radiation Research Institute (JASRI), Japan
Hiroshi Amitsuka	Hokkaido University, Japan
Yoko Sugawara	Kitasato University, Japan
Tadashi Adachi	Sophia University, Japan
Hiroyuki Kishimoto	Sumitomo Rubber Industries, Japan
Yoshie Otake	RIKEN, Japan
Jun Takahara	Kyushu University, Japan
Masahiro Hino	Kyoto University, Japan
Yasuhiro Iye	Chubu University, Japan
Toshiya Otomo	High Energy Accelerator Research Organization (KEK), Japan
Kazuya Aizawa	Japan Atomic Energy Agency (JAEA), Japan
Hiroshi Takada	Japan Atomic Energy Agency (JAEA), Japan
Koichiro Shimomura	High Energy Accelerator Research Organization (KEK), Japan
Yukinobu Kawakita	Japan Atomic Energy Agency (JAEA), Japan
Naritoshi Kawamura	High Energy Accelerator Research Organization (KEK), Japan
Shinichi Itoh	High Energy Accelerator Research Organization (KEK), Japan
Masayasu Takeda	Japan Atomic Energy Agency (JAEA), Japan
Kenji Nakajima	Japan Atomic Energy Agency (JAEA), Japan
Jun-ichi Suzuki	Comprehensive Research Organization for Science and Society (CROSS), Japan

10) Program Advisory Committee (PAC) for Nuclear and Particle Physics Experiments at the J-PARC 50Gev Proton Synchrotron

(*) Chair

Kenkichi Miyabayashi	Nara Womens' University, Japan
Motoi Endo	High Energy Accelerator Research Organization (KEK), Japan
Hirokazu Ishino	Okayama University, Japan
Takahiro Kawabata	Osaka University, Japan
Hiroaki Ohnishi	Tohoku University, Japan
Makoto Oka	Japan Atomic Energy Agency (JAEA) / Tokyo Institute of Technology, Japan
Kohei Yorita	Waseda University, Japan
Patrick Achenbach	Mainz University, Germany
Vincenzo Cirigliano	University of Washington, USA
Laura Fields	Fermi National Accelerator Laboratory (FNAL), USA
David Jaffe	Brookhaven National Laboratory (BNL), USA
Cristina Lazzeroni	University of Birmingham, UK
Kam-Biu Luk	University of California at Berkley, USA
Horst Lenske	University of Giessen, Germany
Kyungseon Joo	University of Connecticut, USA
Rikutarō Yoshida (*)	Argonne National Laboratory, USA

11) TEF Technical Advisory Committee

(*) Chair

Marc Schyns (*)	Belgian Nuclear Research Center(SCK • CEN), Belgium
Michael Butzek	Forschungszentrum Jülich, Germany
Thierry Stora	European Organization for Nuclear Research (CERN), Switzerland
Yukinobu Watanabe	Kyushu University, Japan
Kazuo Hasegawa	National Institutes for Quantum and Radiological Science and Technology (QST), Japan
Georg Müller	Karlsruhe Institute of Technology, Germany
Kei Ito	Kyoto University, Japan

Main Parameters

Present main parameters of Accelerator

Linac	
Accelerated Particles	Negative hydrogen
Energy	400 MeV
Peak Current	50 mA
Pulse Width	0.46 ms for MLF 0.50 ms for MR-FX 0.05 ms for MR-SX
Repetition Rate	25 Hz
Freq. of RFQ, DTL, and SDDL	324 MHz
Freq. of ACS	972 MHz
RCS	
Circumference	348.333 m
Injection Energy	400 MeV
Extraction Energy	3 GeV
Repetition Rate	25 Hz
RF Frequency	0.938 MHz → 1.67 MHz
Harmonic Number	2
Number of RF cavities	12
Number of Bending Magnet	24
Main Ring	
Circumference	1567.5 m
Injection Energy	3 GeV
Extraction Energy	30 GeV
Repetition Rate	~0.4 Hz
RF Frequency	1.67 MHz → 1.72 MHz
Harmonic Number	9
Number of RF cavities	11
Number of Bending Magnet	96

Key parameters of Materials and Life Science Experimental Facility

Injection energy	3 GeV
Repetition rate	25 Hz
Neutron Source	
Target material	Mercury
Number of moderators	3
Moderator material	Liquid hydrogen
Moderator temperature/pressure	20 K/1.5 MPa
Number of neutron beam extraction ports	23
Muon Source	
Target material	Graphite
Number of muon beam extraction ports	4
Neutron Instruments	
Open for user program (general use)	21
Under commissioning/construction	0
Muon Instruments	
Open for user program (general use)	3
Under commissioning/construction	1/0

Events

Events

J-PARC Safety Day (May 23)

"J-PARC Safety Day," the important day following the 2013 radioactive material leak incident at the Hadron Experimental Facility, was held. This year, 350 staff members participated remotely. After the awards ceremony for safety contributions and best practices, a lecture entitled "Improving Ability to Implement On-site Safety through Manuals: Safety Ergonomics Approach" was given by Prof. Akinori KOMATSUBARA of the Faculty of Science and Engineering, Waseda University. Finally, as a new attempt, the safety implementation activities at the Accelerator Facilities, Materials and Life Science Experimental Facility (MLF), Hadron Experimental Facility, and Neutrino Experimental Facility were presented and discussed by all participants.

"Spark Exciting Science" Sponsored by KAKENHI Entitled "World of Cutting-Edge Physics Understood through World's Smallest Spinning Top" (June 18)

Nineteen 5th or 6th grade students from local elementary schools, those in nearby prefectures, and those in Tokyo participated in a part of "Spark ☆ Exciting Science Workshop sponsored by KAKENHI," a program for children to spark their interest in the cutting-edge research being conducted at universities and research institutions that receive financial support from KAKENHI, and engaged in muon beam practice after learning about the elementary particle muon.

The participants experimented to visualize a magnetic field created by magnets and coils, observed the precession movement of a rolling gyroscope and

a handmade spinning top, and built cloud chambers to capture and observe cosmic rays. They also learned about J-PARC, visited the Muon Science Laboratory, and experienced the irradiation of muon beams into a sample. Remarkably, they are the first elementary school students to participate in a muon beam experiment at the MLF.



Monitoring Muon Irradiation

2022 Neutron Industrial Application Report Meeting (July 14 and 15)

J-PARC Center, Ibaraki Prefecture, CROSS, the Industrial Users Society for Neutron Application, and JAEA's JRR-3, which joined as an organizer, held the "Neutron Industrial Application Debriefing Session" at the Akihabara Convention Hall in Tokyo. Over the two days, 141 people attended in person, and 159 attended via the Internet. The results of the newly started joint research at the MLF and JRR-3 were presented, as well as the efforts and contributions to solving issues demanded by society, such as carbon neutrality and DX.

J-PARC Hello Science "Boron Neutron Capture Therapy (BNCT)" (June 24)

Hello Science in June was held at AYA'S LABORATORY Quantum Beam Research Center (AQBRC) with an online combination, and Dr. Fujio Naito, Deputy Director of J-PARC, was the lecturer.

BNCT (Boron Neutron Capture Therapy = irradiation of neutrons to boron drugs, which have the property of accumulating only in cancer cells, to destroy cancer cells) is a type of radiation therapy for cancer. It is being touted as a powerful new treatment method that allows for pinpoint treatment, requires only a single short course of radiation, and is effective against refractory cancers. In developing the small accelerator to be installed in hospitals, the technical expertise of the high-intensity linear accelerator (linac) at J-PARC was used to

construct the Ibaraki BNCT (iBNCT), a treatment device with a 6-m-long linac at the Ibaraki Neutron Medical Research Center (Shirakata, Tokai-mura). After conducting experiments on phantoms, etc., the iBNCT is undergoing non-clinical tests on mice and cells.

A total of 50 people from the medical field and the general public attended the event. Even after the session, many enthusiastic questions indicated a high level of interest.

Eco-Fest Hitachi 2022 (July 23)

"Eco-Fest Hitachi 2022, one of the largest environmental events in Ibaraki Prefecture for learning through experimentation and hands-on experience, was held at the Hitachi Civic Center for the first time in three years. About 50 companies, organizations, schools, and other groups presented their environmental activities and showcased their ecological products at various booths. J-PARC exhibited a superconducting coaster, which was so popular that visitors had to wait for their turns to try it out, a model of J-PARC, posters, etc., and attracted nearly 400 visitors.



Superconductive roller coasters affected kids.

"Let's Make a Spinning Top Tilting and Turning" at Tokai Village Enjoy Summer School 2022 (July 22 and August 2)

In the Enjoy Summer School organized by Tokai Village, J-PARC held lectures on making a top as last year. 16 and 13 fifth and sixth graders gathered at the Tokai Village Library on July 22 and August 2, respectively.

They learned about the relationship between electricity and magnetism. They confirmed that the rotation of the axis of the tops changed when the tops were rotated while tilted or by changing the center of gravity of the tops through the experiments. The lecturer explained that precessional motion was similar to the spin behavior of elementary particles studied at J-PARC.



Observing various light sources with polarization microscopes

“Let’s Make a Kaleidoscope of Light” Craft Class on Kids’ Kasumigaseki Field Trip Day 2022 (August 3 and 4)

The “Kids’ Kasumigaseki Field Trip Day” is a collaborative event among government ministries and agencies in Kasumigaseki to provide children with opportunities to experience and learn about society during their summer vacations. Over the two days, 265 parents and children gathered at the JAEA booth on-site to learn about the principles of spectroscopy by making light kaleidoscopes, which were assembled by drilling star-shaped holes in black paper and folding the cardboard to see rainbow-colored light coming out of the holes, and by listing the similarities and differences in the diffusion of light and the arrangement of colors.

J-PARC Online Facility Open House 2022 (August 27)

The J-PARC Open House, titled “Only Online! The Deepest Part of J-PARC!” was held through a combination of live broadcasts and pre-recorded videos from the accelerator and experimental facilities to provide programs showing the deepest part of J-PARC with nor-



Live Broadcasting from Hadron Experimental Facility

mally unavailable talks by researchers, broadcast via YouTube and niconico Live Broadcast. During the open house, “Hello Science”, the monthly science café, was also held, where Dr. Tsutomu Fukuda, designated assistant professor at the Institute of Materials and Systems for Sustainability Advanced Measurement Technology Center Elementary Particle Measurements Section of Nagoya University, gave a lecture on “Studying Particle Neutrinos and the Mysteries of the Universe with Photographic Film”.

JASIS 2022 Exhibition at Makuhari Messe International Exhibition Hall (September 7-9)

The Materials and Life Science Experimental Facility (MLF) at J-PARC and the JRR-3 research reactor at JAEA participated in JASIS 2022, Japan’s leading exhibition of scientific instruments, analytical systems, and solutions. The ultra-high vacuum pump made of titanium developed at the Accelerator Division of J-PARC attracted many visitors. Nearly 1,500 people visited our booth during the exhibition, many of whom listened intently to the researchers’ explanations.

11th International Workshop on Sample Environment at Scattering Facilities (August 28-September 1)

“11th International Workshop on Sample Environment at Scattering Facilities” was held at Nasu in Tochigi Prefecture, jointly organized by the J-PARC Center, Center of Neutron Science for Advanced Materials of Tohoku University, Comprehensive Research Organization for Science and Society, Frontier Research Center for Applied Atomic Sciences of Ibaraki University, Institute for Solid State Physics of the University of Tokyo, Japan Synchrotron Radiation Research Institute, KEK Institute of Materials Structure Science, and Materials Science Research Center of Japan Atomic Energy Agency.



Group photo in front of the hotel where the workshop was held

Eighty-seven researchers and engineers participated in the workshop and contributed oral and poster presentations on the current operation status of the sample environment and the development of new technologies.

J-PARC Workshop “Progress for Fundamental Physics with Neutrons” (September 28-29)

The J-PARC Center, the Institute of Materials Structure Science of the High Energy Accelerator Research Organization (KEK), and the Institute of Particle and Nuclear Studies of KEK jointly hosted “Progress for Fundamental Physics with Neutrons” at the KEK Tokai Building No.1 and the J-PARC Research Building. The workshop was held in a hybrid format with 15 on-site and 45 remote participants. A total of 16 presentations were made from Japan and abroad, and participants discussed future research directions, applications of the new instruments, and measurement techniques developed for materials.

Workshop at Ozora Marche 2022 in Tokai Village (October 1)

The autumn “Ozora Marche” event was held in Tokai Village for the first time in four years, and the J-PARC Center exhibited crafting lessons for bead bands that change color under ultraviolet light and a superconducting coaster in the children’s corner. More than 500 parents and children visited our booth and had fun with the mysterious behavior of superconducting materials.



Experience of Mysterious Behavior of Superconducting Material

Lecture at KIPP Nakameguro, Children’s After-school Care Program at Nakameguro Elementary School (October 8)

The J-PARC Center held a lecture titled “World’s Smallest? Let’s get to know the elementary particles by

making a mysterious spinning top!” The participants were 14 students from elementary school’s first to sixth grades. They rotated the gyroscope and experimented to see what happened when they changed the center of gravity of the handmade top. The lecturer was Dr. Tsutomu Mibe of the Particle and Nuclear Physics Division.

Workshop at Open house of QST in Naka (October 16)

The J-PARC Center conducted a workshop, “Let’s Make a Kaleidoscope of Light,” at the Naka Fusion Institute of the National Institutes for Quantum Science and Technology open house event. 171 parents and children gathered at the J-PARC booth to learn about spectroscopy’s principles and enjoy making “Kaleidoscopes of Light” crafts.



Observing various kinds of lights with handmade kaleidoscopes

J-PARC Center and ESS ERIC (European Spallation Source ERIC) Celebrate Renewal of Cooperation Agreement in Field of Spallation Neutron Source Development

The renewed cooperation agreement between the J-PARC Center and ESS in the field of spallation neu-

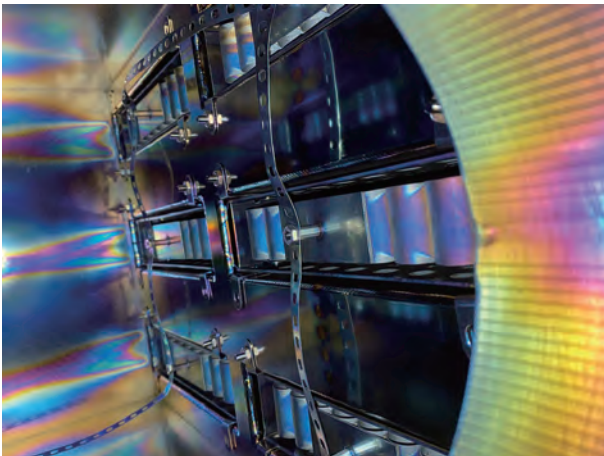


Kobayashi, Director of the J-PARC Center, and Schober, Director General of the ESS handling over the signed agreement.

tron source development, which aims to utilize each other's potential for further development in this field through the exchange of information and technology and the human resources, was signed on June 8, 2022. On October 10, a ceremony to extend the agreement was held in Lund, Sweden, where ESS is located, in the presence of the Japanese Ambassador to Sweden, Mr. Noke Masaki. The signed agreement was handed over between Dr. Kobayashi, Director of J-PARC Center, and Dr. Schober, Director General of ESS.

J-PARC Photo Contest 2022

The annual fall J-PARC Photo Contest, now in its ninth year, received 34 entries from J-PARC staff, users, and others. After careful selection, one Grand Prize winner, two Excellence Award winners, and seven Honorable Mentions were selected. The Grand Prize was awarded to Mr. Masahiko Uota of Accelerator Section 5 for his work entitled "Do specular reflection images in a vacuum duct dream of ray-tracing in a quadrupole magnet?"



Excellence Award
"The art inside the ion pump" by Mr. Masahiko Uota

7th Symposium on Integration of Humanities and Science (November 2 and 3)

The world's most intense negative muon beam, generated at J-PARC's MLF, is being used to study cultural artifacts. The KEK Institute of Materials Structure Science organized the "Symposium on Integration of Humanities and Science" to promote collaboration between cultural heritage researchers and quantum beam researchers. The 7th symposium, "Exploring History with Quantum Beams," featured presentations by experts in archaeology, cultural heritage research, and quantum beams. The symposium aimed to facilitate a non-destructive analysis of cultural heritage. A general

lecture was also held to explain recent achievements to the public. The event was attended by about 70 participants, with 23 oral presentations and three general lectures.



Group photo at the general lecture of the Symposium for the Integration of Humanities and Science

22nd Science Festival for Youth in Hitachi, "Are Magnets and Electricity Good Friends?" (October 23, Hitachi Civic Center)

The 22nd Science Festival for Youth in Hitachi was held on-site for the first time in three years. The J-PARC booth offered a craft workshop on constructing a monopole motor. Dr. Tomohiro Takayanagi explained how the copper wire turns with Fleming's left-hand rule. He also explained that the accelerators at J-PARC operate on the same principle. The children enjoyed the experiment by reversing the magnet's poles and changing the copper wire's shape. They learned how magnets and electricity can work together to create motion.



Dr. Takayanagi explains the principle of single-pole motor.

SACRIE☆ School "Let's Investigate Elementary Particles through Experiments with Tops!" at Hitachi Civic Center (November 5)

Dr. Masashi Otani of Accelerator Section Seven gave lessons to the science experiment class organized by the Hitachi Civic Center Science Museum (SACRIE).

Eight groups of 16 parents and children from the general public attended the morning session. Seventeen children from the Japan Space Youth League of the Hitachi Civic Center Division participated in the afternoon session. Through experiments with compasses, magnets, and gyroscopes, the children had fun learning about the properties of magnets, electric current, and precession.

Won Science Award at 5th Science Photo Contest

Mr. Masahiko Uota of Accelerator Section V, Accelerator Division won the Science Award in the General Category at the 5th Science Photo Contest sponsored by the Union of Organization on Science and Technology (UOST) and co-sponsored by the Ministry of Education, Culture, Sports, Science, and Technology. His photo work was entitled "Do specular reflection images in quadrupole magnet ducts dream of ray tracing?" and also won the Grand Prize in the J-PARC Photo Contest 2022.



"Do specular reflection images in quadrupole magnet ducts dream of ray tracing?" by Mr. Masahiko Uota

Experimental Workshop "Let's Make Spinning Top Spinning on Tilted!" at Tama Rokuto Science Museum at Tama Rokuto Science Museum (January 15)

The J-PARC Center, together with KEK and Tamarokuto Science Center, hosted a science experiment event to make a spinning top spin on tilted and investigate the relationship between electricity and magnets. The workshop, conducted by Dr. Masashi Otani of the Accelerator Division of J-PARC Center and Ms. Yuka Ibaraki of Nagoya University, was held for students from 4th grade to high school. Nine students attended both the morning and afternoon classes and enthusiastically participated in experiments on magnets and electric

currents using a directional magnet, observing precession using a gyroscope, and creating a state in which no precession occurs by shifting the center of gravity using a handmade spinning top.

17th Tokai Forum "Towards Social Implementation of Research and Development Achievements" (February 9)

The Tokai forum is held annually to help local residents understand the activities of the Tokai Area of the Japan Atomic Energy Agency (JAEA). This year, the forum was held face-to-face for the first time in four years, and 100 people attended the event at the Tokai Culture Center, which was also streamed online. The director of the J-PARC Center Kobayashi gave an overview of the accelerators and neutron experiments. Then, Dr. Kamiya, Sub Leader of Accelerator Section III, presented a report titled "Development of Energy-Saving and Space-saving Ultra-High Vacuum Pumps Using Vacuum Technology of J-PARC Accelerator."

T2K Collaboration Meeting Held (February 6-10)

A T2K Collaboration Meeting was held at the AYA'S LABORATORY Quantum Beam Research Center (AQ-BRC). This was the first on-site meeting in the past three years, and 115 collaborators, including researchers from overseas, participated. The neutrino beam period is scheduled to start in April after a two-year-long shutdown for the Main Ring (MR) upgrade. In the near future, the neutrino beam power will exceed 750 kW, which is the first goal since the start of the experiment in 2009. The upgrade of the nearby detectors at the J-PARC site is also underway. These developments were reported and actively discussed at the meeting.



Group photo of attendees

J-PARC Hello Science "Story of Vacuum Aiming Toward Complete Emptiness" (February 24)

Dr. Junichiro Kamiya of the Accelerator Division Section III gave the February Hello Science lecture. He introduced the over 2,000 years long history of vacuums starting with the ancient Greeks. In the 17th century, a series of experiments were conducted in Europe to prove the existence of vacuum. One of them, the Magdeburg hemisphere experiment, was demonstrated by the participants of this lecture. Dr. Kamiya also explained the vacuum technology that aimed to almost empty and the application of this technology. He also introduced the possibility of applying the technology to various industries, such as medicine and logistics.



Magdeburg hemisphere experiment

Quantum Beam Science Festa 2022 with the 14th MLF Symposium and the 40th PF* Symposium (March 13-15)

The Quantum Beam Science Festa, consisting of the MLF Symposium and the PF, KEK Photon Factory, Symposium, is held annually under the auspices of the KEK Institute for Materials Structure Science, the J-PARC Center, the Comprehensive Research Organization for Science and Society (CROSS), the PF Users Association (PF-UA), and the J-PARC MLF Users Society. For the first time in a long time, the Quantum Beam Science Festa was held in person with about 400 participants at Tsukuba International Conference Center and online with 475 participants. The MLF Symposium was held online with about 290 participants. The Quantum Beam Science Festa featured two keynote lectures, six parallel sessions, and about 230 poster presentations, with the keynote lectures broadcast online and attended by more than 100 accounts.

3rd International Workshop on Hadron Facility Expansion Project (March 14-16)

The workshop consisted of a plenary session and three parallel sessions on hadron physics, strangeness nuclear physics, and flavor physics, the main research areas at the J-PARC Hadron Experimental Facility (HEF) was held at AQBRC, KEK Tokai 1st Building and online. Eighty-nine talks were presented, discussing the extension project of HEF and the latest state of physics research, both experimental and theoretical aspects. Of the 188 registered participants, 59 were from foreign institutions, about 60 were present in person, and ten came from overseas.



Group photo of online participants

Visitors

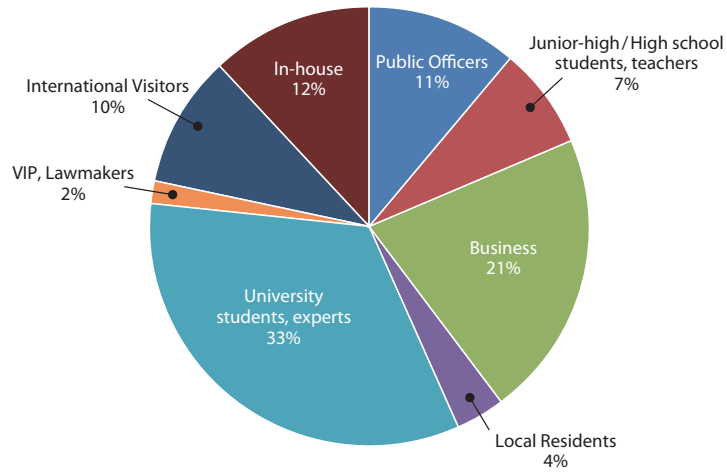
David Gurgendze, Rector of Georgian Technical University (November 4th)

Beate Heinemann, Director of Particle Physics of Deutsches Elektronen-Synchrotron DESY (November 11th)

George Freeman, Minister for Science, Research and Innovation, Department for Business, Energy and Industrial Strategy (December 14th)

Abdul Rahim Bin Harun, Director General of Malaysian Nuclear Agency (March 14th)

There were 1,102 visitors to J-PARC for the period from April 2022 to the end of March 2023.



Publications

Publications in Periodical Journals

- A-001
M. Otani
Muon cooling and acceleration
AAPPS bulletin, 32, 6 (2022)
- A-002
K. Ohishi, *et al.*
Operando Muon Spin Rotation and Relaxation Measurement on LiCoO₂ Half-Cell
ACS Appl. Energy Mater., 5, 12538–12544 (2022).
- A-003
H. Kawaura, *et al.*
Effects of Lithium Bis(oxalate)Borate Electrolyte Additive on the Formation of a Solid Electrolyte Interphase on Amorphous Carbon Electrodes by Operando Time-Slicing Neutron Reflectometry
ACS Appl. Mater. Interfaces, 14, 24526–24535 (2022).
- A-004
T. T. Chuong, *et al.*
Giant Carbon Nano-Test Tubes as Versatile Imaging Vessels for High-Resolution and in situ Observation of Proteins
ACS Appl. Mater. Interfaces, 14, 26507–26516 (2022).
- A-005
W. Yoshimune, *et al.*
Interfacial Distribution of Nafion Ionomer Thin Films on Nitrogen-Modified Carbon Surfaces
ACS Appl. Mater. Interfaces, 14, 53744–53754 (2022).
- A-006
M. Inutsuka, *et al.*
Effect of Oligomer Segregation on the Aggregation State and Strength at the Polystyrene/Substrate Interface
ACS Macro Lett., 11, 504–509 (2022).
- A-007
E. Saiki, *et al.*
Evidence of Long Two-Dimensional Folding Chain Structure Formation of Poly(vinylidene fluoride) in N-Methylpyrrolidone Solution: Total Form Factor Determination by Combining Multiscattering Data
ACS Omega, 7, 22825–22829 (2022).
- A-008
E. Saiki, *et al.*
Elongated Rodlike Particle Formation of Methyl Cellulose in Aqueous Solution
ACS Omega, 7, 28849–28859 (2022).
- A-009
K. Ohishi, *et al.*
Hard Carbon Studied with Positive Muon Spin Rotation and Relaxation
ACS Phys. Chem. Au, 2, 98–107 (2022).
- A-010
T. Kawasaki, *et al.*
Rearrangement of Hydrogen Bonds in Dehydrated Raffinose Tetrahydrate: A Time-of-Flight Neutron Diffraction Study
Acta Crystallogr. Sect. C Struct. Chem., 78, 743–748 (2022).
- A-011
Y. Terasawa, *et al.*
Single-Crystal Structure Analysis of Non-Deuterated Triglycine Sulfate by Neutron Diffraction at 20 and 298 K: A New Disorder Model for the 298 K Structure
Acta Crystallogr. Sect. E Crystallogr. Commun., 78, 306–312 (2022).
- A-012
T. Chatake, *et al.*
Protonation States of Hen Egg-White Lysozyme Observed Using D/H Contrast Neutron Crystallography
Acta Crystallogr. Sect. Struct. Biol., 78, 770–778 (2022).
- A-013
K. Okada, *et al.*
Effect of Hydrogen on Evolution of Deformation Microstructure in Low-Carbon Steel with Ferrite Microstructure
Acta Mater., 225, 117549 (2022).
- A-014
D. Wei, *et al.*
Metalloid Substitution Elevates Simultaneously the Strength and Ductility of Face-Centered-Cubic High-Entropy Alloys
Acta Mater., 225, 117571 (2022).
- A-015
M. Liu, *et al.*
Achieving Excellent Mechanical Properties in Type 316 Stainless Steel by Tailoring Grain Size in Homogeneously Recovered or Recrystallized Nanostructures
Acta Mater., 226, 117629 (2022).
- A-016
K. Sakaki, *et al.*
Displacement of Hydrogen Position in Di-Hydride of V-Ti-Cr Solid Solution Alloys
Acta Mater., 234, 118055 (2022).
- A-017
R. Zheng, *et al.*
Rediscovery of Hall-Petch Strengthening in Bulk Ultrafine Grained Pure Mg at Cryogenic Temperature: A Combined in-situ Neutron Diffraction and Electron Microscopy Study
Acta Mater., 238, 118243 (2022).
- A-018
R. S. Ramadhan, *et al.*
Mechanical Surface Treatment Studies by Bragg Edge Neutron Imaging
Acta Mater., 239, 118259 (2022).
- A-019
Q. Li, *et al.*
Large Tunable Thermal Expansion in Ferroelastic Alloys by Stress
Acta Mater., 240, 118350 (2022).
- A-020
B. Guo, *et al.*
Unexpected Dynamic Transformation from α Phase to β Phase in Zirconium Alloy Revealed by in-situ Neutron Diffraction during High Temperature Deformation
Acta Mater., 242, 118427 (2022).
- A-021
T. Sawaguchi, *et al.*
Evidence Supporting Reversible Martensitic Transformation under Cyclic Loading on Fe–Mn–Si–Al Alloys Using in situ Neutron Diffraction
Acta Mater., 242, 118494 (2022).
- A-022
K. Ozawa, *et al.*
Towards the Measurement of the Mass Modifications of Vector Mesons in a Finite Density Matter
Acta Physica Polonica A 142, 399–401 (2022)
- A-023
X. Xu, *et al.*
Tough Yet Flexible Superelastic Alloys Meet Biomedical Needs
Adv. Mater. Process., 180, 35–37 (2022).
- A-024
M. Ohira, *et al.*
Star-Polymer–DNA Gels Showing Highly Predictable and Tunable Mechanical Responses
Adv. Mater., 34, 2108818 (2022).
- A-025
T. Odaira, *et al.*
Flexible and Tough Superelastic Co–Cr Alloys for Biomedical Applications
Adv. Mater., 34, 2202305 (2022).
- A-026
K. Okamoto, *et al.*
Impact of Na Concentration on the Phase Transition Behavior and H– Conductivities in the Ba–Li–Na–H–O Oxyhydride System
Adv. Sci., 10, 2203541 (2022).
- A-027
E. Nomura, *et al.*
Magnetization Process of Cubic Fe₃O₄ Submicron Particles Studied by Polarized Small-Angle Neutron Scattering
AIP Adv., 12, 035034 (2022).

- A-028
T. Ohashi, *et al.*
Structure of Basaltic Glass at Pressures up to 18 Gpa
Am. Mineral., 107, 325–335 (2022).
- A-029
K. Kino, *et al.*
Nondestructive Quantitative Imaging for Spatially Nonuniform Degradation in a Commercial Lithium-Ion Battery Using a Pulsed Neutron Beam
Appl. Phys. Express, 15, 027005 (2022).
- A-030
K. Hayashi, *et al.*
Determination of Site Occupancy of Boron in 6H–SiC by Multiple-Wavelength Neutron Holography
Appl. Phys. Lett., 120, 132101 (2022).
- A-031
K. Akutsu-Suyama, *et al.*
New Design of a Sample Cell for Neutron Reflectometry in Liquid–Liquid Systems and Its Application for Studying Structures at Air–Liquid and Liquid–Liquid Interfaces
Appl. Sci., 12, 1215 (2022).
- A-032
Y. Hirota, *et al.*
Hydrogen Dynamics in Hydrated Chitosan by Quasi-Elastic Neutron Scattering
Bioengineering, 9, 599 (2022).
- A-033
T. Sogabe, *et al.*
Effect of Water Activity on the Mechanical Glass Transition and Dynamical Transition of Bacteria
Biophys. J., 121, 3874–3882 (2022).
- A-034
Y. Kameda, *et al.*
Neutron Diffraction with $34\text{ S}/\text{nat S}$ Isotopic Substitution Method on the Solvation Structure of S8 Molecule in Concentrated CS₂ Solutions
Bull. Chem. Soc. Jpn., 95, 1481–1485 (2022).
- A-035
S. H. Song, *et al.*
Rational Design of Li Off-Stoichiometric Ni-Rich Layered Cathode Materials for Li-Ion Batteries
Chem. Eng. J., 448, 137685 (2022).
- A-036
A. Hoshikawa, *et al.*
Observation of Hydrogen Bonding Network in Hydrogen Sulfide Hydrate Using Neutron Diffraction
Chem. Phys. Lett., 812, 140274 (2022).
- A-037
L. Zheng, *et al.*
Universal Dynamical Onset in Water at Distinct Material Interfaces
Chem. Sci., 13, 4341–4351 (2022).
- A-038
C. Tsutsumi-Arai, *et al.*
Antimicrobial Surface Processing of Polymethyl Methacrylate Denture Base Resin Using a Novel Silica-Based Coating Technology
Clin. Oral Investig., 27, 1043–1053 (2022).
- A-039
N. V. Mdllovu, *et al.*
Design of Doxorubicin Encapsulated pH-/Thermo-Responsive and Cationic Shell-Crosslinked Magnetic Drug Delivery System
Colloids Surf. B Biointerfaces, 209, 112168 (2022).
- A-040
M. Akamatsu, *et al.*
Controlled Recombination Rate of Lophyl Radicals in Cationic Surfactant Micelles
Colloids Surf. Physicochem. Eng. Asp., 638, 128319 (2022).
- A-041
Y. Furuie, *et al.*
Cross-Scale Analysis of Temperature Compensation in the Cyanobacterial Circadian Clock System
Commun. Phys., 5, 75 (2022).
- A-042
K. Komatsu
Neutrons Meet Ice Polymorphs
Crystallogr. Rev., 28 224–297 (2022).
- A-043
J. Kamiya, *et al.*
Evaluation of titanium vacuum chamber as getter pump
e-Journal of Surface Science and Nanotechnology (Internet), 20(2), p.107 - 118, 2022/05
- A-044
Y. Hino, *et al.*
Characterization of the correlated background for a sterile neutrino search using the first dataset of the JSNS² experiment
Eur. Phys. J. C 82, 331(2022)
- A-045
A. Abed Abud, *et al.*
Scintillation light detection in the 6-m drift-length ProtoDUNE Dual Phase liquid argon TPC
Eur. Phys. J. C 82, 618(2022)
- A-046
K. Abe, *et al.*
Separation of track- and shower-like energy deposits in ProtoDUNE-SP using a convolutional neural network
Eur. Phys. J. C 82, 903 (2022)
- A-047
M. Shibata, *et al.*
Micellar Aggregation and Thermogelation of Amphiphilic Random Copolymers in Water Hierarchically Dependent on Chain Length
Eur. Polym. J., 168, 111091 (2022).
- A-048
N. Kitamura, *et al.*
Effects of Ca Substitution on the Local Structure and Oxide–Ion Behavior of Layered Perovskite Lanthanum Nickelate
Front. Mater., 9, 954729 (2022).
- A-049
D. Gong, *et al.*
Nematic Fluctuations in the Non-Superconducting Iron Pnictide BaFe_{1.9–x}Ni_{0.1}Cr_xAs₂
Front. Phys., 10, 886459 (2022).
- A-050
K. Yamashita, *et al.*
Improvement of Nano-Polycrystalline Diamond Anvil Cells with Zr-Based Bulk Metallic Glass Cylinder for Higher Pressures: Application to Laue-TOF Diffractometer
High Press. Res., 42, 121–135 (2022).
- A-051
T. Hattori, *et al.*
Development of a Hybrid Piston Cylinder Cell for Quasielastic Neutron Scattering Experiments up to 1 GPa
High Press. Res., 42, 226–235 (2022).
- A-052
S. Machida, *et al.*
Investigation of Null-Matrix Alloy Gaskets for a Diamond-Anvil-Cell on High Pressure Neutron Diffraction Experiments
High Press. Res., 42, 303–317 (2022).
- A-053
H. Iimura, *et al.*
Design of a Strong X-Y Coupling Beam Transport Line for J-PARC Muon g-2/EDM Experiment
IEEE Trans. Appl. Supercond., 32, 4004705 (2022)
- A-054
M. Abe, *et al.*
Design Method of Active Shield Steering Magnet for Fine Tuning of Muon Injection Orbit Into g-2/EDM Precision Measurements Magnet
IEEE Trans. Appl. Supercond., 32, 4007505 (2022)
- A-055
N. Sumi, *et al.*
Construction Status of the Superconducting Magnet System for the COMET Experiment
IEEE Trans. Appl. Supercond., 32, 4101204 (2022)
- A-056
K. Oda, *et al.*
Developments of a Pulse Kicker System for

the Three-Dimensional Spiral Beam Injection of the J-PARC Muon $g-2$ /EDM Experiment
IEEE Trans. Appl. Supercond., 32, 4101504 (2022)

A-057

M. Yoshida, *et al.*
Repetitive Irradiation Tests at Cryogenic Temperature by Neutrons and Protons on Stabilizer Materials of Superconductor
IEEE Trans. Appl. Supercond., 32, 7100405 (2022)

A-058

K. Sasaki, *et al.*
Development of Precise Shimming Technique With Materials Having Low Saturation Magnetization
IEEE Trans. Appl. Supercond., 32, 9002107 (2022)

A-059

H. Tada, *et al.*
Development of Magnetic Field Mapping System for the MuSEUM Experiment With High Precision Using CW-NMR Probes
IEEE Trans. Appl. Supercond., 32, 9002205 (2022)

A-060

H. Iinuma, *et al.*
Design of a Strong X-Y Coupling Beam Transport Line for J-PARC Muon $g-2$ /EDM Experiment
IEEE Trans. Appl. Supercond., 32, 4004705 (2022)

A-061

H. Hirayama, *et al.*
Control of the Rotatable-Quadrupole Magnet Angle for a 3-D Spiral Injection Test Experiment
IEEE Trans. Appl. Supercond., 32, 4005705 (2022)

A-062

M. Abe, *et al.*
Design Method of Active Shield Steering Magnet for Fine Tuning of Muon Injection Orbit Into $g-2$ /EDM Precision Measurements Magnet
IEEE Trans. Appl. Supercond., 32, 4007505 (2022)

A-063

Y. Fuwa, *et al.*
Development of Combined-Function Multipole Permanent Magnet for High-Intensity Beam Transportation
IEEE Trans. Appl. Supercond., 32, 6, 4006705 (2022)

A-064

T. Takayanagi, *et al.*
Evaluation of Eddy Currents Dependent on Excitation Pattern in Design of Pulse Electromagnets
IEEE Trans. Appl. Supercond., 32, 6, 1401405 (2022)

A-065

Y. Iwamiya, *et al.*
Photocatalytic Silica-Resin Coating for Environmental Protection of Paper as a

Plastic Substitute

Ind. Eng. Chem. Res., 61, 6967–6972 (2022).

A-066

K. Takaya, *et al.*
A Real-Time Gas Monitoring System Based on Ion Mobility Spectrometry for Workplace Environmental Measurements
Ind. Health, 60, 40–46 (2021).

A-067

T. Yajima, *et al.*
High-Pressure Synthesis of Transition-Metal Oxyhydrides with Double-Perovskite Structures
Inorg. Chem., 61, 2010–2016 (2022).

A-068

M. K. Sugumar, *et al.*
Preparation of Li-Excess and Li-Deficient Antiperovskite Structured $\text{Li}_{2+x}\text{OH}_{1-x}\text{Br}$ and Their Effects on Total Ionic Conductivity
Inorg. Chem., 61, 4655–4659 (2022).

A-069

Y. Yasuda, *et al.*
Visualization of the Working Fluid in a Flat-Plate Pulsating Heat Pipe by Neutron Radiography
Int. J. Heat Mass Transf., 185, 122336 (2022).

A-070

D. Wei, *et al.*
Mechanical Behaviors of Equiatomic and Near-Equiatomic Face-Centered-Cubic Phase High-Entropy Alloys Probed Using in situ Neutron Diffraction
Int. J. Plast., 158, 103417 (2022).

A-071

D. Wei, *et al.*
Si-Addition Contributes to Overcoming the Strength-Ductility Trade-off in High-Entropy Alloys
Int. J. Plast., 159, 103443 (2022).

A-072

Y. Oba, *et al.*
Characterization of Deformation by Cold Rolling in Ferritic Steel Containing Cu Particles Using Neutron Transmission Analysis
ISIJ Int., 62, 173–178 (2022).

A-073

S. Harjo, *et al.*
Revisit Deformation Behavior of Lath Martensite
ISIJ Int., 62, 1990–1999 (2022).

A-074

M. Koyama, *et al.*
Microstructure and Plasticity Evolution During Lüders Deformation in an Fe-5Mn-0.1C Medium-Mn Steel
ISIJ Int., 62, 2036–2042 (2022).

A-075

M. Koyama, *et al.*
Hierarchical Deformation Heterogeneity during Lüders Band Propagation in an Fe-5Mn-0.1C Medium Mn Steel Clarified through *in situ* Scanning Electron Microscopy
ISIJ Int., 62, 2043–2053 (2022).

A-076

H. Sato, *et al.*
Visualising Martensite Phase Fraction in Bulk Ferrite Steel by Superimposed Bragg-Edge Profile Analysis of Wavelength-Resolved Neutron Transmission Imaging
ISIJ Int., 62, 2319–2330 (2022).

A-077

H. Uchima, *et al.*
Impact of Dislocation Density and Mobility on Yielding Behavior in Quenched Medium-Carbon Martensitic Steel Tempered at Low Temperature
ISIJ Int., 62, 998–1003 (2022).

A-078

T. Murakawa, *et al.*
Re-Evaluation of Protein Neutron Crystallography with and without X-Ray/Neutron Joint Refinement
IUCr, 9, 342–348 (2022).

A-079

Z. Deng, *et al.*
Multifunctional Nanostructured NiTi Alloy with Invar, Elinvar and Rinvar Properties
J. Alloys Compd., 909, 164682 (2022).

A-080

D. Yun, *et al.*
Stress Contribution of B2 Phase in $\text{Al}_{0.7}\text{CoCrFeNi}$ Eutectic High Entropy Alloy
J. Alloys Compd., 918, 165673 (2022).

A-081

K. Fukui, *et al.*
Room-Temperature Fast H^- Conduction in Oxygen-Substituted Lanthanum Hydride
J. Am. Chem. Soc., 144, 1523–1527 (2022).

A-082

T. Kumada, *et al.*
Structure Analysis of a Buried Interface between Organic and Porous Inorganic Layers Using Spin-Contrast-Variation Neutron Reflectivity
J. Appl. Crystallogr., 55, 1147–1153 (2022).

A-083

K. Ikeda, *et al.*
Pressure Cells for in situ Neutron Total Scattering: Time and Real-Space Resolution during Deuterium Absorption
J. Appl. Crystallogr., 55, 1631–1639 (2022).

A-084

F. Malamud, *et al.*

Non-Destructive Characterization of the Spatial Variation of γ/γ' Lattice Misfit in a Single-Crystal Ni-Based Superalloy by Energy-Resolved Neutron Imaging
J. Appl. Crystallogr., 55, 228–239 (2022).

A-085

K. Tatsumi, *et al.*

Optimization and Inference of Bin Widths for Histogramming Inelastic Neutron Scattering Spectra
J. Appl. Crystallogr., 55, 533–543 (2022).

A-086

T. Kawasaki, *et al.*

Operando Structure Observation of Pyroelectric Ceramics during Power Generation Cycle
J. Appl. Phys., 131, 134103 (2022).

A-087

M. Hiraishi, *et al.*

Ambipolarity of Diluted Hydrogen in Wide-Gap Oxides Revealed by Muon Study
J. Appl. Phys., 132, 105701 (2022).

A-088

Y. Sakuda, *et al.*

Improved Oxide-Ion and Lower Proton Conduction of Hexagonal Perovskite-Related Oxides Based on $\text{Ba}_7\text{Nb}_4\text{MoO}_{20}$ by Cr^{6+} Doping
J. Ceram. Soc. Jpn., 130, 442–447 (2022).

A-089

Y. Mitsuya, *et al.*

Energy-Resolved Neutron Imaging with Glass Gas Electron Multiplier and Dynamic Time-over-Threshold Method
J. Instrum., 17, C01006 (2022).

A-090

A. Abed Abud, *et al.*

Design, construction and operation of the ProtoDUNE-SP Liquid Argon TPC
J. Instrum., 17, P01005 (2022)

A-091

N. Muto, *et al.*

A Novel Nuclear Emulsion Detector for Measurement of Quantum States of Ultracold Neutrons in the Earth's Gravitational Field
J. Instrum., 17, P07014 (2022).

A-092

B. Yee-Rendon, *et al.*

Beam physics design of a 30-MW beam transport to the target for an accelerator-driven subcritical system
J. Instrum., 17, P10005 (2022)

A-093

K. Abe, *et al.*

Scintillator ageing of the T2K near detectors from 2010 to 2021
J. Instrum., 17, P10028 (2022)

A-094

K. Abe, *et al.*

Neutron tagging following atmospheric neutrino events in a water Cherenkov detector
J. Instrum., 17, P10029 (2022)

A-095

R. A. Jameson, *et al.*

Improved bunching and longitudinal emittance control in an RFQ
J. Instrum., 17, P12011 (2022)

A-096

K. Futatsukawa, *et al.*

Development of the novel and superior adaptive beam-loading compensation system calculated in the frequency domain for the J-PARC Linac
J. Instrum., 17, T11002 (2022)

A-097

W. Gong, *et al.*

In-situ Observation of Twinning and Detwinning in AZ31 Alloy
J. Magnes. Alloys, 10, 3418–3432 (2022).

A-098

K. Okamoto, *et al.*

Stabilization of a High H^- -Conducting Phase via K Doping of Ba–Li Oxyhydride
J. Mater. Chem. A, 10, 23023–23027 (2022).

A-099

D. Wei, *et al.*

Strengthening of High-Entropy Alloys via Modulation of Cryo-Pre-Straining-Induced Defects
J. Mater. Sci. Technol., 129, 251–260 (2022).

A-100

J. Yang, *et al.*

Mictomagnetism and Suppressed Thermal Conduction of the Prototype High-Entropy Alloy CrMnFeCoNi
J. Mater. Sci. Technol., 99, 55–60 (2022).

A-101

H. Abe, *et al.*

Spontaneous Formations of Nanoconfined Water in Ionic Liquids by Small-Angle Neutron Scattering
J. Mol. Liq., 346, 117035 (2022).

A-102

W. Q. Zhang, *et al.*

Structure of an Aqueous RbCl Solution in the Gigapascal Pressure Range by Neutron Diffraction Combined with Empirical Potential Structure Refinement Modeling
J. Mol. Liq., 348, 118080 (2022).

A-103

T. Yamaguchi, *et al.*

Neutron Scattering on an Aqueous Sodium Chloride Solution in the Gigapascal Pressure Range

J. Mol. Liq., 365, 120181 (2022).

A-104

K. Yoshida, *et al.*

The Translational, Rotational, and Phonon Dynamics of Water in ZrO_2 /Water Nanofluid
J. Mol. Liq., 366, 120218 (2022).

A-105

R. Motokawa, *et al.*

Nanoscope Structure of Borosilicate Glass with Additives for Nuclear Waste Vitrification
J. Non-Cryst. Solids, 578, 121352 (2022).

A-106

D. Ito, H, *et al.*

Spatial Distribution and Preferred Orientation of Crystalline Microstructure of Lead-Bismuth Eutectic
J. Nucl. Mater., 569, 153921 (2022).

A-107

G. Ariyoshi, *et al.*

Development of a miniature electromagnet probe for the measurement of local velocity in heavy liquid metals
J. Nucl. Sci. Technol., 59, 1071 (2022)

A-108

G. Rovira, *et al.*

KeV-Region Analysis of the Neutron Capture Cross-Section of ^{237}Np
J. Nucl. Sci. Technol., 59, 110–122 (2022).

A-109

K. Yamamoto, *et al.*

Design and actual performance of J-PARC 3 GeV rapid cycling synchrotron for high-intensity operation
J. Nucl. Sci. Technol., 59, 1174 - 1205 (2022)

A-110

H. Nakano, *et al.*

Development of a neutron beam monitor with a thin plastic scintillator for nuclear data measurement using spallation neutron source
J. Nucl. Sci. Technol., 59, 1499-1506 (2022).

A-111

S. Endo, *et al.*

Neutron Capture and Total Cross-Section Measurements and Resonance Parameter Analysis of Niobium-93 below 400 eV
J. Nucl. Sci. Technol., 59, 318–333 (2022).

A-112

G. Rovira, *et al.*

KeV-neutron capture cross-section measurement of ^{197}Au with a Cr-filtered neutron beam at the ANNRI beamline of MLF/J-PARC
J. Nucl. Sci. Technol., 59, 647-655 (2022).

A-113

H. Iwamoto, *et al.*

Measurement of 107-MeV proton-induced

- double-differential thick target neutron yields for Fe, Pb, and Bi using a fixed-field alternating gradient accelerator at Kyoto University
J. Nucl. Sci. Technol., 60, 435 (2022)
- A-114
G. Rovira, *et al.*
 ^{241}Am Neutron Capture Cross Section in the KeV Region Using Si and Fe-Filtered Neutron Beams
J. Nucl. Sci. Technol., 60, 489–499 (2022).
- A-115
A. Kimura, *et al.*
Neutron Total and Capture Cross-Section Measurements of ^{155}Gd and ^{157}Gd in the Thermal Energy Region with the Li-Glass Detectors and NaI(Tl) Spectrometer Installed in J-PARC-MLF-ANNRI
J. Nucl. Sci. Technol., 60, 678–696 (2022).
- A-116
M. Uyama, *et al.*
Neutron Reflectometry & Simultaneous Measurements of Rheology and Small Angle Neutron Scattering Studies for Polyether Modified Silicone Vesicle Systems
J. Oleo Sci., 71, 1625–1637 (2022).
- A-117
T. Tominaga, *et al.*
Experimental Evidence of Slow Mode Water in the Vicinity of Poly(ethylene oxide) at Physiological Temperature
J. Phys. Chem. B, 126, 1758–1767 (2022).
- A-118
I. Umegaki, *et al.*
Negative Muon Spin Rotation and Relaxation Study on Battery Anode Material, Spinel $\text{Li}_4\text{Ti}_5\text{O}_{12}$
J. Phys. Chem. C, 126, 10506–10514 (2022).
- A-119
T. Sato, *et al.*
Effect of Co-Substitution on Hydrogen Absorption and Desorption Reactions of YMgNi_4 -Based Alloys
J. Phys. Chem. C, 126, 16943–16951 (2022).
- A-120
S. Hori, *et al.*
Revealing the Ion Dynamics in $\text{Li}_{10}\text{GeP}_2\text{S}_{12}$ by Quasi-Elastic Neutron Scattering Measurements
J. Phys. Chem. C, 126, 9518–9527 (2022).
- A-121
M. Nakano, *et al.*
Energetic and Structural Insights into Phospholipid Transfer from Membranes with Different Curvatures by Time-Resolved Neutron Scattering
J. Phys. Chem. Lett., 13, 6024–6030 (2022).
- A-122
R. Akiyama, *et al.*
Direct Probe of the Ferromagnetic Proximity Effect at the Interface of SnTe/Fe Heterostructure by Polarized Neutron Reflectometry
J. Phys. Chem. Lett., 13, 8228–8235 (2022).
- A-123
M. Aizawa, *et al.*
Protein Condensation at Nanopore Entrances as Studied by Differential Scanning Calorimetry and Small-Angle Neutron Scattering
J. Phys. Chem. Lett., 13, 8684–8691 (2022).
- A-124
S. Shimono, *et al.*
Structural Phase Transition in Cobalt Oxyfluoride $\text{Co}_3\text{Sb}_4\text{O}_6\text{F}_6$ Observed by High-Resolution Synchrotron and Neutron Diffraction
J. Phys. Chem. Solids, 163, 110568 (2022).
- A-125
T. Yamanaka, *et al.*
Enhancement of Electrical Conductivity to Metallization of $\text{Mn}_{3-x}\text{Fe}_x\text{O}_4$ Spinel and Postspinel with Elevating Pressure
J. Phys. Chem. Solids, 167, 110721 (2022).
- A-126
C. Kim, *et al.*
Antiferromagnetic Kitaev Interaction in $J_{\text{eff}} = 1/2$ Cobalt Honeycomb Materials $\text{Na}_3\text{Co}_2\text{SbO}_6$ and $\text{Na}_2\text{Co}_2\text{TeO}_6$
J. Phys. Condens. Matter, 34, 045802 (2022).
- A-127
K. Kataoka, *et al.*
Pyrochlore Oxide $\text{Hg}_2\text{Os}_2\text{O}_7$ on Verge of Metal–Insulator Boundary
J. Phys. Condens. Matter, 34, 135602 (2022).
- A-128
T. Xie, *et al.*
Spin Fluctuations in the 112-Type Iron-Based Superconductor $\text{Ca}_{0.82}\text{La}_{0.18}\text{Fe}_{0.96}\text{Ni}_{0.04}\text{As}_2$
J. Phys. Condens. Matter, 34, 474001 (2022).
- A-129
K. Kakimoto, *et al.*
Magnetism of $\text{Al}_x\text{Fe}_{2-x}\text{GeO}_5$ with Andalusite Structure
J. Phys. Soc. Jpn., 91, 054704 (2022).
- A-130
K. Kakimoto, *et al.*
Sinusoidal Magnetic Structure of Andalusite-Type $\text{Al}_x\text{Fe}_{2-x}\text{GeO}_5$ with $x = 0.09$ and 0.1
J. Phys. Soc. Jpn., 91, 054707 (2022).
- A-131
N. Metoki, *et al.*
Hyperfine Splitting and Nuclear Spin Polarization in NdPd_5Al_2 and $\text{Nd}_3\text{Pd}_{20}\text{Ge}_6$
J. Phys. Soc. Jpn., 91, 054710 (2022).
- A-132
T. Matsumura, *et al.*
Cycloidal Magnetic Ordering in Noncentrosymmetric EuIrGe_3
J. Phys. Soc. Jpn., 91, 073703 (2022).
- A-133
D. Ueta, *et al.*
Anomalous Magnetic Moment Direction under Magnetic Anisotropy Originated from Crystalline Electric Field in van Der Waals Compounds CeTe_3 and CeTe_2Se
J. Phys. Soc. Jpn., 91, 094706 (2022).
- A-134
M. Soda, *et al.*
Magnetic Diffuse and Quasi-Elastic Scatterings in Frustrated Magnet YBaCo_4O_7
J. Phys. Soc. Jpn., 91, 094707 (2022).
- A-135
M. Nasu, *et al.*
Neutron Imaging of Generated Water inside Polymer Electrolyte Fuel Cell Using Newly-Developed Gas Diffusion Layer with Gas Flow Channels during Power Generation
J. Power Sources, 530, 231251 (2022).
- A-136
K. Saito, *et al.*
Oxide-Ion and Proton Conductivity of the Ordered Perovskite $\text{BaY}_{1/3}\text{Ga}_{2/3}\text{O}_{2.5}$
J. Solid State Chem., 306, 122733 (2022).
- A-137
F. Abudinen, *et al.*
Combined analysis of Belle and Belle II data to determine the CKM angle ϕ_3 using $B^+ \rightarrow D(K^0 h^+ h^-) h^+$ decays
Journal of High Energy Physics, 02, 63 (2022)
- A-138
S.X. Li, *et al.*
First measurement of the $\Lambda_c^+ \rightarrow p \eta'$ decay
Journal of High Energy Physics, 03, 90 (2022)
- A-139
K. Inami, *et al.*
An improved search for the electric dipole moment of the τ lepton
Journal of High Energy Physics, 04, 110 (2022)
- A-140
F. Abudinen, *et al.*
Search for charged lepton flavor violating decays of $Y(1S)$
Journal of High Energy Physics, 05, 95 (2022)
- A-141
S. Sasada, *et al.*
Strain Distribution Visualization of Punched Electrical Steel Sheets Using Neutron Bragg-Edge Transmission Imaging
Jpn. J. Appl. Phys., 61, 046004 (2022).
- A-142
K. Shimokita, *et al.*

Neutron Reflectivity Study on the Suppression of Interfacial Water Accumulation between a Polypropylene Thin Film and Si Substrate Using a Silane-Coupling Agent
Langmuir, 38, 12457–12465 (2022).

A-143
K. Yamaoka, *et al.*
Interfacial Selective Study on the Gelation Behavior of Aqueous Methylcellulose Solution via a Quartz Crystal Microbalance
Langmuir, 38, 4494–4502 (2022).

A-144
D. Ihara, *et al.*
Cononsolvency of Poly[2-(methacryloyloxy)ethyl phosphorylcholine] in Ethanol–Water Mixtures: A Neutron Reflectivity Study
Langmuir, 38, 5081–5088 (2022).

A-145
Y. Xie, *et al.*
Hydrophobicity of the Pentafluorosulfanyl Group in Side Chains of Polymethacrylates by Evaluation with Surface Free Energy and Neutron Reflectivity
Langmuir, 38, 6472–6480 (2022).

A-146
Y. Higaki, *et al.*
Zwitterionic Poly(carboxybetaine) Brush/Albumin Conjugate Films: Structure and Lubricity
Langmuir, 38, 9278–9284 (2022).

A-147
T. Tominaga, *et al.*
Data Collection for Dilute Protein Solutions via a Neutron Backscattering Spectrometer
Life, 12, 675 (2022).

A-148
S. Imai, *et al.*
Water-Assisted Microphase Separation of Cationic Random Copolymers into Sub-5 Nm Lamellar Materials and Thin Films
Macromolecules, 55, 9113–9125 (2022).

A-149
M. Kumagai, *et al.*
In situ Neutron Diffraction Analysis of Microstructural Evolution-Dependent Stress Response in Austenitic Stainless Steel under Cyclic Plastic Deformation
Mater. Des., 221, 110965 (2022).

A-150
K. S. N. Sessa, *et al.*
Demonstrating a Duplex TRIP/TWIP Titanium Alloy via the Introduction of Metastable Retained β -Phase
Mater. Res. Lett., 10, 754–761 (2022).

A-151
H. Dannoshita, *et al.*
Evolution of Dislocation Structure

Determined by Neutron Diffraction Line Profile Analysis during Tensile Deformation in Quenched and Tempered Martensitic Steels
Mater. Sci. Eng. A, 854, 143795 (2022).

A-152
P. Thirathipiwat, *et al.*
In-situ Neutron Diffraction Study on a Dislocation Density in a Correlation with Strain Hardening in Al–Mg Alloys
Mater. Sci. Eng. A, 855, 143956 (2022).

A-153
T.-N. Lam, *et al.*
Estimating Fine Melt Pool, Coarse Melt Pool, and Heat Affected Zone Effects on the Strengths of Additive Manufactured AlSi10Mg Alloys
Mater. Sci. Eng. A, 856, 143961 (2022).

A-154
D. Egusa, *et al.*
Quantitative X-Ray Diffraction Analysis of Solute-Enriched Stacking Faults in Hcp-Mg Alloys Based on Peak Asymmetry Analysis
Mater. Today Commun., 31, 103344 (2022).

A-155
R. Miyazaki, *et al.*
Reverse Monte Carlo Analysis of NaI-Li Solid Electrolyte Based on the Neutron Total Scattering Data
Mater. Today Commun., 32, 104014 (2022).

A-156
S. M. Suturen, *et al.*
Structural Peculiarities of ϵ -Fe₂O₃/GaN Epitaxial Layers Unveiled by High-Resolution Transmission Electron Microscopy and Neutron Reflectometry
Mater. Today Commun., 33, 104412 (2022).

A-157
E. Rathore, *et al.*
Enhanced Covalency and Nanostructured-Phonon Scattering Lead to High Thermoelectric Performance in n-Type PbS
Mater. Today Energy, 24, 100953 (2022).

A-158
H. Sasaki, *et al.*
Characterization of Precipitated Phase in Cu–Ni–Si Alloy by Small-Angle X-Ray Scattering, Small Angle Neutron Scattering and Atom Probe Tomography
Mater. Trans., 63, 1384–1389 (2022).

A-159
N. R. Jaladurgam, *et al.*
Load Redistribution in Eutectic High Entropy Alloy AlCoCrFeNi_{2.1} during High Temperature Deformation
Materialia, 22, 101392 (2022).

A-160
Y. Wang, *et al.*

Evolution of Austenite Lattice Parameter during Isothermal Transformation in a 0.4 C Low Alloyed Steel
Materialia, 27, 101685 (2022).

A-161
T. Yamada
Quasi Elastic Neutron Scattering Study on Water Dynamics in Nafion Membrane
MEMBRANE, 47, 207–212 (2022).

A-162
M.-M. Schiavone, *et al.*
On the Proton Conduction Pathways in Polyelectrolyte Membranes Based on Syndiotactic-Polystyrene
Membranes, 12, 143 (2022).

A-163
Y. Onuki, *et al.*
Microstructure Formation and Carbon Partitioning with Austenite Decomposition during Isothermal Heating Process in Fe–Si–Mn–C Steel Monitored by in situ Time-of-Flight Neutron Diffraction
Metals, 12, 957 (2022).

A-164
K. Yamanaka, *et al.*
Dislocation Density of Electron Beam Powder Bed Fusion Ti–6Al–4V Alloys Determined via Time-Of-Flight Neutron Diffraction Line-Profile Analysis
Metals, 13, 86 (2022).

A-165
K. Shiomi
Search for Rare Kaon Decays at the J-PARC KOTO Experiment
Moscow University Physics Bulletin, 77, 254 (2022)

A-166
Q. Li, *et al.*
Ferroelectric Ordering in Nanosized PbTiO₃
Nano Lett., 22, 9405–9410 (2022).

A-167
R. Takagi, *et al.*
Square and Rhombic Lattices of Magnetic Skyrmions in a Centrosymmetric Binary Compound
Nat. Commun., 13, 1472 (2022).

A-168
P. Luo, *et al.*
Q-Dependent Collective Relaxation Dynamics of Glass-Forming Liquid Ca_{0.4}K_{0.6}(NO₃)_{1.4} Investigated by Wide-Angle Neutron Spin-Echo
Nat. Commun., 13, 2092 (2022).

A-169
Y. Yu, *et al.*
The ω^3 Scaling of the Vibrational Density of States in Quasi-2D Nanoconfined Solids
Nat. Commun., 13, 3649 (2022).

- A-170
L. Chen, *et al.*
Anisotropic Magnon Damping by Zero-Temperature Quantum Fluctuations in Ferromagnetic CrGeTe₃
Nat. Commun., 13, 4037 (2022).
- A-171
S. Xu, *et al.*
Non-Hookean Large Elastic Deformation in Bulk Crystalline Metals
Nat. Commun., 13, 5307 (2022).
- A-172
F. Takeiri, *et al.*
Hydride-Ion-Conducting K₂NiF₄-Type Ba–Li Oxyhydride Solid Electrolyte
Nat. Mater., 21, 325–330 (2022).
- A-173
A. D. Hillier, *et al.*
Muon Spin Spectroscopy
Nat. Rev. Methods Primer, 2, 4 (2022).
- A-174
J. Pacio, *et al.*
Advanced Thermal-Hydraulic experiments and instrumentation for heavy liquid metal reactors
Nucl. Eng. Des. 399, 112010 (2022)
- A-175
A. Kobayashi, *et al.*
Impedance reduction by a SiC-loaded flange and its application to the J-PARC main ring septum magnet
Nucl. Instrum. Methods Phys. Res. A, 1031, 16651 (2022)
- A-176
H. Okita, *et al.*
Improvement of longitudinal beam tracking simulation considering the frequency response of the cavity gap voltage monitor
Nucl. Instrum. Methods Phys. Res. A, 1041, p.167361_1 - 167361_7 (2022)
- A-177
V. Andrieux, *et al.*
The large COMPASS polarized solid ammonia target for Drell-Yan measurements with a pion beam
*Nucl. Instrum. Methods Phys. Res. A*1025, 166069 (2022)
- A-178
K. Abe, *et al.*
First gadolinium loading to Super-Kamiokande
*Nucl. Instrum. Methods Phys. Res. A*1027, 166248 (2022)
- A-179
Y. Akazawa, *et al.*
Development and application of CATCH: A cylindrical active tracker and calorimeter system for hyperon–proton scattering experiments
*Nucl. Instrum. Methods Phys. Res. A*1029, 166430 (2022)
- A-180
N. Muramatsu, *et al.*
SPRING-8 LEPS2 beamline: A facility to produce a multi-GeV photon beam via laser Compton scattering
*Nucl. Instrum. Methods Phys. Res. A*1033, 166677 (2022)
- A-181
T. Ishikawa, *et al.*
Time resolution of a 1.8-m long BC-420 plastic scintillator bar with metal-packaged H11934 photomultiplier tubes
*Nucl. Instrum. Methods Phys. Res. A*1039, 167164 (2022)
- A-182
S. Nakasuga, *et al.*
Commissioning of the electron identification system for Dilepton measurement in pA collisions at J-PARC
*Nucl. Instrum. Methods Phys. Res. A*1041, 167335 (2022)
- A-183
H. Nishiguchi, *et al.*
Vacuum-Compatible, Ultra-Thin-Wall Straw Tracker; Detector construction, Thinner straw R&D, and the brand-new graphite-straw development
*Nucl. Instrum. Methods Phys. Res. A*1042, 167373 (2022)
- A-184
M. Fujita, *et al.*
Development of a Ge detector array and an in-beam calibration system for highly precise measurement of Ξ^- atomic X-rays
*Nucl. Instrum. Methods Phys. Res. A*1042, 167439 (2022)
- A-185
C. Zhang, *et al.*
Modeling the diffusion of muonium in silica aerogel and its application to a novel design of multi-layer target for thermal muon generation
*Nucl. Instrum. Methods Phys. Res. A*1042, 167443 (2022)
- A-186
K. Horie, *et al.*
Measurement of Residual μ^+ Polarization in Various Scintillating Materials to Search for T-Violating μ^+ Polarization in $K^+ \rightarrow \pi^0 \mu^+ \nu$ Decay
Nucl. Instrum. Methods Phys. Res. Sect. Accel. Spectrometers Detect. Assoc. Equip., 1037, 166932 (2022).
- A-187
K. Isegawa, *et al.*
Fast Phase Differentiation between Liquid–Water and Ice by Pulsed Neutron Imaging with Gated Image Intensifier
Nucl. Instrum. Methods Phys. Res. Sect. Accel. Spectrometers Detect. Assoc. Equip., 1040 167260 (2022).
- A-188
F. Nemoto, *et al.*
Performance of Position-Sensitive Flat-Panel and Resister Type Photomultiplier Tube Detector on Neutron Reflectometer SOFIA at J-PARC
Nucl. Instrum. Methods Phys. Res. Sect. Accel. Spectrometers Detect. Assoc. Equip., 1040, 166988 (2022).
- A-189
H. Takeshita, *et al.*
Measurement of nuclide production cross sections for proton-induced reactions on ^{nat}Ni and ^{nat}Zr at 0.4, 1.3, 2.2, and 3.0 GeV
Nucl. Instrum. Methods Phys. Res. B 527, 17 (2022)
- A-190
M. Kawano, *et al.*
Effects of Self-Hydrogen Bonding among Formamide Molecules on the UCST-Type Liquid–Liquid Phase Separation of Binary Solutions with Imidazolium-Based Ionic Liquid, [CnMim][TFSI], Studied by NMR, IR, MD Simulations, and SANS
Phys. Chem. Chem. Phys., 24, 13698–13712 (2022).
- A-191
K. Yamaguchi, *et al.*
Kinetics of the Interfacial Curing Reaction for an Epoxy–Amine Mixture
Phys. Chem. Chem. Phys., 24, 21578–21582 (2022).
- A-192
T. Yamanaka, *et al.*
Magnetic and Structure Transition of Mn_{3-x}Fe_xO₄ Solid Solutions under High-Pressure and High-Temperature Conditions
Phys. Chem. Miner., 49, 41 (2022).
- A-193
B. Yee-Rendon, *et al.*
Beam dynamics studies for fast beam trip recovery of the Japan Atomic Energy Agency accelerator-driven subcritical system
Phys. Rev. Accel. Beams, 25, 080101 (2022)
- A-194
Y. Nakazawa, *et al.*
High-power test of an interdigital H-mode drift tube linac for the J-PARC muon g-2 and electric dipole moment experiment
Phys. Rev. Accel. Beams, 25, 110101 (2022)
- A-195
Y. Nakazawa, *et al.*
High-power test of an interdigital H-mode drift tube linac for the J-PARC

- Phys. Rev. Accel. Beams*, 25, 110101(2022)
- A-196
M.-Y. Huang, *et al.*
Performance of the correlated painting based on the mechanical structure of the anticorrelated painting scheme
Phys. Rev. Accel. Beams, 25, 110401 (2022)
- A-197
T. Yasui, *et al.*
Suppression of the eighth-order space-charge-induced resonance
Phys. Rev. Accel. Beams, 25, 121001 (2022)
- A-198
M. Saito, *et al.*
Indirectly cooled secondary-particle production target at J-PARC Hadron Experimental Facility
Phys. Rev. Accel. Beams, 25, 63001 (2022)
- A-199
H. Kadowaki, *et al.*
Spin and Quadrupole Correlations by Three-Spin Interaction in the Frustrated Pyrochlore Magnet $Tb_{2+x}Ti_{2-x}O_{7+y}$
Phys. Rev. B, 105, 014439 (2022).
- A-200
K. Ikeuchi, *et al.*
Spin Excitations Coupled with Lattice and Charge Dynamics in $La_{2-x}Sr_xCuO_4$
Phys. Rev. B, 105, 014508 (2022).
- A-201
M. Watanabe, *et al.*
Contrasting Magnetic Structures in $SrLaCuSbO_6$ and $SrLaCuNbO_6$: Spin -1/2 Quasi-Square-Lattice J_1 - J_2 Heisenberg Antiferromagnets
Phys. Rev. B, 105, 054414 (2022).
- A-202
M. Saito, *et al.*
Structures of Magnetic Excitations in the Spin -1/2 Kagome-Lattice Antiferromagnets $Cs_2Cu_3SnF_{12}$ and $Rb_2Cu_3SnF_{12}$
Phys. Rev. B, 105, 064424 (2022).
- A-203
K. Matan, *et al.*
Breakdown of Linear Spin-wave Theory and Existence of Spinon Bound States in the Frustrated Kagome-Lattice Antiferromagnet
Phys. Rev. B, 105, 134403 (2022).
- A-204
M. Fujihala, *et al.*
Relief of Spin Frustration through Magnetic Anisotropy in the Quasi-One-Dimensional $S = 1/2$ Antiferromagnet $Na_2CuSO_4Cl_2$
Phys. Rev. B, 105, 144410 (2022).
- A-205
Y. Kojima, *et al.*
Magnons and Spinons in Ba_2CoTeO_6 : A Composite System of Isolated Spin-1/2 Triangular Heisenberg-like and Frustrated Honeycomb Ising-like Antiferromagnets
Phys. Rev. B, 105, L020408 (2022).
- A-206
Y. Imai, *et al.*
Zigzag Magnetic Order in the Kitaev Spin-Liquid Candidate Material $RuBr_3$ with a Honeycomb Lattice
Phys. Rev. B, 105, L041112 (2022).
- A-207
S.-H. Do, *et al.*
Damped Dirac Magnon in the Metallic Kagome Antiferromagnet $FeSn$
Phys. Rev. B, 105, L180403 (2022).
- A-208
M. Micoulaut, *et al.*
Structural Properties of Chalcogenide Glasses and the Isocoordination Rule: Disentangling Effects from Chemistry and Network Topology
Phys. Rev. B, 106, 014206 (2022).
- A-209
K. Tomiyasu, *et al.*
Observation of Topological Z_2 Vortex Fluctuations in the Frustrated Heisenberg Magnet $NaCrO_2$
Phys. Rev. B, 106, 054407 (2022).
- A-210
R. Tripathi, *et al.*
Quantum Critical Spin-Liquid-like Behavior in the $S = 1/2$ Quasikagome-Lattice Compound $CeRh_{1-x}Pd_xSn$ Investigated Using Muon Spin Relaxation and Neutron Scattering
Phys. Rev. B, 106, 064436 (2022).
- A-211
B. Gao, *et al.*
Magnetic Field Effects in an Octupolar Quantum Spin Liquid Candidate
Phys. Rev. B, 106, 094425 (2022).
- A-212
Y. Ishii, *et al.*
Partial Breakdown of Translation Symmetry at a Structural Quantum Critical Point Associated with a Ferroelectric Soft Mode
Phys. Rev. B, 106, 134111 (2022).
- A-213
T. Hattori, *et al.*
Hydrogen Vibration Excitations of $ZrH_{1.8}$ and $TiH_{1.84}$ up to 21 GPa by Incoherent Inelastic Neutron Scattering
Phys. Rev. B, 106, 134309 (2022).
- A-214
Z. Jin, *et al.*
Chern Numbers of Topological Phonon Band Crossing Determined with Inelastic Neutron Scattering
Phys. Rev. B, 106, 224304 (2022).
- A-215
M. Hiraishi, *et al.*
Local Electronic Structure of Dilute Hydrogen in β - Ga_2O_3 Probed by Muons
Phys. Rev. B, 107, L041201 (2022).
- A-216
J. Koga, *et al.*
Angular Distribution of γ Rays from the p -Wave Resonance of ^{118}Sn
Phys. Rev. C, 105, 054615 (2022).
- A-217
U.A. Acharya, *et al.*
Kinematic dependence of azimuthal anisotropies in $p+Au$, $d+Au$, and ^3He+Au at $\sqrt{s_{NN}} = 200$ GeV
Phys. Rev. C, 105, 24901 (2022)
- A-218
T. Ishikawa, *et al.*
Coherent photoproduction of the neutral pion and η -meson on the deuteron at incident energies below 1.15 GeV
Phys. Rev. C, 105, 45201 (2022)
- A-219
U.A. Acharya, *et al.*
Systematic study of nuclear effects in $p+Al$, $p+Au$, $p+Au$, and ^3He+Au collisions at $\sqrt{s_{NN}} = 200$ GeV using π^0 production
Phys. Rev. C, 105, 64902 (2022)
- A-220
U. Acharya, *et al.*
Measurement of $\psi(2S)$ nuclear modification at backward and forward rapidity in $p+p$, $p+Al$, and $p+Au$ collisions at $\sqrt{s_{NN}} = 200$ GeV
Phys. Rev. C, 105, 64912 (2022)
- A-221
S. Endo, *et al.*
Measurement of the Transverse Asymmetry of γ Rays in the $^{117}Sn(n, \gamma)^{118}Sn$ Reaction
Phys. Rev. C, 106, 064601 (2022).
- A-222
U. Acharya, *et al.*
 ϕ meson production in $p+Al$, $p+Au$, $d+Au$, and ^3He+Au collisions at $\sqrt{s_{NN}} = 200$ GeV
Phys. Rev. C, 106, 14908 (2022)
- A-223
T. Hashimoto, *et al.*
Differential cross sections and photon beam asymmetries of η photoproduction on the proton at $E_\gamma = 1.3$ -2.4 GeV
Phys. Rev. C, 106, 35201 (2022)
- A-224
X.L. Wang, *et al.*
Study of $\gamma\gamma \rightarrow \gamma\psi(2S)$ at Belle
Phys. Rev. D, 105, 112011 (2022)
- A-225
E. Waheed, *et al.*
Study of $\bar{B}^0 \rightarrow D^+h^-(h=K/\pi)$ decays at Belle

- Phys. Rev. D*, 105, 12003 (2022)
- A-226
B. Wang, *et al.*
Measurement of $B(B_s \rightarrow D_s X)$ with B_s semileptonic tagging
Phys. Rev. D, 105, 12004 (2022)
- A-227
G.D. Alexeev, *et al.*
Exotic meson $\pi_1(1600)$ with $J^{PC} = 1^{-+}$ and its decay into $\rho(770)\pi$
Phys. Rev. D, 105, 12005 (2022)
- A-228
B. Bhuyan, *et al.*
Search for the decay $B\eta \rightarrow \eta\eta$
Phys. Rev. D, 105, 12007 (2022)
- A-229
Wren A. Yamada, *et al.*
Near-threshold spectrum from a uniformized Mittag-Leffler expansion: Pole structure of the $Z(3900)$
Phys. Rev. D, 105, 14034 (2022)
- A-230
X.Y. Gao, *et al.*
Search for tetraquark states $X_{cc\bar{s}\bar{s}}$ in $D_s^+ D_s^+$ ($D_s^+ D_s^{*+}$) final states at Belle
Phys. Rev. D, 105, 32002 (2022)
- A-231
U.A. Acharya, *et al.*
Transverse-single-spin asymmetries of charged pions at midrapidity in transversely polarized $p+p$ collisions at $\sqrt{s} = 200$ GeV
Phys. Rev. D, 105, 32003 (2022)
- A-232
U.A. Acharya, *et al.*
Transverse single spin asymmetries of forward neutrons in $p+p$, $p+Al$, and $p+Au$ collisions at $\sqrt{s_{NN}} = 200$ GeV as a function of transverse and longitudinal momenta
Phys. Rev. D, 105, 32004 (2022)
- A-233
R.U. Abbasi, *et al.*
Observation of variations in cosmic ray single count rates during thunderstorms and implications for large-scale electric field changes
Phys. Rev. D, 105, 62002 (2022)
- A-234
A. Abed Abud, *et al.*
Low exposure long-baseline neutrino oscillation sensitivity of the DUNE experiment
Phys. Rev. D, 105, 72006 (2022)
- A-235
T. Bloomfield, *et al.*
Measurement of the branching fraction and CP asymmetry for $\$B \rightarrow \bar{D}^0\pi$ decays
Phys. Rev. D, 105, 72007 (2022)
- A-236
Y. Li, *et al.*
Measurements of the branching fractions of $\Xi_c^0 \rightarrow \Lambda K\eta$, $\Xi_c^0 \rightarrow \Sigma^0 K\eta$, and $\Xi_c^0 \rightarrow \Sigma^+ K^-$ decays at Belle
Phys. Rev. D, 105, L011102 (2022)
- A-237
C. Hadjivasiliou, *et al.*
Search for B^0 meson decays into Λ and missing energy with a hadronic tagging method at Belle
Phys. Rev. D, 105, L051101 (2022)
- A-238
Y.B. Li, *et al.*
First test of lepton flavor universality in the charmed baryon decays $\Omega_c^0 \rightarrow \Omega-\ell^+\nu_\ell$ using data of the Belle experiment
Phys. Rev. D, 105, L091101 (2022)
- A-239
M. Pavin, *et al.*
Measurement of proton-carbon forward scattering in a proof-of-principle test of the EMPHATIC spectrometer
Phys. Rev. D, 106, 112008 (2022)
- A-240
T. Czank, *et al.*
Search for $Z' \rightarrow \mu^+\mu^-$ in the $L_\mu - L_\tau$ gauge-symmetric model at Belle
Phys. Rev. D, 106, 12003 (2022)
- A-241
H.B. Jeon, *et al.*
Search for the radiative penguin decays $B^0 \rightarrow K\eta K\eta\gamma$ in the Belle experiment
Phys. Rev. D, 106, 12006 (2022)
- A-242
U. Gebauer, *et al.*
Measurement of the branching fractions of the $B^+ \rightarrow \eta\ell^+\nu_\ell$ and $B^+ \rightarrow \eta'\ell^+\nu_\ell$ decays with signal-side only reconstruction in the full q^2 range
Phys. Rev. D, 106, 32013 (2022)
- A-243
E. Gramellini, *et al.*
Measurement of the $\pi^- - Ar$ total hadronic cross section at the LArIAT experiment
Phys. Rev. D, 106, 52009 (2022)
- A-244
R. Matsumoto, *et al.*
Search for proton decay via $p \rightarrow \mu^+ K^0$ in 0.37 megaton-years exposure of Super-Kamiokande
Phys. Rev. D, 106, 72003 (2022)
- A-245
Y. Hidaka, *et al.*
Complementarity and causal propagation of decoherence by measurement in relativistic quantum field theories
Phys. Rev. D, 106, 76018 (2022)
- A-246
M. Bogomilov, *et al.*
Multiple Coulomb scattering of muons in lithium hydride
Phys. Rev. D, 106, 92003 (2022)
- A-247
T. Pang, *et al.*
Search for the decay $B\eta \rightarrow \eta'K\eta$
Phys. Rev. D, 106, L051103 (2022)
- A-248
S.-M. Chang, *et al.*
Mechanism of Endosomal Escape by pH-Responsive Nucleic-Acid Vectors
Phys. Rev. E, 106, 034408 (2022).
- A-249
T. Hashimoto, *et al.*
Measurements of Strong-Interaction Effects in Kaonic-Helium Isotopes at Sub-eV Precision with X-Ray Microcalorimeters
Phys. Rev. Lett., 128, 112503 (2022)
- A-250
Y.C. Chen, *et al.*
Measurement of Two-Particle Correlations of Hadrons in e^+e^- Collisions at Belle
Phys. Rev. Lett., 128, 142005 (2022)
- A-251
K. Miwa, *et al.*
Precise Measurement of Differential Cross Sections of the $\Sigma^- p \rightarrow \Lambda n$ Reaction in Momentum Range 470–650 MeV/c
Phys. Rev. Lett., 128, 72501 (2022)
- A-252
S. Jia, *et al.*
Search for a Light Higgs Boson in Single-Photon Decays of $Y(1S)$ Using $Y(2S) \rightarrow \pi^+\pi^- Y(1S)$ Tagging Method
Phys. Rev. Lett., 128, 81804 (2022)
- A-253
W. Yao, *et al.*
Excitations in the Ordered and Paramagnetic States of Honeycomb Magnet $\text{Na}_2\text{Co}_2\text{TeO}_6$
Phys. Rev. Lett., 129, 147202 (2022).
- A-254
Wren A. Yamada, *et al.*
Analytic Map of Three-Channel S Matrix: Generalized Uniformization and Mittag-Leffler Expansion
Phys. Rev. Lett., 129, 192001 (2022)
- A-255
M. Fujihala, *et al.*
Birchite $\text{Cd}_2\text{Cu}_2(\text{PO}_4)_2\text{SO}_4 \cdot 5\text{H}_2\text{O}$ as a Model Antiferromagnetic Spin-1/2 Heisenberg $J_1 - J_2$ Chain
Phys. Rev. Mater., 6, 114408 (2022).
- A-256
S. Shamoto, *et al.*
Magnetic Bragg Peak Enhancement under

- Ultrasound Injection
Phys. Rev. Res., 4, 013245 (2022).
- A-257
Y. Ohmasa, *et al.*
Rotation of Complex Ions with Ninefold Hydrogen Coordination Studied by Quasielastic Neutron Scattering and First-Principles Molecular Dynamics Calculations
Phys. Rev. Res., 4, 033215 (2022).
- A-258
M. Matsuura, *et al.*
Phonon Renormalization Effects Accompanying the 6 K Anomaly in the Quantum Spin Liquid Candidate κ -(BEDT-TTF)₂Cu₂(CN)₃
Phys. Rev. Res., 4, L042047 (2022).
- A-259
S. Bao, *et al.*
Neutron Spectroscopy Evidence on the Dual Nature of Magnetic Excitations in a van Der Waals Metallic Ferromagnet Fe_{2.72}GeTe₂
Phys. Rev. X, 12, 011022 (2022).
- A-260
X. Li, *et al.*
Giant Magnetic In-Plane Anisotropy and Competing Instabilities in Na₃Co₂SbO₆
Phys. Rev. X, 12, 041024 (2022).
- A-261
H. Ito, *et al.*
Measurement of structure dependent radiative $K^+ \rightarrow e^+\nu\gamma$ decays using stopped positive kaons
Physics Letters B, 835, 136913 (2022)
- A-262
Y. Fujimoto, *et al.*
Equation of state of neutron star matter and its warm extension with an interacting hadron resonance gas
Physics Letters B, 835, 137524 (2022)
- A-263
H. Aoyama, *et al.*
Cryptoasset networks: Flows and regular players in Bitcoin and XRP
*PLoS ONE*17, e0273068 (2022)
- A-264
M. Yoshida, *et al.*
Conformation and Structure of Hydroxyethyl Cellulose Ether with a Wide Range of Average Molar Masses in Aqueous Solutions
Polymers, 14, 4532 (2022).
- A-265
A. Koda, *et al.*
Organic Molecular Dynamics and Charge-carrier Lifetime in Lead Iodide Perovskite MAPbI₃
Proc. Natl. Acad. Sci., 119, e2115812119 (2022).
- A-266
K. Yamashita, *et al.*
Atomic Distribution and Local Structure in Ice VII from in situ Neutron Diffraction
Proc. Natl. Acad. Sci., 119, e2208717119 (2022).
- A-267
W. Higemoto, *et al.*
Direct Measurement of the Evolution of Magnetism and Superconductivity toward the Quantum Critical Point
Proc. Natl. Acad. Sci., 119, e2209549119 (2022).
- A-268
J. Sheng, *et al.*
Two-Dimensional Quantum Universality in the Spin-1/2 Triangular-Lattice Quantum Antiferromagnet Na₂BaCo(PO₄)₂
Proc. Natl. Acad. Sci., 119, e2211193119 (2022).
- A-269
Y. Hidaka, *et al.*
Foundations and applications of quantum kinetic theory
Progress in Particle and Nuclear Physics, 127, 103989 (2022)
- A-270
Y. Shobuda
Two-dimensional resistive-wall impedance with finite thickness; Its mathematical structures and their physical meanings
PTEP (Internet), 2022(5), p.053G01_1 - 053G01_44, (2022)
- A-271
M. Chimura, *et al.*
Beam emittance growth due to the strong space-charge field at low energy of a high-intensity ion linac and its mitigation using an octupole magnetic field
PTEP (Internet), 2022(6), p.063G01_1 - 063G01_26, (2022)
- A-272
T. Yasui, *et al.*
Beam optics for the compensation of third-order structure resonances
PTEP 2022, 013G01 (2022)
- A-273
Y. Hidaka, *et al.*
Symmetry protected topological phases of matter
PTEP 2022, 04A001 (2022)
- A-274
Y. Hidaka, *et al.*
Global 4-group symmetry and 't Hooft anomalies in topological axion electrodynamics
PTEP 2022, 04A103 (2022)
- A-275
M. Otani
First muon acceleration and muon linear accelerator for measuring the muon anomalous magnetic moment and electric dipole moment
PTEP 2022, 052C01 (2022)
- A-276
T. Hayata, *et al.*
Lattice Lindblad simulation
PTEP 2022, 053B03 (2022)
- A-277
R.L. Workman, *et al.*
REVIEW OF PARTICLE PHYSICS
PTEP 2022, 083C01 (2022)
- A-278
T. Nanamura, *et al.*
Measurement of differential cross sections for Σ^+p elastic scattering in the momentum range 0.44–0.80 GeV/c
PTEP 2022, 093D01 (2022)
- A-279
M. Fujita, *et al.*
 Ξ^- atomic X-ray spectroscopy using a counter-emulsion hybrid method
PTEP 2022, 123D01 (2022)
- A-280
M. Nishida, *et al.*
Neutron Stress Measurement of W/Ti Composite in Cryogenic Temperatures Using Time-of-Flight Method
Quantum Beam Sci., 7, 8 (2022).
- A-281
E. Wakai, *et al.*
Development of Innovative Materials and Measurement Systems used for Radiation Environment
Research & Development in Material Science, 16, 1859 (2022)
- A-282
E. Wakai, *et al.*
Titanium/Titanium Oxide Particle Dispersed W-TiC Composites for High Irradiation Applications
Research & Development in Material Science, 16, 1879 (2022)
- A-283
T. Fujiwara, *et al.*
Neutron Flat-Panel Detector Using In–Ga–Zn–O Thin-Film Transistor
Rev. Sci. Instrum., 93, 013304 (2022).
- A-284
J. Abe, *et al.*
Development of Triaxial Compressive Apparatus for Neutron Experiments with Rocks
Rev. Sci. Instrum., 93, 025103 (2022).
- A-285
K. Akutsu-Suyama, *et al.*
Heavy Water Recycling for Producing Deuterium Compounds

RSC Adv, 12, 24821–24829 (2022).

A-286

N. Okita, *et al.*

The Origin of Stability and High $\text{Co}^{2+/3+}$ Redox Utilization for FePO_4 -Coated $\text{LiCo}_{0.90}\text{Ti}_{0.05}\text{PO}_4/\text{MWCNT}$ Nanocomposites for 5 V Class Lithium Ion Batteries
RSC Adv, 12, 26192–26200 (2022).

A-287

Y. Hanazono, *et al.*

Revisiting the Concept of Peptide Bond Planarity in an Iron-Sulfur Protein by Neutron Structure Analysis
Sci. Adv, 8, eabn2276 (2022).

A-288

Y. Qin, *et al.*

Field-Tuned Quantum Effects in a Triangular-Lattice Ising Magnet
Sci. Bull., 67, 38–44 (2022).

A-289

K. Iida, *et al.*

Magnon Mode Transition in Real Space
Sci. Rep., 12, 20663 (2022).

A-290

E. Nocerino, *et al.*

Nuclear and Magnetic Spin Structure of the Antiferromagnetic Triangular Lattice Compound LiCrTe_2 Investigated by μ^+ SR, Neutron and X-Ray Diffraction
Sci. Rep., 12, 21657 (2022).

A-291

H. Hashimoto, *et al.*

Structure of Alumina Glass
Sci. Rep., 12, 516 (2022).

A-292

I.-H. Chiu, *et al.*

Non-Destructive 3D Imaging Method Using Muonic X-Rays and a CdTe Double-Sided Strip Detector
Sci. Rep., 12, 5261 (2022).

A-293

M. Maeda, *et al.*

Effect of Sample Density in Prompt γ -Ray Analysis
Sci. Rep., 12, 6287 (2022).

A-294

H. Kwon, *et al.*

Work Hardening Behavior of Hot-Rolled Metastable $\text{Fe}_{50}\text{Co}_{25}\text{Ni}_{10}\text{Al}_5\text{Ti}_5\text{Mo}_5$ Medium-Entropy Alloy: in situ Neutron Diffraction Analysis
Sci. Technol. Adv. Mater., 23, 579–586 (2022).

A-295

T. Nakamura, *et al.*

Formation and Evolution of Carbonaceous Asteroid Ryugu: Direct Evidence from Returned Samples
Science, 379, eabn8671 (2022).

A-296

M.-Y. Luo, *et al.*

Grain-Size-Dependent Microstructure Effects on Cyclic Deformation Mechanisms in CoCrFeMnNi High-Entropy-Alloys
Scr. Mater., 210, 114459 (2022).

A-297

D. Wei, *et al.*

Regulation of Strength and Ductility of Single-Phase Twinning-Induced Plasticity High-Entropy Alloys
Scr. Mater., 216, 114738 (2022).

A-298

N. Tsuchida, *et al.*

Stress Partitioning between Bcc and Cementite Phases Discussed from Phase Stress and Dislocation Density in Martensite Steels
Scr. Mater., 222, 115002 (2022).

A-299

W. Gong, *et al.*

Compressive Deformation Behavior of AZ31 Alloy at 21K: An in-situ Neutron Diffraction Study
Scr. Mater., 225, 115161 (2022).

A-300

E. Zhao, *et al.*

Quantifying the Anomalous Local and Nanostructure Evolutions Induced by Lattice Oxygen Redox in Lithium-Rich Cathodes
Small Methods, 6, 2200740 (2022).

A-301

F. Nemoto, *et al.*

Neutron Reflectometry-Based in situ Structural Analysis of an Aligning Agent Additive for the Alignment of Nematic Liquid Crystals on Solid Substrates
Soft Matter, 18, 545–553 (2022).

A-302

F. Song, *et al.*

Tracer Diffusion Coefficients Measurements on LaPO_4 -Dispersed LAMP by Means of Neutron Radiography
Solid State Ion., 377, 115873 (2022).

A-303

Y. Makida, *et al.*

SMES Model Device Cooled by Liquid Hydrogen Flow through Thermosiphon Loop
TeionKogaku (低温工学), Vol 57, 241 (2022)

A-304

W. Shen, *et al.*

Relationship between Interfacial Adsorption of Additive Molecules and Reduction of Friction Coefficient in the Organic Friction Modifiers-ZDDP Combinations
Tribol. Int., 167, 107365 (2022).

A-305

N. Yamashita, *et al.*

Interfacial Structure and Tribological Property of Adsorbed Layer Formed by Dibasic Acid Ester Derivative
Tribol. Online, 17, 246–256 (2022).

A-306

S. Makimura

Frontiers of Target, Beam Window, and Its Materials in the Proton Accelerator Field
Vacuum and Surface Science (表面と真空) 65, 577 (2022)

Conference Reports and Books

B-001

M. Segawa, *et al.*

Investigation of Radioactive Samples for Neutron Capture Reaction Measurements Using Energy-Resolved Neutron Imaging
Ann. Nucl. Energy, 167, 108828 (2022).

B-002

S. Kanda

A Search for Atomic Parity Violation in Muonic Atoms Using a High-Intensity Pulsed Muon Beam at J-PARC
EPJ Web Conf., 262, 01010 (2022).

B-003

S. Fukumura, *et al.*

Proposal for New Measurements of Muonic Helium Hyperfine Structure at J-PARC
EPJ Web Conf., 262, 01012 (2022).

B-004

T. Higuchi, *et al.*

Prospects for a Neutron EDM Measurement with an Advanced Ultracold Neutron Source at TRIUMF
EPJ Web Conf., 262, 01015 (2022).

B-005

Y. Kawakita, *et al.*

Recent Progress on DNA ToF Backscattering Spectrometer in MLF, J-PARC
EPJ Web Conf., 272, 02002 (2022).

B-006

R. Kajimoto, *et al.*

Possible Future Upgrades of the Direct-Geometry Chopper Spectrometer 4SEASONS
EPJ Web Conf., 272, 02007 (2022).

- B-007
K. Nakajima, *et al.*
Possible Options for Efficient Wide-Band Polychromatic Measurements Using Chopper Spectrometers at Pulsed Sources
EPJ Web Conf., 272, 02012 (2022).
- B-008
S. Yoshida, *et al.*
Grain Orientation Dependence of Deformation Microstructure Evolution and Mechanical Properties in Face-Centered Cubic High/Medium Entropy Alloys
IOP Conf. Ser. Mater. Sci. Eng., 1249, 012027 (2022).
- B-009
S. Sato, *et al.*
Development of a Pulse-Width-Discriminating ^3He Position-Sensitive Detector System
J. Neutron Res., 24, 427–434 (2022).
- B-010
A. Ueno, *et al.*
Impurities reduction conditionings to recover best beam quality of J-PARC cesiated RF-driven H⁻ ion source with new parts exposed to plasma
J. Phys. Conf. Ser., 2244, 012029_1 - 012029_5 (2022)
- B-011
Y. Yamada, *et al.*
Non-destructive beam spatial profile measurement using a gas sheet monitor for a high-intensity ion beam
J. Phys. Conf. Ser., 2244, 012077_1 - 012077_6 (2022)
- B-012
T. Shibata, *et al.*
Numerical study of different electron density observed in Hydrogen and Deuterium ion source plasmas
J. Phys. Conf. Ser., 2244, 12002 (2022)
- B-013
T. Shibata, *et al.*
Soundness evaluation of J-PARC RF ion source after 5-month continuous operation
J. Phys. Conf. Ser., 2244, 12041 (2022)
- B-014
T. D. Vu, *et al.*
Narrow-Area Bragg-Edge Transmission of Iron Samples Using Superconducting Neutron Sensor
J. Phys. Conf. Ser., 2323, 012028 (2022).
- B-015
H. Shishido, *et al.*
Neutron Imaging toward Epithermal Regime Using a Delay Line Current-Biased Kinetic-Inductance Detector
J. Phys. Conf. Ser., 2323, 012029 (2022).
- B-016
T.D. Vu, *et al.*
Narrow-area Bragg-edge transmission of iron samples using superconducting neutron sensor
J. Phys. Conf. Ser., 2374, 12028 (2022)
- B-017
H. Shishido, *et al.*
Neutron Imaging toward Epithermal Regime using a Delay Line Current-Biased Kinetic-Inductance Detector
J. Phys. Conf. Ser., 2374, 12029 (2022)
- B-018
T. Kosaka, *et al.*
Development of Low Temperature Analog Readout (LTARS 2018) for LAr-TPCs
J. Phys. Conf. Ser., 2374, 12077 (2022)
- B-019
T. Arihara, *et al.*
Development of the in-situ Calibration System using LEDs and Light Guide Plates for the SuperFGD
J. Phys. Conf. Ser., 2374, 12118 (2022)
- B-020
P.K. Saha, *et al.*
Recent results of beam loss mitigation and extremely low beam loss operation of J-PARC RCS
J. Phys. Conf. Ser., 2420, 012040, 2023
- B-021
M. Kitaguchi
T-violation in neutron scattering
JPS Conf. Proc., 37, 011010 (2022).
- B-022
H. Akatsuka, *et al.*
Study of Thin Iron Films for Polarization Analysis of Ultracold Neutrons
JPS Conf. Proc., 37, 020801 (2022).
- B-023
T. Ino, *et al.*
Optically Polarized Alkali Metal Cell for Muonic Helium Measurements
JPS Conf. Proc., 37, 021208 (2022).
- B-024
R. Matsumiya, *et al.*
The Precision nEDM Measurement with UltraCold Neutrons at TRIUMF
JPS Conf. Proc., 37, 20701 (2022)
- B-025
T. Ishikawa, *et al.*
Coherent neutral-pion and eta-meson photoproduction on the deuteron
JPS Conf. Proc., 37, 21003 (2022)
- B-026
F. Suekane, *et al.*
A Plan for Decay at Rest $\nu_e + \text{Pb}$ Cross Section Measurement: DaRveX
PoSNUFACT2021, 402, 194 (2022).
- B-027
S. Kanda
Toward a High-Precision Measurement of the Muon Lifetime with an Intense Pulsed Muon Beam at J-PARC
PoSNUFACT2021, 402, 215 (2022).
- B-028
G. Ariyoshi, *et al.*
Flow measurement in high temperature liquid metal by using electro-magnet probe
Proc. 19th International Topical Meeting on Nuclear Reactor Thermal Hydraulics (NURETH-19, 2022)
- B-029
H. Obayashi, *et al.*
Application of Noncontact Type of Ultrasonic Flowmeter for High Temperature LBE Flow
Proc. 19th International Topical Meeting on Nuclear Reactor Thermal Hydraulics (NURETH-19, 2022)
- B-030
B. Yee-Rendon, *et al.*
Progress on SRF Linac Development for the Accelerator-Driven Subcritical System at JAEA
Proc. 20th International Conference on RF Superconductivity (SRF'21), pp. 372-375 (2022)
- B-031
J. Tamura, *et al.*
Present Status of the Spoke Cavity Prototyping for the JAEA-ADS Linac
Proc. 20th International Conference on RF Superconductivity (SRF'21), pp. 612-615 (2022)
- B-032
P.K. Saha, *et al.*
ACHIEVEMENT OF LOW BEAM LOSS AT HIGH-INTENSITY OPERATION OF J-PARC 3 GeV RCS
Proc. Ann. Mtg PASJ, 1 (2022)
- B-033
S. Mizobata, *et al.*
OVERVIEW OF THE J-PARC LINAC KLYSTRON TEST STAND
Proc. Ann. Mtg PASJ, 1041 (2022)
- B-034
T. YASUI, *et al.*
RESULTS OF HIGH REPETITION BEAM COMMISSIONING IN J-PARC MR
Proc. Ann. Mtg PASJ, 151 (2022)
- B-035
T. Asami, *et al.*
HIGH-PRECISION OPTICS MEASUREMENT USING COD RESPONSE IN J-PARC MAIN RING
Proc. Ann. Mtg PASJ, 161 (2022)
- B-036
S. Iwata, *et al.*
COUNTERMEASURES FOR THE FAILURE

OF THE NEW SEPTUM MAGNET FOR FAST EXTRACTION IN J-PARC MAIN RING
Proc. Ann. Mtg PASJ, 170 (2022)

B-037

F. Tamura, *et al.*

EFFECTS OF THE LONGITUDINAL IMPEDANCES ON NON-ADIABATIC BUNCH MANIPULATION AT FLATTOP OF J-PARC MR
Proc. Ann. Mtg PASJ, 175 (2022)

B-038

A. KOBAYASHI, *et al.*

PROGRESS OF EVALUATION OF BEAM COUPLING IMPEDANCE REDUCTION FOR THE EDDY-CURRENT TYPE SEPTUM MAGNET IN J-PARC MR
Proc. Ann. Mtg PASJ, 19 (2022)

B-039

T. Ito, *et al.*

CAVITY CLEANING FOR SUPPRESSION OF MULTIPACTOR OCCURED AT J-PARC SDTL
Proc. Ann. Mtg PASJ, 193 (2022)

B-040

Y. Nakazawa, *et al.*

HIGH-POWER TEST OF AN APF IH-DTL PROTOTYPE FOR THE MUON LINAC
Proc. Ann. Mtg PASJ, 197 (2022)

B-041

K. Sumi, *et al.*

DESIGN OF COUPLER CELLS IN THE DISK-LOADED STRUCTURE FOR THE MUON LINAC
Proc. Ann. Mtg PASJ, 202 (2022)

B-042

R. Kitamura, *et al.*

LONGITUDINAL MEASUREMENT OF HIGH-INTENSITY BEAM WITH BUNCH-SHAPE MONITOR IN FRONT-END
Proc. Ann. Mtg PASJ, 212 (2022)

B-043

M. Nomura, *et al.*

IMAGE RECOGNITION TECHNOLOGY IS USED TO OBTAIN MOMENTUM DISTRIBUTION AND LONGITUDINAL BEAM SHAPE FROM MOUNTAIN PLOT IMAGE
Proc. Ann. Mtg PASJ, 215 (2022)

B-044

H. Iinuma, *et al.*

DEMONSTRATION OF THREE-DIMENSIONAL SPIRAL INJECTION FOR J-PARC MUON g-2/ EDM EXPERIMENT
Proc. Ann. Mtg PASJ, 218 (2022)

B-045

Y. Fukao, *et al.*

DEVELOPMENT OF THE SIC MUON BEAM MONITOR FOR THE COMET EXPERIMENT
Proc. Ann. Mtg PASJ, 224 (2022)

B-046

M. Chimura, *et al.*

Development of quadrupole-octupole combined magnet for emittance-growth mitigation in the J-PARC Linac
Proc. Ann. Mtg PASJ, 237 - 241 (2022)

B-047

T. Sugimoto, *et al.*

PERFORMANCE OF NEW IMPEDANCE MATCHING CIRCUIT FOR J-PARC MR INJECTION KICKER MAGNET
Proc. Ann. Mtg PASJ, 247 (2022)

B-048

T. Shibata, *et al.*

THE REDUCTION OF THE LEAKAGE FIELD OF THE NEW SEPTUM MAGNETS FOR FAST EXTRACTION IN J-PARC-MR
Proc. Ann. Mtg PASJ, 253 (2022)

B-049

H. Okita, *et al.*

EVALUATION OF HIGHER HARMONICS GENERATED IN ACCELERATION GAPS DURING THE HIGH POWER BEAM ACCELERATION AT J-PARC RCS
Proc. Ann. Mtg PASJ, 262 (2022)

B-050

P.K. Saha, *et al.*

STATUS OF POP DEMONSTRATION OF 400 MeV H- LASER STRIPPING AT J-PARC RCS
Proc. Ann. Mtg PASJ, 272 (2022)

B-051

S. Yamada

PROPOSAL FOR A UNIDIRECTIONAL GATEWAY FROM EPICS CHANNEL ACCESS TO HTTP USING WEB TECHNOLOGIES
Proc. Ann. Mtg PASJ, 296 (2022)

B-052

H. Takahashi, *et al.*

DEVELOPMENT OF BEAM WINDOW PROTECTION UNIT FOR J-PARC LINAC
Proc. Ann. Mtg PASJ, 300 (2022)

B-053

K. Agari, *et al.*

DEVELOPMENT OF TEMPERATURE-MEASUREMENT AND CONTROL SYSTEM FOR NEW PRODUCTION TARGET AT J-PARC HADRON EXPERIMENTAL FACILITY
Proc. Ann. Mtg PASJ, 309 (2022)

B-054

A. Toyoda, *et al.*

DEVELOPMENT OF HIGH SENSITIVITY RESIDUAL GAS IONIZATION PROFILE MONITOR FOR J-PARC HADRON HIGH-P BEAMLINE(3)
Proc. Ann. Mtg PASJ, 327 (2022)

B-055

R. Kitamura, *et al.*

STUDIES OF BEAM DIAGNOSTICS WITH BUNCH-SHAPE MONITOR FOR HIGH-POWER AND LOW-BETA H- BEAM

Proc. Ann. Mtg PASJ, 330 (2022)

B-056

Y. Sato, *et al.*

SIGNAL RESPONSE OF THE RESIDUAL GAS IONIZATION CURRENT MONITOR IN J-PARC HADRON EXPERIMENTAL FACILITY
Proc. Ann. Mtg PASJ, 338 (2022)

B-057

H. Iinuma, *et al.*

DESIGN WORK OF PULSED RADIAL KICK FIELD FOR J-PARC MUON g-2/EDM EXPERIMENT
Proc. Ann. Mtg PASJ, 385 (2022)

B-058

K. Miura, *et al.*

UPGRADE OF MAIN MAGNET POWER SUPPLY SYSTEM IN J-PARC MR FOR HIGH-REPETITION RATE OPERATION
Proc. Ann. Mtg PASJ, 400 (2022)

B-059

H. Watanabe, *et al.*

DESIGN OF GAS BEARING FOR ROTATING-DISK-TYPE SECONDARY-PARTICLE PRODUCTION TARGET AT J-PARC HADRON EXPERIMENTAL FACILITY
Proc. Ann. Mtg PASJ, 427 (2022)

B-060

S. Nagayama, *et al.*

Study of non-destructive slow beam extraction method in particle accelerator
Proc. Ann. Mtg PASJ, 503 - 507(2022)

B-061

R. Kurasaki, *et al.*

DEVELOPMENT OF A LARGE-DIAMETER PILLOW-SEAL USING WELDED STAINLESS-STEEL PLATES (2)
Proc. Ann. Mtg PASJ, 521 (2022)

B-062

T. Sasaki, *et al.*

DEVELOPMENT OF A WIDE DYNAMIC-RANGE BEAM PROFILE MONITOR USING OTR AND FLUORESCENCE FOR INJECTED BEAMS IN J-PARC MAIN RING (3)
Proc. Ann. Mtg PASJ, 560 (2022)

B-063

M. Abe, *et al.*

TWO-DIMENSIONAL MAGNETIC FIELD RECONSTRUCTION FOR SIMULATION OF SPIRAL INJECTION IN MUON G-2/EDM PRECISION MEASUREMENTS MAGNET
Proc. Ann. Mtg PASJ, 605 (2022)

B-064

F. Muto, *et al.*

DEVELOPMENT OF RADIATION-RESISTANT DISPLACEMENT SENSOR FOR MONITORING ROTATING PRODUCTION TARGET AT J-PARC HADRON FACILITY
Proc. Ann. Mtg PASJ, 634 (2022)

- B-065
H. Watanabe, *et al.*
EVALUATION OF PURE TUNGSTEN MADE WITH METAL 3D PRINTER
Proc. Ann. Mtg PASJ, 65 (2022)
- B-066
K. Shinto, *et al.*
OUTGASSING CHARACTERISTICS FROM THE J-PARC-MADE INTERNAL ANTENNA FOR A HIGH-INTENSITY RADIO-FREQUENCY H- ION SOURCE
Proc. Ann. Mtg PASJ, 675 (2022)
- B-067
M. Tomizawa, *et al.*
DEVELOPMENT OF BEAM OPTICS CORRECTION TOOL FOR J-PARC MAIN RING
Proc. Ann. Mtg PASJ, 711 (2022)
- B-068
F. Kobayashi, *et al.*
COUNTERMEASURES AGAINST NOISE OF INVERTER-CONTROLLED MULTI-STAGE ROOT PUMPS IN J-PARC LINAC BEAM DUMP
Proc. Ann. Mtg PASJ, 726 (2022)
- B-069
K. Satou, *et al.*
DEVELOPMENT OF SIGNAL ATTENUATOR WITH LOW REFLECTION AND LOW DISTORTION FOR NEW BPM SIGNAL ACQUISITION SYSTEM OF J-PARC MR
Proc. Ann. Mtg PASJ, 751 (2022)
- B-070
M. Shirakata, *et al.*
BEAM COLLIMATOR SYSTEM WHICH CONSISTS OF SEVEN UNITS IN J-PARC MAIN RING
Proc. Ann. Mtg PASJ, 756 (2022)
- B-071
S. Makimura, *et al.*
DEVELOPMENT OF BEAM WINDOW WITH A LARGE DIAMETER, A THIN WALL THICKNESS, AND A LARGE PROOF PRESSURE OUT OF Ti-6Al-4V THROUGH ADDITIVE MANUFACTURING
Proc. Ann. Mtg PASJ, 79 (2022)
- B-072
Y. Kawabata, *et al.*
VERIFICATION OF ROBOT UTILIZATION IN ACCELERATOR TUNNEL
Proc. Ann. Mtg PASJ, 83 (2022)
- B-073
T. Shibata, *et al.*
Evaluation of RF antenna lifetime after long-term operation of J-PARC ion source
Proc. Ann. Mtg PASJ, 863 (2022)
- B-074
K. Okabe, *et al.*
BEAM SUTUDY ON MEBT1 AT THE J-PARC LINEAC
Proc. Ann. Mtg PASJ, 885 (2022)
- B-075
R. Muto, *et al.*
SIMULATION STUDY ON THE BEAM SPILL STRUCTURE OF THE SLOW EXTRACTION AT J-PARC MAIN RING
Proc. Ann. Mtg PASJ, 893 (2022)
- B-076
S. Iwata, *et al.*
THE INSTALLATION OF THE NEW SEPTUM MAGNETS FOR FAST EXTRACTION IN J-PARC MAIN RING
Proc. Ann. Mtg PASJ, 901 (2022)
- B-077
Y. Sugiyama, *et al.*
NEXT GENERATION LLRF CONTROL SYSTEM FOR J-PARC MR
Proc. Ann. Mtg PASJ, 92 (2022)
- B-078
Y. Hashimoto, *et al.*
A MULTI-RIBBON BEAM PROFILE MONITOR IN A BEAM DUMP LINE OF J-PARC MR
Proc. Ann. Mtg PASJ, 931 (2022)
- B-079
N. Yoshimura, *et al.*
EVALUATION FOR UPDATING THE INTRA-BUNCH FEEDBACK AT J-PARC MAIN RING
Proc. Ann. Mtg PASJ, 936 (2022)
- B-080
Ersin CICEK, *et al.*
INSTALLATION AND TEST OF THE PHASE DRIFT MONITOR AT J-PARC LINAC
Proc. Ann. Mtg PASJ, 97 (2022)
- B-081
T. Ito, *et al.*
Cavity cleaning for suppression of multipactor occurred at the J-PARC SDTL
Proc. Ann. Mtg. PASJ (internet), 193-196(2022)
- B-082
Y. Nakazawa, *et al.*
HIGH-POWER TEST OF AN APF IH-DTL PROTOTYPE FOR THE MUON LINAC
Proc. Ann. Mtg. PASJ (internet), 197-201 (2022)
- B-083
Y. Sumi, *et al.*
DESIGN OF COUPLER CELLS IN THE DISK-LOADED STRUCTURE FOR THE MUON LINAC
Proc. Ann. Mtg. PASJ (internet), 202-206 (2022)
- B-084
R. Kitamura, *et al.*
Longitudinal measurement of high-intensity beam with bunch-shape monitor in front-end
Proc. Ann. Mtg. PASJ (internet), 212-214 (2022)
- B-085
T. Takayanagi, *et al.*
Semiconductor pulse power supplies for accelerators at J-PARC
Proc. Ann. Mtg. PASJ (internet), 242-246 (2022)
- B-086
R. Kitamura, *et al.*
Studies of beam diagnostics with bunch-shape monitor for high-power and low-beta H- beam
Proc. Ann. Mtg. PASJ (internet), 330-332 (2022)
- B-087
K. Nii, *et al.*
REPORTS OF ELECTRO-POLISHING IMPLEMENTATION FOR QUARTER-WAVE RESONATORS (2)
Proc. Ann. Mtg. PASJ (internet), 601-604 (2022)
- B-088
K. Shinto, *et al.*
Outgassing Characteristics from the J-PARC-made internal antenna for a high-intensity radio-frequency H- ion source
Proc. Ann. Mtg. PASJ (internet), 675-679 (2022)
- B-089
F. Kobatashi, *et al.*
Countermeasures against noise of inverter-controlled multi-stage root pump in J-PARC linac beam dump
Proc. Ann. Mtg. PASJ (internet), 726-730 (2022)
- B-090
T. Shibata, *et al.*
Evaluation of RF antenna lifetime after long-term operation of J-PARC ion source
Proc. Ann. Mtg. PASJ (internet), 863-867 (2022)
- B-091
K. Hirano, *et al.*
Multiple irradiation experiment of tungsten materials by negative hydrogen ion beam (1) Study of beam target materials
Proc. Atomic Energy Society of Japan, 3H08 (2022)
- B-092
M. Fukuda, *et al.*
Multiple irradiation experiment of tungsten materials by negative hydrogen ion beam (2) Evaluation as material for ITER divertor
Proc. Atomic Energy Society of Japan, 3H09 (2022)
- B-093
K. Tokunaga, *et al.*
Multiple irradiation experiment of tungsten materials by negative hydrogen ion beam (3) Observation of material degradation by multiple irradiation
Proc. Atomic Energy Society of Japan, 3H10 (2022)
- B-094
M. Kamibayashi, *et al.*
Single Bit Upsets Versus Burst Errors of Stacked-Capacitor DRAMs Induced by High-Energy Neutron -SECCED Is No Longer Effective-
Proc. Eur. Conf. Radiat. Its Eff. Compon. Syst. RADECS (2022).

- B-095
H. Hotchi, *et al.*
1 MW J-PARC RCS Beam Operation and Further Beyond
Proc. HB2021, MOIP1 (2022)
- B-096
B. Yee-Rendon, *et al.*
Status of the JAEA-ADS Superconducting LINAC Design
Proc. HB2021, MOP04 (2022)
- B-097
T. Toyama, *et al.*
Beam Instability Issue and Transverse Feedback System in the MR of J-PARC
Proc. HB2021, THAC1 (2022)
- B-098
M. Tomizawa, *et al.*
Slow Extraction Operation at J-PARC Main Ring
Proc. HB2021, THDC1 (2022)
- B-099
K. Satou, *et al.*
MERITS OF PULSE MODE OPERATION OF RESIDUAL GAS IONIZATION PROFILE MONITOR FOR J-PARC MAIN RING
Proc. IBIC2022, 434 (2022)
- B-100
R. Kitamura
First Measurement of Longitudinal Profile of High-Power and Low-Energy H⁻ Beam by Using Bunch Shape Monitor with Graphite Target
Proc. IBIC2022, 532 (2022)
- B-101
M. Yamamoto, *et al.*
Influence of a positive grid biasing on RF system in J-PARC RCS
Proc. IPAC2022 (Internet), 1336 - 1338 (2022)
- B-102
Y. Sumi, *et al.*
FABRICATION AND LOW-POWER TEST OF DISK-AND-WASHER CAVITY FOR MUON ACCELERATION
Proc. IPAC2022 (Internet), 1534-1537 (2022)
- B-103
Y. Shobuda, *et al.*
Measurements of radiation fields from a ceramic break
Proc. IPAC2022 (Internet), 1663 - 1666 (2022)
- B-104
Y. Takeuchi, *et al.*
muon g-2 and electric dipole moment experiment
Proc. IPAC2022 (Internet), 94-97 (2022)
- B-105
H. Okita, *et al.*
DESIGN STUDIES ON A HIGH-POWER WIDE-
- BAND RF COMBINER FOR CONSOLIDATION OF THE DRIVER AMPLIFIER OF THE J-PARC RCS
Proc. IPAC2022, 1333 (2022)
- B-106
M. Yamamoto, *et al.*
INFLUENCE OF A POSITIVE GRID BIASING ON RF SYSTEM IN J-PARC RCS
Proc. IPAC2022, 1336 (2022)
- B-107
Y. Takeuchi, *et al.*
FABRICATION AND LOW-POWER TEST OF DISK-AND-WASHER CAVITY FOR MUON ACCELERATION
Proc. IPAC2022, 1534 (2022)
- B-108
P.K. Saha, *et al.*
RECENT RESULTS OF BEAM LOSS MITIGATION AND EXTREMELY LOW BEAM LOSS OPERATION OF J-PARC RCS
Proc. IPAC2022, 1616 (2022)
- B-109
S. Iwata, *et al.*
SIMULATION STUDY OF FAST EXTRACTION IN THE ABSENCE OF ONE SEPTUM MAGNET FOR J-PARC MAIN RING
Proc. IPAC2022, 2100 (2022)
- B-110
S. Iwata, *et al.*
UPGRADE OF SEPTUM MAGNETS FOR FAST EXTRACTION IN J-PARC MAIN RING
Proc. IPAC2022, 2103 (2022)
- B-111
K. Hasegawa, *et al.*
STATUS AND UPGRADE PLAN OF THE MR RING RF SYSTEMS IN J-PARC
Proc. IPAC2022, 2131 (2022)
- B-112
T. Shibata, *et al.*
THE NEW EDDY CURRENT TYPE SEPTUM MAGNET FOR UPGRADING OF FAST EXTRACTION IN MAIN RING OF J-PARC
Proc. IPAC2022, 2428 (2022)
- B-113
T. Shibata, *et al.*
THE REDUCTION OF THE LEAKAGE FIELD OF THE INJECTION SEPTUM MAGNET IN MAIN RING OF J-PARC
Proc. IPAC2022, 2774 (2022)
- B-114
T. Shibata, *et al.*
THE NEW HIGH FIELD SEPTUM MAGNET FOR UPGRADING OF FAST EXTRACTION IN MAIN RING OF J-PARC
Proc. IPAC2022, 2788 (2022)
- B-115
C. Ohmori, *et al.*
- 20-YEAR COLLABORATION ON SYNCHROTRON RF BETWEEN CERN AND J-PARC
Proc. IPAC2022, 3130 (2022)
- B-116
T. Sugimoto, *et al.*
IMPROVEMENT OF MATCHING CIRCUIT FOR J-PARC MAIN RING INJECTION KICKER MAGNET
Proc. IPAC2022, 316 (2022)
- B-117
K. Sumi, *et al.*
DESIGN AND BEAM DYNAMICS STUDY OF DISK-LOADED STRUCTURE FOR MUON LINAC
Proc. IPAC2022, 94 (2022)
- B-118
Y. Nakazawa, *et al.*
HIGH-POWER TEST OF AN APF IH-DTL PROTOTYPE FOR THE MUON LINAC
Proc. LINAC2022 (Internet), 275-278(2022)
- B-119
Y. Takeuchi, *et al.*
END-TO-END SIMULATIONS AND ERROR STUDIES OF THE J-PARC MUON LINAC
Proc. LINAC2022 (Internet), 562-564(2022)
- B-120
Y. Kono, *et al.*
THE MUON LINAC PROJECT AT J-PARC
Proc. LINAC2022 (Internet), 636-640(2022)
- B-121
J. Tamura, *et al.*
ACCELERATION EFFICIENCY OF TE-MODE STRUCTURES FOR PROTON LINACS
Proc. LINAC2022, 177-179 (2022)
- B-122
J. Tamura, *et al.*
Current Status of the Spoke Cavity Prototyping for the JAEA-ADS Linac
Proc. LINAC2022, 180-183 (2022)
- B-123
Ersin CICEK, *et al.*
IMPLEMENTATION OF AN ADVANCED M TCA.4-BASED DIGITIZER FOR MONITORING COMB-LIKE BEAM AT THE J-PARC LINAC
Proc. LINAC2022, 219 (2022)
- B-124
Y. Nakazawa, *et al.*
HIGH-POWER TEST OF AN APF IH-DTL PROTOTYPE FOR THE MUON LINAC
Proc. LINAC2022, 275 (2022)
- B-125
B. Yee-Rendon, *et al.*
Overview of ADS Projects in the World
Proc. LINAC2022, 310-313 (2022)
- B-126
Y. Fuwa, *et al.*

Design of Beam Focusing System with Permanent Magnet for J-PARC LINAC MEBT1
Proc. LINAC2022, 364-376 (2022)

B-127

Y. Takeuchi, *et al.*
END-TO-END SIMULATIONS AND ERROR STUDIES OF THE J-PARC MUON LINAC
Proc. LINAC2022, 562 (2022)

B-128

Y. Kondo, *et al.*
THE MUON LINAC PROJECT AT J-PARC
Proc. LINAC2022, 636 (2022)

B-129

Min YANG, *et al.*
APPLICATIONS OF TIMING READ-BACK SYSTEM IN J-PARC MAIN RING
Proc. PCaPAC2022, 8 (2022)

B-130

D. Barrow, *et al.*
T2KSK Joint ν Oscillation Sensitivity
Proceedings of Science, NOW2022, 8 (2022)

B-131

崔烘福, *et al.*
中性子イメージング技術を用いた接着系あと施工アンカーにおける 接着剤未充填部の特定手法
日本地震工学会・大会2022, (2022).

KEK Reports

C-001

Safety Division, J-PARC Center
Annual Report on the Activities of Safety in J-PARC, FY2021
KEK Internal 2022-007

C-002

Belle Collaboration
Measurement of Two-Particle Correlations of Hadrons in e^+e^- Collisions at Belle
KEK Preprint 2021-57; Belle Preprint 2021-32

C-003

Belle Collaboration
Search for the decay $B_s \rightarrow \eta' K S_0$
KEK Preprint 2021-58; Belle Preprint 2022-01

C-004

Belle Collaboration
Search for charged lepton flavor violating decays of $Y(1S)$
KEK Preprint 2021-59; Belle Preprint 2022-02

C-005

Belle Collaboration
Search for $B_0 \rightarrow K_S^0 K_S^0 \gamma$ decays at Belle
KEK Preprint 2021-62; Belle Preprint 2022-03

C-006

Belle Collaboration
Measurements of the branching fractions $B(\bar{B}^0 \rightarrow D^{*+}\pi^-)$ and $B(\bar{B}^0 \rightarrow D^{*+}K^-)$ and tests of QCD factorization
KEK Preprint 2022-1; Belle Preprint 2022-10

C-007

Belle Collaboration
Two-particle angular correlations in $e^+e^- \rightarrow \text{hadronic final states}$ in two reference coordinates at Belle
KEK Preprint 2022-10; Belle Preprint 2022-11

C-008

Belle Collaboration
First search for the weak radiative decays $\Lambda_c^+ \rightarrow \Sigma^+\gamma$ and $\Xi_c^0 \rightarrow \Xi^0\gamma$
KEK Preprint 2022-11; Belle Preprint 2022-12

C-009

Belle Collaboration
Search for $X(3872) \rightarrow \pi^+\pi^-\pi^0$ at Belle
KEK Preprint 2022-12; Belle Preprint 2022-13

C-010

Belle II Collaboration
Measurement of the Λ_c^+ lifetime
KEK Preprint 2022-13; Belle II Preprint 2022-003

C-011

Belle Collaboration
Observation of $\Omega(2012) \rightarrow \Xi(1530)$ K-bar and measurement of the couplings of $\Omega(2012) \rightarrow \Xi(1530)$ K-bar and $\Xi(1530)$ K-bar
KEK Preprint 2022-14; Belle Preprint 2022-14

C-012

Belle Collaboration
Measurement of the B^+/B_0 production ratio in e^+e^- collisions at the $Y(4S)$ resonance using $B \rightarrow J/\psi(\text{II})K$ decays at Belle
KEK Preprint 2022-15; Belle Preprint 2022-15

C-013

Belle Collaboration
Measurement of the branching fraction and search for CP Violation in $D^0 \rightarrow K_S^0 K_S^0 \pi^+\pi^-$ decays at Belle
KEK Preprint 2022-19; Belle Preprint 2022-16; UCHP-22-002

C-014

Belle Collaboration
Measurement of the branching fractions for Cabibbo-suppressed decays $D^+ \rightarrow K^+K^-\pi^+\pi^0$ and $D_s^+ \rightarrow K^+\pi^-\pi^+\pi^0$ at Belle
KEK Preprint 2022-2; Belle Preprint 2022-04

C-015

Belle Collaboration
Search for baryon CP violation, measurement of branching fractions and decay asymmetry parameters for $\Lambda_c^+ \rightarrow \Lambda h^+$ and $\Lambda_c^+ \rightarrow \Sigma^0 h^+(h=K,\pi)$
KEK Preprint 2022-22; Belle Preprint 2022-17; UCHP-22-04

C-016

Belle Collaboration
First measurement of the $B^+ \rightarrow \pi^+\pi^0\pi^0$ branching fraction and CP asymmetry
KEK Preprint 2022-23; Belle Preprint 2022-18

C-017

Belle II Collaboration
Observation of $e^+e^- \rightarrow \omega\chi_{\text{BJ}}(1P)$ and search

for $X_{\text{b}} \rightarrow \omega Y(1S)$ at \sqrt{s} near 10.75 GeV
KEK Preprint 2022-24; Belle II Preprint 2022-004

C-018

Belle Collaboration
Measurements of branching fractions of $\Lambda_c^+ \rightarrow \Sigma^+\eta$ and $\Lambda_c^+ \rightarrow \Sigma^+\eta'$ and asymmetry parameters of $\Lambda_c^+ \rightarrow \Sigma^+\pi^0$, $\Lambda_c^+ \rightarrow \Sigma^+\eta$, and $\Lambda_c^+ \rightarrow \Sigma^+\eta'$
KEK Preprint 2022-25; Belle Preprint 2022-19

C-019

Belle II Collaboration
Measurement of the Ω_c^0 lifetime at Belle II
KEK Preprint 2022-26; Belle II Preprint 2022-005

C-020

Belle Collaboration
Evidence for the singly Cabibbo-suppressed decay $\Omega_c^0 \rightarrow \Xi^-\pi^+$ and search for $\Omega_c^0 \rightarrow \Xi^-K^+$ and $\Omega_c^0 \rightarrow \Omega^-K^+$ decays at Belle
KEK Preprint 2022-28; Belle Preprint 2022-20

C-021

Belle Collaboration
Observation of a Threshold Cusp at the $\Lambda\eta$ Threshold in the pK^- Mass Spectrum with $\Lambda_c^+ \rightarrow pK^-\pi^+$ Decays
KEK Preprint 2022-29; Belle Preprint 2022-21

C-022

Belle Collaboration
Search for $D^+ \rightarrow K^- K_S^0 \pi^+\pi^+\pi^0$ at Belle
KEK Preprint 2022-3; Belle Preprint 2022-05

C-023

Belle Collaboration
Studies of $e^+e^- \rightarrow \eta\phi$ via Initial State Radiation
KEK Preprint 2022-30; Belle Preprint 2022-22

C-024

Belle Collaboration
Search for rare decays $B^+ \rightarrow D_s^{*+}\eta$, $D_s^{*+}\bar{K}^0$, $D^{*+}\eta$, and D^+K^0
KEK Preprint 2022-31; Belle Preprint 2022-23

C-025

Belle Collaboration
Measurement of branching fractions of $\Lambda_c^+ \rightarrow p K_S^0 K_S^0$ and $\Lambda_c^+ \rightarrow p K_S^0 \eta$ at Belle
KEK Preprint 2022-33; Belle Preprint 2022-24

- C-026
Belle Collaboration
Study of $B^+ \rightarrow p \bar{n} \pi^0$
KEK Preprint 2022-34; Belle Preprint 2022-25
- C-027
Belle Collaboration
Study of $e^+ e^- \rightarrow \Sigma^0 \bar{\Sigma}^0$ and $\Sigma^+ \bar{\Sigma}^-$ by Initial State Radiation Method at Belle
KEK Preprint 2022-35; Belle Preprint 2022-26
- C-028
Belle Collaboration
Search for heavy neutrino in tau decays at Belle
KEK Preprint 2022-36; Belle Preprint 2022-27
- C-029
Belle Collaboration
Measurement of the mass and width of the $\Lambda_c(2625)^+$ and the branching ratios of $\Lambda_c(2625)^+ \rightarrow \Sigma_c^0 \pi^+$ and $\Lambda_c(2625)^+ \rightarrow \Sigma_c^+ \pi^-$
KEK Preprint 2022-37; Belle Preprint 2022-28
- C-030
Belle Collaboration
First observation of $\Lambda \pi^+$ and $\Lambda \pi^-$ signals near the $\bar{K}N$ ($I=1$) mass threshold in $\Lambda_c^+ \rightarrow \Lambda^+ \pi^+ \pi^+ \pi^-$ decay
KEK Preprint 2022-38; Belle Preprint 2022-29
- C-031
Belle II Collaboration
Search for lepton-flavor-violating tau decays to a lepton and an invisible boson at Belle II
KEK Preprint 2022-39; Belle II Preprint 2022-007
- C-032
Belle Collaboration
Measurement of the branching fraction of $\Xi_c^0 \rightarrow \Lambda_c^+ \pi^-$ at Belle
KEK Preprint 2022-4; Belle Preprint 2022-06
- C-033
Belle II Collaboration
Search for an invisible Z' in a final state with two muons and missing energy at Belle II
KEK Preprint 2022-40; Belle II Preprint 2022-008
- C-034
Belle Collaboration
Search for the lepton flavour violating decays $B^+ \rightarrow K^+ \tau^\pm \ell^\mp$ ($\ell = e, \mu$) at Belle
KEK Preprint 2022-41; Belle Preprint 2022-30
- C-035
Belle Collaboration
First observation of $B \rightarrow \bar{D}_1 (\rightarrow \bar{D} \pi^+ \pi^-) \ell^+ \nu_\ell$ and measurement of the $B \rightarrow \bar{D}^{(*)} \pi \ell^+ \nu_\ell$ and $B \rightarrow \bar{D}^{(*)} \pi^+ \pi^- \ell^+ \nu_\ell$ branching fractions with hadronic tagging at Belle
KEK Preprint 2022-44; Belle Preprint 2022-32
- C-036
Belle Collaboration
Angular analysis of the low $M(K^+ K^-)$ mass enhancement in $B^+ \rightarrow K^+ K^- \pi^+$ decays
KEK Preprint 2022-5; Belle Preprint 2022-07
- C-037
Belle II Collaboration
Search for a dark photon and an invisible dark Higgs in $\mu^+ \mu^-$ and missing energy final states with the Belle II experiment
KEK Preprint 2022-6; Belle II Preprint 2022-001
- C-038
Belle Collaboration
Evidence of a new excited charmed baryon decaying to $\Sigma_c(2455)^{0,+} \pi^\pm$
KEK Preprint 2022-7; Belle Preprint 2022-08
- C-039
Belle Collaboration
Measurement of two-photon decay width of $\chi_{c2}(1P)$ in $\gamma\gamma \rightarrow \chi_{c2}(1P) \rightarrow J/\psi\gamma$ at Belle
KEK Preprint 2022-8; Belle Preprint 2022-09
- C-040
Belle II Collaboration
Measurement of Lepton Mass Squared Moments in $B \rightarrow X_c \ell \bar{\nu}_\ell$ Decays with the Belle II Experiment
KEK Preprint 2022-9; Belle II Preprint 2022-002
- C-041
I. Yamane
Laser Charge-Exchange of J-PARC 400 MeV H-Beam with 2 Pulse Laser Storage Ring
KEK Report 2022-1
- C-042
I. Yamane
Laser Charge-Exchange Injection for High Intensity Proton Accelerator
KEK Report 2022-4
- C-043
2022年度サマーチャレンジ編集委員会、土手昭伸、長谷川雅也 (KEK, Tsukuba)
第16回大学生・高校生のための素粒子・原子核スクール サマーチャレンジ: 宇宙、物質、生命—21世紀の謎に挑む 2022講義テキスト、2022年8月17日~26日 (To be filed on the bookshelf: P0.22:S:8.16.1 KSC22-010)

JAEA Reports

- D-001
R. Kitamura
Highly durable and multifunctional ion beam monitor
JAEA Technology Seeds, 8, p. 68
- D-002
H. Iwamoto, *et al.*
Radiation shielding analysis of the upper structure of an accelerator-driven system
JAEA-Research 2021-012 (2022)
- D-003
K. Nakano, *et al.*
Measurement of Nuclide Production Cross-sections in High-energy Proton-induced Spallation Reactions at J-PARC
JAEA-Research 2021-014 (2022)
- D-004
K. Nakano, *et al.*
Neutronic Analysis of Beam Window and LBE of an Accelerator-Driven System
JAEA-Research 2021-018 (2022)
- D-005
Safety Division, J-PARC Center
Annual Report on the Activities of Safety in J-PARC, FY2021
JAEA-Review 2022-074(2022)
- D-006
S. Saito, *et al.*
Development of High Temperature LBE Corrosion Test Loop "OLLOCHI"
JAEA-Technology 2021-034 (2022)
- D-007
H. Obayashi, *et al.*
Development of Mock-up Test Loop (IMMORTAL) for LBE Spallation Target
JAEA-Technology 2021-035 (2022)
- D-008
A. Ono, *et al.*
加速器装置メンテナンスを安全に進める上での注意点と要領
JAEA-Technology 2021-044, p.53, 2022/03

Others

E-001

H. Aoyagi, *et al.*

Reports on the 11th International Beam
Instrumentation Conference, IBIC2022
Kasokuki 19, No. 4, p. 237

E-002

R. Kitamura, *et al.*

BEAM PROFILE MONITOR
*Unexamined patent publication bulletin, JP,2022-
027504*

J-PARC

JAPAN PROTON ACCELERATOR RESEARCH COMPLEX

High Energy Accelerator Research Organization (KEK)
Japan Atomic Energy Agency (JAEA)



2-4 Shirakata, Tokai-mura, Naka-gun, Ibaraki 319-1195, Japan



<https://j-parc.jp/>